DEVELOPMENT OF A MATHEMATICAL MODEL CONSIDERING NUTRIENTS KINETICS FOR ASSESSING UMGENI RIVER WATER QUALITY

By

Olowe Kayode Oluwafemi

Student No: 215082179

Submitted in fulfilment of the academic requirements for the degree of Doctor of Philosophy in Civil Engineering

College of Agriculture, Engineering and Science,

University of KwaZulu-Natal,

Howard College Campus, Durban.

May 2018

SUPERVISOR: Dr Muthukrishna vellaisamy Kumarasamy

DECLARATION

Supervisor:

As the candidate's Supervisor I agree/do not agree to the submission of this dissertation.

Signed :…….(Dr Muthukrishna vellaisamy Kumarasamy) Date.……

Candidate:

I **Olowe Kayode Oluwafemi**, declare that:

1. The research reported in this thesis, except where otherwise indicated, is my original research.

2. This thesis has not been submitted for any degree or examination at any other university.

3. This thesis does not contain other persons' data, pictures, graphs or other information, unless specifically acknowledged as being sourced from other persons.

4. This thesis does not contain other persons' writing, unless specifically acknowledged as being sourced from other researchers. Where other written sources have been quoted, then:
   a. Their words have been re-written, but the general information attributed to them has been referenced
   b. Where their exact words have been used, then their writing has been placed in italics and inside quotation marks and referenced.

5. This thesis does not contain text, graphics or tables copied and pasted from the Internet, unless specifically acknowledged, and the source being detailed in the thesis and in the References sections.

…….. ……

Olowe Kayode Oluwafemi Date

ACKNOWLEDGEMENTS

All praises and adoration be to almighty God who has been my helper and for protecting me on this fruitful journey. To God be the Glory.

My profound gratitude goes to my supervisor Dr Muthukrishna vellaisamy Kumarasamy for his immense wealth of experience and constructive feedback throughout this research. I admire your passion and your excellent work ethic.

I would like to thank Water Research Commission and JW Nelson Fund for providing funding to support this study.

My sincere appreciation goes to my wonderful parents, Mr. and Mrs. T.B. Olowe for their prayers, financial, and moral support accorded me throughout the pursuit of my programme. Thank you for believing in me and for sharing in my aspirations.

I wish to express my sincere appreciation to the following individuals (Engr. Kayode Ibijola, Engr. Joy Adu, Nxusa Nomandla, Ooma Chetty, Deji Ogunode, Kazeem, Labulo Ayo, Gboyega Ola, Engr. Tope Fatukasi, Engr. Ope Makinde, Engr. Owoola, Prof. Gbenga Tedela and Prof. Oyegoke). Thank you for your constant support and encouragement during the course of my study.

To my beautiful wife, Adekunle Adesola Olowe, thank you for enduring my absence, supporting my dreams, in fact you are my joy.

To my families and friends, Wura, Collins, Balogun, Abbey, Tayo, Martins, Dayo, Mrs Joke Aregbesola, Mrs Ola Joseph, Kehinde, Femi Omodara, Victor and Kolajo. You are highly recognized.

ABSTRACT

Surface water is an essential component of the natural environment which needs to be sheltered from all sources of contamination because human and aquatic animals depend on it for their survival. However, the discharge of organic wastes into water bodies has deteriorated its quality and placed economic restrictions on water use. Anthropogenic inputs of nutrients into the water column has become one of the vast water quality problems around the world. This result in the reduction of dissolved oxygen level and promotes algae growth in the water body. Therefore, there is a need for the development of an effective nutrient management strategy which is essential in protecting the water body. Standard practice is to use water quality models as an important part of environmental valuation tools for modeling and controlling the surface water pollution. Water quality models have been a useful tool in maintaining the water quality status and evaluating the fate of pollutants in different water bodies.

Numerous methods are available for solving solute transport in natural streams and rivers. However, existing methods are flawed either because of their limitation in application to a natural water body due to their inaccurate in estimating model parameters or their failure to simulate the advection component of solute transport. The Hybrid cell in series (HCIS) model which is a conceptualized model serves as an alternative method to solve solute transport in a natural river. It overcomes the difficulties associated with the existing approaches such as Fickian based models by converting its second – order partial differential equation to a first - order ordinary differential equation which could be solved analytically. Additionally, the conceptual hybrid model was able to include advection component to its process which overcomes the difficulty associated with mixing cells model.

In this study, additional components to the conceptualized hybrid cells in series model have developed for the first order kinetic reaction of Ammonia (NH_3), Nitrite (NO_2) and Nitrate (NO_3) along with advection and dispersion processes using mass balance concept. A basic hybrid model which consist of a plug flow cell and two different thoroughly mixed cells all connected in series is developed to predict nutrients solute transport in a river from a point source of pollution. Analytical solutions of the HCIS model along with the nutrients kinetics were obtained using Laplace transformation. A C-Sharp programming language was then used to implement the analytical solutions obtained for these models where a user-friendly software package was developed. The developed models were used to predict the temporal and spatial variation of the nutrients concentration in the water body.

The potential of the developed model has been tested using hypothetical data and a field data obtained from uMgeni River to predict the effect of ammonia, nitrite, and nitrate nutrients concentration along the selected river reach. The data collected from several sampling locations along the study area from January 2014 to December 2014 were used to verify the model's efficiency. The prediction of ammonia, nitrite and nitrate concentration using the developed HCIS models have shown excellent agreement with field data of the uMgeni River, South Africa. Thus, the analytical solutions obtained can accurately predict the nutrients solute transport in uMgeni River. Further, the study has shown that the response of hybrid models matched satisfactorily with the numerical solution of Fickian based Advection-Dispersion Equation model which was solved with explicit finite difference method.

The performance of the model was validated using statistical tools based on the coefficient of determination (R^2) which was carried out at a 95 percent level of confidence between the observed and simulated data. It was observed from the correlation that the observed and simulated values of the nutrients concentration in the river demonstrated a high correlation coefficient (R^2) and the standard error (SE) was low for all components of the model (NH_3, NO_2, and NO_3). Hence, the results show that the developed model has demonstrated high accuracy and provide a novel tool for predicting ammonia, nitrite, and nitrate concentration distributions in the River.

This research work presents the development and application of HCIS model for predicting the concentration of nutrients, i.e., NH_3, NO_2, and NO_3 in water bodies. Based on the study, the hybrid model is effective in predicting the spatiotemporal concentration of ammonia, nitrite, and nitrate nutrients in the natural water body. However, the influence of high rainfall event significantly increases the nutrient concentrations of the river which was not considered in the current model. Thus, this gives a prospect for the consideration of non–point source pollution component in the hybrid model formulation.

TABLE OF CONTENTS

List of Figures

List of Tables

ABBREVIATIONS

ADZ:	Aggregated Dead Zone Model
ADE:	Advection-Dispersion Equation
BOD:	Biological Oxygen Demand
CIS:	Cells in Series Model
CBOD:	Carbonaceous biochemical oxygen demand
DO:	Dissolved Oxygen
DWS:	Department of Water and Sanitation
DWAF:	Department of Water Affairs
HCIS:	Hybrid Cells in Series Model
NH_3:	Ammonia concentration
NO_2:	Nitrite concentration
NO_3:	Nitrate concentration
NSE	Nash-Sutcliffe efficiency coefficient
PO_4:	phosphate
R^2	Coefficient of determination
RMSE	Root mean square error
RSR	RMSE observations standard deviation ratio
SAWS:	South African Weather Services
WW:	Water Works
WWW:	Wastewater Works

NOMENCLATURE

α	Nitrogen fraction of algae biomass
ρ	Algae respiration rate coefficient
μ	Algal growth rate coefficient
Δx	Size of Hybrid unit
δ_3	Benthic release of ammonia nitrogen
δ (.)	Dirac delta function
A	Cross-sectional area of flow
A_g	Algal biomass concentration
$C_a(x, t)$	Ammonia concentration in space and time
C_a^*	Laplace transform of C_a
$C_{a,\,1}$	Concentration of ammonia in the plug flow cell
$C_{a,\,2}$	Concentration of ammonia in the first mixing cell
$C_{a,\,3}$	Concentration of ammonia in the second mixing cell
$C_b(x, t)$	Nitrite concentration in space and time
C_b^*	Laplace transform of C_b
$C_{b,\,1}$	Concentration of nitrite in the plug flow cell
$C_{b,\,2}$	Concentration of nitrite in the first mixing cell
$C_{b,\,3}$	Concentration of nitrite in the second mixing cell
$C_c(x, t)$	Nitrate concentration in space and time
C_c^*	Laplace transform of C_c
$C_{c,\,1}$	Concentration of nitrate in the plug flow cell
$C_{c,\,2}$	Concentration of nitrate in the first mixing cell
$C_{c,\,3}$	Concentration of nitrate in the second mixing cell
C_R	Boundary concentration
C-t	Concentration – time

d	mean stream depth (m),
D_L	Longitudinal dispersion co-efficient
F	Fraction of algal nitrogen uptake from the ammonia pool
H	Depth of flow
k_a	ammonia oxidation rate coefficient
k_b	Nitrite oxidation rate coefficient
K_c	denitrification rate coefficient
$K_{HCIS-NH3}$	Unit step response function of hybrid model with ammonia concentration
$K_{HCIS-NO2}$	Unit step response function of hybrid model with nitrite concentration
$K_{HCIS-NO3}$	Unit step response function of hybrid model with nitrate concentration
n	Cell number
P_e	Peclet number
PN	Algal preference factor
Q	Flow rate
S	Slope
t	time
T_1	Residence time of plug flow cell
T_2	Residence time of first mixed cell
T_3	Residence time of second mixed cell
u	mean flow velocity
U (.)	Step function
U_*	Shear flow velocity
W	Width of the channel
x	distance

CHAPTER 1: INTRODUCTION

1.1. Research Background

In many countries, including South Africa, poor water quality poses a significant threat to human health and aquatic animals. Due to the industrialization and continuously growing population, water pollution has increased considerably in recent times. Surface water is a significant element of our natural habitat which must be safeguarded from all forms of contamination. Rivers and streams offer a different number of benefits in the social and economic development for human activities ranging from irrigation, drinking, recreational, agricultural, and industrial use (Pimentel *et al.*, 2004; Arthington *et al*., 2010). However, the water bodies get polluted by the effluent from anthropogenic activities which results in significant quantities of nutrients in the water columns. Continuous discharge of nutrients in the surface water results in the eutrophication of the water body. Eutrophication prompts the water quality degradation, in particular, depletion of the dissolved oxygen concentration (Karadzic *et al.*, 2010; Kumar, 2011; Foley *et al.*, 2012; Savci, 2012). Many rivers in South Africa, including the uMgeni River, are under threat because of an influx of nutrient pollutants. Eutrophication has been a crucial public health concern which has a dramatic impact on the aquatic ecosystem. Thus, the water quality deterioration calls for regular monitoring of the surface water so that the health of the aquatic ecosystems would be maintained. As water quality monitoring is time-consuming and labour intensive, water quality models are significant tools for simulating water quality parameters and controlling the surface water pollution (Santhi, 2006; Wang *et al.*, 2013).

Nitrogen (N) is an essential component which supports any life form on earth. It is a vital component of the ecosystem because it affects the productivity of the water body. However, an increase in nitrogen components in surface water leads to water quality deterioration. Nitrogen cycling is a complex process in the water bodies which must be understood as it affects the ecosystem functioning. The nitrogen component exists in different forms in surface water as dissolved nitrogen gas, reduced inorganic and oxidized compounds ammonia (NH_3), nitrite (NO_2), nitrate (NO_3) and organic nitrogen compounds (Zheng *et al.*, 2002; Schlesinger *et al.*, 2006). There are different means through which nitrogen may be deposited into the surface water which includes the following: atmospheric deposition; point sources from sewage treatment plants and industrial effluents, diffuse sources from

the catchment area because of agricultural inputs (Paerl, 1997; Howarth, 2008). Additionally, cyanobacteria which convert atmospheric nitrogen into ammonia (Paerl *et al.*, 2011).

A study of nutrients' fate and transport is vital to control/regulate the rate of discharge of nutrient pollutants for the safety of the aquatic habitat's health. Solute transport in water bodies influenced by physical, chemical and biological processes (Gooseff *et al.*, 2008). Several hydrologic and biochemical processes should be taken into consideration when describing the governing mechanisms behind pollutant transport in water bodies. Some of these processes that influence the movement and spread of pollutants in a water body include advection, dispersion, sorption, and sedimentation processes which have been described by several researchers (Fischer *et al.*, 1979; Nordin and Troutman, 1980; Kumarasamy *et al.*, 2011). Advection and dispersion are the primary processes for controlling solute transport in water bodies and are recognized as a one-dimensional transport model known as a Fickian dispersion model (Chatwin, 1980). Advection is due to a bulk fluid movement which is influenced by the flow velocity. The dispersion could be described as the spreading of pollutants in the water bodies resulting from shear stress and molecular diffusion caused by random motion in a fluid (Fischer *et al.*, 1979; Rutherford, 1994). The increase in flow rate will prompt an increment in the longitudinal dispersion in the surface water. Many investigators have applied different methods to study solute transport in rivers and streams, which include advection-dispersion equation and the conceptual mixing cells model.

1.2. Research Motivation

Adolph Fick developed a relationship between the molecular diffusion and heat transfer using the process of Fourier's law in the year 1855 (Fischer *et al.*, 1979). He described the method of solute movement in the water body where it was observed that the pollutant concentration changes from a higher level to a lower concentration as it moved downstream. Further studies were carried out on the diffusion theory of fluids using the concepts of Fick's method by G.I. Taylor in the year 1921. Also, in the year 1953 and 1954, additional research was carried out by him describing the process of the mechanism of dispersion for both laminar and turbulent flow conditions through a pipe (Gosh, 2001). Elder (1959) used the analysis to take account of the effects of vertical shear, and Fischer (1966) used it to estimate longitudinal dispersion in open channels. Several researchers have used laboratory

studies to verify Taylor's theory in applying it to a pipe and open channel (Fischer 1966; Sayre and Chang, 1968). Generalising the transport of solute in a natural river to a one-dimensional behaviour by assuming the vertical and transverse concentration gradients are relatively insignificant. Thus, the advection-dispersion (ADE) equation was formulated using the analysis in Fisher *et al*. (1979). A controlled volume was assumed where conservation of mass method was used coupled with the Fick's law of diffusion to formulate the ADE model as described in Eq. (1.1).

$$\frac{\partial(AC)}{\partial t} = -\frac{\partial(AuC)}{\partial x} + \frac{\partial}{\partial x}\left(AD_L \frac{\partial C}{\partial x}\right) \tag{1.1}$$

C is described as the pollutant concentration (mg/l), D_L represents the longitudinal dispersion coefficient (m^2/s), u denotes the mean flow velocity (m/s), and A represents the area of the channel (m^2). Eq. (1.1) was simplified to determine the classical advection-dispersion equation by assuming a regular channel with uniform flow velocity, as presented below:

$$\frac{\partial(AC)}{\partial t} = -\frac{u\partial C}{\partial x} + D_L \frac{\partial^2 C}{\partial x^2} \tag{1.2}$$

The following assumptions used in solving the one-dimensional Advection-Dispersion Equation. The river was presumed to be spatially uniform, where the channel area and the flow of the river do not fluctuate in space. The dispersion coefficient (D_L) was assumed to be constant in all directions, and a constant velocity in the downstream (x) direction was considered for a given flow. Furthermore, the mass of the pollutant is uniformly spread across the cross-sectional area. Finally, the solute thoroughly mixed in the river, and its concentration varies only in the downstream (x) direction, ignoring fluxes through other planes. The approach has been widely used by Chatwin (1985), Cameron and Klute (1977), Fischer *et al*. (1979), Hart (1995), Runkel (1998), Lees *et al.* (2000) to study solute transport in different water bodies. However, the method has a problem in its application to a natural water body (Chatwin and Allen, 1985; Ghosh *et al.,* 2008; Kumarasamy, 2015). The observed data at a downstream location from the source of injection of pollutant does not indicate a Gaussian shape as predicted by the AD model. Besides, there are problems in determining the accurate longitudinal dispersion coefficient (D_L) in the natural water body which is another limitation of the model. Thus, many conceptual models were developed to serve as an alternative to the ADE model, and they have been applied to simulate solute transport in water bodies.

The Cells-in-Series (CIS) model was developed to serve as an alternative to the Advection-Dispersion method of studying pollutant transport in rivers and streams (Bear, 1972; Banks, 1974; Stefan and Demetracopoulos, 1981). The CIS model presumed a conceptualized river reach to consist of a series of mixed cells having equal filling time. The model assumes the concentration of pollutants from the previous cell will be the input to the succeeding cell. Banks (1974) described an ordinary first-order differentiation for mass transport as the fundamental equation of the CIS model as shown:

$$V\frac{d\bar{C}_o}{dt} = QC_1 - Q\bar{C}_o \tag{1.3}$$

Where Q is the rate of flow (m^3/s), C_1 is inflow concentration (mg/l), C_o represents the average concentration within a cell (mg/l), and V describes the volume of each cell (m^3).

First order ordinary differential method was implemented by the CIS model to formulate its solution. However, its limitation was that the relationship between the number of cells, the travel time of solute and dispersive properties was fixed for a set of same tanks (Beer, 1983; Rutherford, 1994). Furthermore, it was observed that it could not simulate the advection component of solute transport and could not adequately reproduce the persistent skewness which is usually observed in the C-t curves in rivers and streams (Banks, 1974; Kumarasamy, 2015). Hence, the model failed to simulate the longer tail associated with C-t curves in waterways.

Beer and Young (1983), developed a new model known as Aggregated Dead Zone (ADZ) to tackle the problem associated with the CIS model in simulating the advection component of solute transport. The conceptualized ADZ modeling approach was introduced to serve as an alternative model in simulating the advective and dispersive behaviour of pollutants in rivers with a transient storage mechanism (Rutherford, 1994). Furthermore, the dead zone process in the model is primarily responsible for the major cause of dispersion in the natural water body. It was assumed that inclusion of transient storage in the ADZ model accounts for the elevated tails and the persistence of the skewness observed in the C-t profiles which were not catered for in the previous models. Therefore, the ADZ model describes the observed C-t patterns of a natural river adequately and simulate solute transport in rivers and streams satisfactorily when compared to previous models such as the ADE and CIS models. The limitation of the ADZ model was the difficulty in computing the model parameters (Rutherford, 1994; Lee *et al*., 2000).

The hybrid cell-in-series (HCIS) model was developed as an alternative method to solve solute transport in natural water bodies and solve the limitation associated with previous models (Ghosh, 2001; Kumarasamy, 2015). The HCIS model consists of a series of hybrid units, and each unit is comprised of a plug flow zone and two thoroughly mixed zones of different residence times as presented in Fig 1.1.

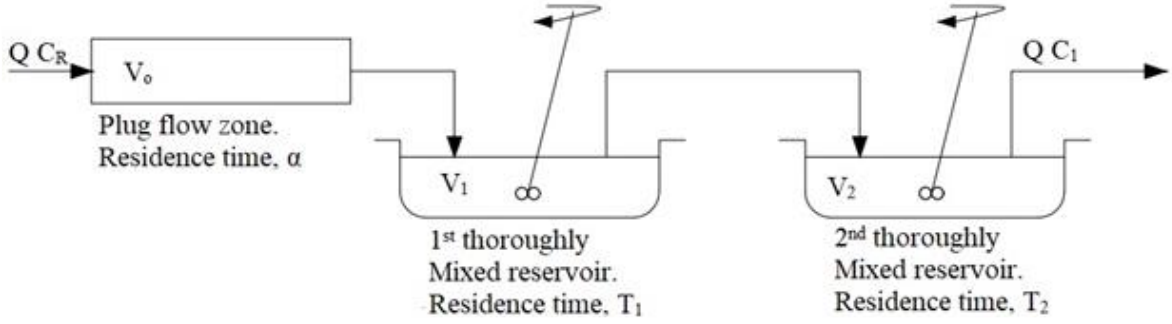

Figure 1.1: A Conceptualised Hybrid Model (Ghosh 2001)

The developed model was used in studying the advection and dispersion component of solute movement in a water column. The process which takes place in the plug flow cell signifies the advection component, and the two thoroughly mixed zones represent both advection and dispersion. The HCIS model has demonstrated some merits over the former models as described by Ghosh *et al*. (2004). The model equation is a first–order ordinary differential equations that can be solved analytically. Also, the model could describe the advection component of solute transport due to the introduction of a plug flow zone. Thus, the inclusion of the compartment has allowed for the estimating of the first arrival time of pollutant in a river reach. Furthermore, it can incorporate additional solute kinetic reactions to its three compartments, and the resulting equation would be solved analytically. Therefore, the model has been able to demonstrate its ability in simulating solute transport in natural water. The model was initially conceptualized to simulate conservative pollutant in surface water (Ghosh, 2001). Since then, the model has been expanded considering various pollutant transport and reaction processes in water bodies. It has been developed to simulate pollutant sorption and decay processes in a water body (Kumarasamy et al. 2011; 2013). Additionally, Kumarasamy (2015) applied the model for simulating dissolved oxygen concentration in streams by adding De-oxygenation and Re-aeration component to the model.

Due to the flexibility and strength of the HCIS model, development of new model components of the HCIS model are aimed to evaluate the nutrient (ammonia, nitrite, and nitrate) pollutants in a natural river. The new models will be calibrated and applied to assess the nutrient pollutants concentrations along the uMgeni River. Thus, the outcome of this research will be useful to the decision makers on how to control and monitor the level of nutrient pollution in surface water and to thereby make the water safe for the use of aquatic animals and human consumption.

1.3. Research Questions

Is the HCIS model capable of simulating the concentration of ammonia, nitrite, and nitrate solute transport in a river?

How is the HCIS model, coupled with nutrient kinetics, useful to simulate ammonia, nitrite and nitrate concentrations along uMgeni River?

Is the output of the research valuable and significant in simulating nutrients pollutant in a river?

1.4. Aims and Objectives

The primary aim of the present study is to formulate a mathematical model for pollutant transport considering nutrient kinetics and to develop a user-friendly software package for nutrient simulation in natural rivers and streams. The objectives to achieve the aim of this research include several essential steps which are:

i) to review existing water quality models;
ii) formulation and development of HCIS model coupled with first-order kinetic reactions of Ammonia, Nitrite, and Nitrate nutrient;
iii) to compare the behaviours of the HCIS models with the numerical approach of Fickian based ADE model coupled with first-order kinetic reactions NH_3, NO_2, and NO_3;
iv) to develop a user-friendly software package using a C# programming language;
v) to test the proposed model with data collected from uMgeni River.

1.5. Outline of the Study

The thesis comprises of seven chapters, references, and appendices. Chapter one outlines the general introduction and background of the previous studies on the method of solving pollutant transport in surface water. The section highlighted the objectives of this research.

Chapter two presents the review of existing literature on water quality models. The water quality models in the study are described based on their development, intended use, model strength, application, and limitations.

The development of analytical solutions of the HCIS model coupled with the first-order reaction of ammonia through the hybrid unit is described in chapter three. In this chapter, a comparison of the analytical solution of the HCIS model is compared with the numerical solution of the ADE model.

Chapter four provides the analytical solution of the conceptual hybrid cells-in-series model component incorporating first-order kinetic reaction of nitrite along with advection and dispersion. The developed model is compared with the numerical solution of the advection-dispersion equation model. Also, the model will be used to evaluate the spatial and temporal variation of nitrite pollutant in a natural water body.

Chapter five deals with the mathematical formulation of the HCIS model considering the first-order kinetic reaction of nitrate. The simplified mathematical model is used to simulate the spatial and temporal variation of nitrate concentration in a river for hypothetical problems. Analytical solutions of the HCIS-NO_3 model are compared with the numerical solutions of the Fickian-based ADE model in this chapter.

Chapter six describes the application of the new model performance in simulating the nutrient concentration, i.e., ammonia, nitrite, and nitrate in the uMgeni River. The model calibration was done using the observation at one sampling site and validated with observed data at other sampling locations.

Chapter seven focuses on the relevant findings of this research, the general conclusions, and recommendations for future development. Finally, references and appendices are presented.

CHAPTER 2: LITERATURE REVIEW

2.1. Introduction

Streams are an essential area of the environment that serves as a source of water for human consumption and abode for aquatic animals. Industrialisation, urbanization and agricultural practices discharge an enormous quantity of organic and inorganic pollutants into the water bodies. These result in the scarcity of quality water for the proper functioning of the ecosystem (Yang *et al.,* 2013; Kumarasamy, 2015). The pollution of various water bodies is increasing due to the discharge of different sources of pollutants (Mazaheri *et al.,* 2015), which can be grouped into conservative and non-conservative by their nature. On account of these various pollutants entering the water bodies with an increase in concentration, it is essential to make the stream safe from any form of pollutants. The increase in the rate of nutrient pollutants' discharge into water bodies has resulted in a eutrophication process which results in the growth of algae and reduction of the dissolved oxygen (DO) (Yang *et al.,* 2008; Conley *et al*., 2009). Stream water deterioration has been one of the most serious environmental threats facing our environment. The decrease in the concentration of dissolved oxygen in the water column has resulted in major damage to the freshwater quality and reduction in the population of the aquatic animals in water bodies (Cox, 2003; Seibel, 2011). Streams act as a carrier of discharged pollutants and disperse within the water bodies due to the combined effects of diffusion and the advection process (Jaiswal *et al*., 2011). Adequate assessment of dissolved oxygen and nutrients in the stream is essential for preserving the ecosystem's integrity and regulating the pollutants disposed of in the streams. Thus, it is essential to monitor and keep appropriate nutrient levels sufficient for the survival of sea animals and humans.

Sharma and Kansal (2013), demonstrated that the development of water quality models is essential for predicting pollutants in surface water. Water quality models (WQM) are decision support tools for simulating the fate of contaminants in the water columns and assessing their associated risks (Chapra, 2008; Wang *et al*., 2013). Estimation of pollutants through monitoring is a difficult task that requires a continuous update of existing models and development of new WQM for accurate measurement of solute transport in the water bodies. Streeter and Phelps did the first significant research on water quality modeling in 1925 for simulating BOD and DO in the river system (Cox, 2003; Chapra, 2008; Gotovtsev, 2014). WQM can be classified as a simulation model and optimization model (Chapra, 2008; Sharma and Kansal, 2013). The simulation model describes all

models which represent changes in water quality in some mathematical form. It includes all types of mechanistic models which are deterministic. Besides, optimization models are generally used to find the least number of alternative data before carrying out a simulation model. The magnitude and quality of input data available determine the complexity of the model in simulating water quality parameters. However, it is best to implement simple models in simulating solute transport in different water bodies before complex models, because they are more complicated. The fundamental principle governing model formulation is the law of conservation of mass, momentum, and conservation of energy (Chapra, 2008)**.** Therefore, to develop a water quality model, there are different formulations which must be followed, and each formulation depends on the different types of parameters to be modelled. Advection, dispersion, and molecular diffusion are the primary processes that cause changes in pollutant concentration along the water bodies (Jirka and Weitbrecht, 2005; Chapra, 2008; Wang *et al.,* 2012). Pollutant decay and kinetic reactions can be incorporated in the water quality models to give a clear understanding of the pollutants' impact and ecosystem response.

2.2. Existing Water Quality Models

The rapid development in computer technology and mathematics techniques has brought improvement to water quality management, which has ensued in the expansion of different modeling tools. In determining which models are the most useful, it is necessary to evaluate the existing WQM. Various water quality models are widely used, which all have their advantages and limitations. The study reviewed seven major water quality models: AQUATOX, QUAL2E, WASP, CEUALRIV1, MIKE11, SWAT, and SIMCAT, which are currently available for different water bodies and are mostly mechanistic models. Also, the review describes their capabilities and applications to different water bodies. The study will help to select a suitable model for different water quality problems. Furthermore, the limitations associated with the existing WQM have prompted the advancement of new models to simulate pollutant transport under various environmental conditions.

2.2.1. AQUATOX

The model was developed by USEPA to predict the fate of different contaminants and their effects on the aquatic environment (Park *et al*., 2008; Sharma and Kansal, 2013). It is a mechanistic environmental model with the aim of predicting ecological stressors and their effects on the ecosystem. It simulates various water quality parameters which include nutrients, sediment, and toxic

chemicals. Also, their impacts on the aquatic animals and plants are reproduced by the model (Park and Clough, 2004; Bingli *et al*., 2008). Sharma and Kansal (2013) stated that the model integrates its algorithms from the clean model which is used for the biological aquatic ecosystem model. In addition, it simulates close to twenty parameters within the aquatic habitat simultaneously which makes the model one of the best WQM. Moreover, the public can access the model freely online and can be combined with some watershed models which make it better than some water quality models.

2.2.1.1. Model System

The AQUATOX model is quite sophisticated and a suitable WQM to predict various pollutants in a well-mixed ecosystem. The model is designed as a mechanistic model with spatial and temporal resolutions to determine the fate of contaminants in an aquatic habitat (Sharma and Kansal, 2013). It assumes the river to be comprised of different well-mixed segments with each time step and uses average flow data for its operation. Moreover, the model equation was solved using the principle of fourth and fifth order Runge-Kutta integration techniques. The fifth-order differential equation solution was used to correct the error observed with the fourth-order solution. Consequently, the model can be used to understand the impact of various water quality parameters on aquatic habitats.

2.2.1.2. Model Application

AQUATOX can be used to identify the different environmental stressors that are causing ecological impairment and predict the impact of pollutants on the ecosystem. The model has been used to simulate the effect of various environmental stressors such as nutrients, sediments, organic waste, toxic substance, temperature, periphyton, phytoplankton, and macrophytes in the water bodies. It has been applied to numerous water bodies by different researchers to predict the effect of pollutants on aquatic habitats. Blancher (2010) used the model for predicting the effect of eutrophication within the Braden River reservoir, Bradenton Florida, and a high concentration of nutrients in the water body affects the quality of the river. According to Shu *et al*. (2012), the model was used to predict the concentration of nutrients in Lake Nansi, China. It was discovered that the quality of Lake Nansi has a moderate eutrophication condition. It was also used to simulate some nutrient parameters in Vimtim stream, Nigeria (Anyadike *et al*., 2013). Their results indicate that the predicted values have a definite trend with the observed values. Akkoyunlu and Karaaslan (2015) used the model to simulate nutrient and sediment concentration in Morgan Lake, Turkey, and it was discovered that the source of nutrient

pollutants in the lake were linked to pesticides and sediments. Additionally, the lake has been exposed to intensive organic pollution. From the study, the Aquatox model is a valuable tool for decision-makers in the management of river quality. It could be used to simulate pollutants in different water columns which include ponds, rivers, streams and, vertically stratified lakes (Shoemaker *et al*., 2005).

2.2.1.3. Model limitation

The model cannot model metals and cannot be linked with hydrodynamic models. Also, the internal nutrient is not represented in algae bioenergetics. Moreover, it assumes a unit volume of water when simulating the change in nutrients, chemical and sediment concentrations in the water body.

2.2.2. QUAL2E

QUAL2E is a steady state model for predicting contaminants in stretching rivers and well-mixed lakes (Brown and Barnwell, 1987), and was developed by the United States Environmental Insurance Agency (USEPA) (Cox, 2003). It assumes the river to be a one-dimensional model which predicts the significant responses of nutrient cycles, sediment, algae formation, environmental damages and their effects on the concentration of DO in the water body (Birgand, 2004). It is used to predict the spatial and temporal variations of some parameters such as temperature, nutrients, BOD and DO concentrations within the water column (Kannel *et al.,* 2011). Furthermore, it can be used to know the effect of different sources of pollutants discharged into water bodies and how it affects the water quality parameters. Moreover, the impact of algae growth and death rate on dissolved oxygen in the water system can be predicted using the model.

2.2.2.1. Model system

The numerical scheme which describes the model is a one-dimensional advection-dispersion equation which was solved by a mass balance method. The water body to be simulated will be discretized into different reaches and assumed to have the same length. However, the geometric properties and pollutants kinetics may change between the reaches. The reaches will be chosen based on either there is a massive change in pressure within the water system and parameters to be simulated in the water body. The separation of every reach will be controlled by utilizing a GPS alongside topographic maps. The differential equation of the QUAL2E model is presented below and numerically solved with the

implicit finite difference method. Besides, an empirical approach was used to estimate the longitudinal dispersion coefficient of the river.

$$\frac{\partial C}{\partial t} = \frac{\partial\left(A_x D_L \frac{\partial c}{\partial x}\right)}{A_x \partial x} - \frac{\partial\left(A_x UC\right)}{A_x \partial x} + \frac{dC}{dt} + \Delta S \tag{2.1}$$

where, C = concentration (mg/l); x = distance (m); t = time (s); Ax = Area of the river reach (m^2); D_L = dispersion coefficient (m^2/s); u = Average flow velocity (m/s); S = the sink or source of pollutants (mg/l).

The QUAL2E model simulates the real components and constituents that relate to the dissolved oxygen concentration. The significant sinks or source included in the equation are biochemical oxygen demand, algae reactions, and nutrient reactions. Also, QUAL2E can show the reaeration that happens when water is spilling over dams.

2.2.2.2. Model applications

The QUAL2E model is developed to simulate different water quality parameters such as dissolved oxygen, nutrients and, conservative pollutants in water bodies (Cox, 2003). A few applications of QUAL2E models can be found in Ning *et al.* (2001), where the model was used to predict the concentrations of BOD and DO along the Kao-Ping River Basin, Taiwan. Park and Lee (2002) used the model to simulate the nutrient concentration of the Nakdong River, Korea, and from their results the model represents the field data very well. Also, it was applied to the Yangtze River to simulate some water quality parameters, and it was discovered that the predicted values agreed well with the measured data (Zhang *et al*., 2006). Purandara *et al*. (2012) applied the model to assess the effect of point and non-point source pollution of the Ghataprabha River, Karnataka, India, where the result indicated that the quality of water within the river is highly acceptable. It was observed that an increase in river flow leads to a reduction in dissolved oxygen.

2.2.2.3. Model limitation

A QUAL2E model cannot be applied to a river that experiences temporal variation in its flow. It models organic nitrogen, ammonia, nitrates, and nitrites but neglects macrophytes, suspended sediment movement, and denitrification processes. It cannot model variable flow conditions due to its steady-state assumption. The QUAL2E model has certain dimensional limitations which are imposed during programme development which include: the reaches should not be more than 25, the computational element should not be more than 20 per reach or a total of 250. Furthermore, the headwater and junction elements should have a maximum value of seven.

2.2.3. WASP

The model was developed by the United States Environmental Protection Agency to simulate pollutants transport in water bodies (Connolly and Winfield, 1984; Yang *et al*., 2007). The model can be applied in one, two or three-dimensional flows. It could be used to predict various parameters which include conservative and non-conservative pollutants within the water column (Wool *et al*., 2006). WASP is a dynamic model programme, which follows a box modeling approach and can be used in solving different flow conditions along the aquatic habitat (Ambrose *et al*., 1993). It consists of seven versions ranging from WASP to WASP7 which has two sub-models used to simulate eutrophication and toxic processes within the water system. The model can be applied to different water bodies which include rivers, streams, lakes, and ponds.

2.2.3.1. Model system

The WASP water quality model consists of DYNHYD and WASP stand-alone computer programmes that could be used independently or combined with each other. The flow of water across the reach within the river system is simulated using the DYNHYD, which is a hydrodynamics programme. Moreover, to simulate the pollutants transport within the water column the WASP programme will be applied. There are two sub-programmes within the model system which are EUTRO and TOXI, respectively. The EUTRO model enables modeling of the conventional pollution which is related to water eutrophication, while the TOXI model is used to simulate toxic pollutants in waterways. The model uses conservation of mass and mass balance equations to solve the model equation. The model requires some input data to solve the mass balance equation. The input data includes, initial and

boundary concentrations, the source of pollutants, kinetic parameter coefficients, the flow characteristics and geometry of the river is also vital in solving the mass balance equation. The model's mass balance equation is described below:

$$\frac{\partial(AC)}{\partial t} = \frac{\partial}{\partial x}\left(-U_x AC + E_x A\frac{\partial C}{\partial x}\right) + A(S_l + S_b) + AS_k \quad (2.2)$$

Where, C is the Concentration of the pollutant (mg/l); A is the river area (m^2); U_x is the advective velocity (m/s); E_x is longitudinal dispersion coefficients (m^2/s); S_b is the boundary loading rate (g/m^3-s), and S_K is the total kinetic transformation rate (g/m^3- s).

2.2.3.2. Model application

This model can simulate some water quality parameters which include: temperature, nitrogen, phosphorus, BOD, coliform bacteria, silica, DO, conservative pollutants, and synthetic organic compounds. The model was successfully used to estimate the level of DO concentration in the Altamaha River estuary, Georgia (Kaufman, 2011). The WASP model was applied by Ernst and Owens (2009) to a vast Texas reservoir to simulate and predict eutrophication content of the lake. Lai *et al*. (2013) used the model to determine the effect of NPS and ammonia pollutants on the Kaoping River Basin, Taiwan, and it was observed that a high flow rate during rainy season caused a high discharge of NPS into its upper section.

2.2.3.3. Model limitations

The complexity of the model requires extensive training for its user to use the model for decision making effectively. The calibration of the model and applying it to simulate some water quality parameters need a long time for its user. Furthermore, the model cannot simulate periphyton and microalgae.

2.2.4. CE-QUAL-RIV1

The water quality model is a one-dimensional hydrodynamic model developed by the U.S. Army Engineers Waterways Experiment Station (WES) released in 1991 for simulating water quality parameters associated with streams, rivers, and estuaries (Dortch *et al*., 1990; Martin *et al*., 2002;

Sharma and Kansal, 2013). A new version of the model was developed in the year 1995. The model simulates highly unsteady flow conditions of a river system because most models in existence were developed for steady flow conditions (Martin *et al*., 2002). CE-QUAL-RIV1 consists of two codes which include a water quality programme code (RIV1Q) and a hydrodynamic programme code (RIV1H) (Ziemińska-Stolarska and Skrzypski, 2010). The RIV1H code is first applied to the water column to calculate the river hydraulics using the geometric properties of the river and boundary conditions. The RIV1Q code will use the output from RIV1H for its water quality simulation. The RIV1H code uses the four-points implicit solution method of the St. Venant equation to estimate the flow rates, depths, velocities, and widths of the river. Fortran 77 programme language code was used for the model and is available for MS-DOS-based microcomputers.

2.2.4.1. Model system

The model equation is solved using St. Venant equations which comprise of continuity and momentum equations. Fourth-order explicit scheme and implicit scheme were used to solve the ADE equation. More parameters have been added to the governing equation which includes floodplains and cross-section storage flows. The equation presented below describes the equation governing the water quality model.

The continuity equation;

$$\frac{\partial A}{\partial t} + \frac{\partial Q}{\partial t} = q \tag{2.3}$$

The momentum equation;

$$\frac{\partial Q}{\partial t} + U\frac{\partial Q}{\partial x} + gA\frac{\partial h}{\partial x} = gA\left(S_o - S_f - \frac{h_e}{\Delta x}\right) + qU_q \tag{2.4}$$

The one-dimensional advection and dispersion equation coupled with the sink and source are shown below;

$$\frac{\partial \alpha}{\partial t} + U\frac{\partial \alpha}{\partial x} = D\frac{\partial^2 \alpha}{\delta x^2} + \frac{q}{A}(K - a) - K_s\alpha + \sin ks \tag{2.5}$$

Where, Q = flow rate, (m^3/s); U = Average velocity, (m/s); A = area of the channel, (m^2); h = depth, (m) g is the gravitational acceleration; S_o and S_f are the bottom and friction slope respectively; x = length (m); t = time; α = parameters; q is the lateral flow rate (m^3/s); D = dispersion coefficient (m^2/s).

The equations were solved numerically because it has a nonlinear, hyperbolic, and partial differential function. The water quality module, RIV1Q, uses a fourth-order, explicit, finite difference scheme developed by Holly Jr and Preissmann (1977) to solve the fundamental mass balance equation. The data required in the water quality model includes the river geometry, initial flow condition of the water system and inflow water quality concentrations and meteorological data.

2.2.4.2. Model application

CE-QUAL-RIV1 can be applied to simulate the chemical, biological, and physical processes in rivers. It can be used to predict the response of lakes and estuaries to pollutant loading. It could be used to predict a branched stream with numerous hydraulic structures like dams, and estimate the hydraulic and geometric properties of the water body. Furthermore, it can be used to simulate some water quality parameters which include the thermal stratification, growth of algae and macrophytes.

2.2.4.3. Model limitation

The model cannot be used to simulate sediment transport processes within the river system. The one-dimensional assumption of the model is also the limitation of the model. It contains limited eutrophication kinetics in its operation and requires extensive training by its user for them to use the model effectively.

2.2.5. MIKE-11

The model is a deterministic computer programme that simulates unsteady flow in a water system, which was developed by the Danish Hydraulic Institute, Netherlands. It is used to calculate flow and water level in the river system. Also, it can be used as a hydrodynamic model to simulate tidal sections of a water system, and it could be used as a water quality model (Tsakiris and Alexakis, 2012).

The model can simulate more complex water quality problems such as DO, BOD, sediments exchange reactions, the balance of nitrate and ammonium without denitrification, and coliform bacteria (Tsakiris and Alexakis, 2012).

2.2.5.1. Model system

The hydrodynamic model depends on the formulation of the Saint Venant equations which was solved by implicit finite difference method. It can be applied to one and two-dimensional unsteady flow in water columns. The model can use kinematic, diffusive dynamic, vertically integrated mass and momentum equations for its simulation. The hydrodynamic module is solved using the continuity and momentum equation to determine the water level and the rate of flow. The other modules of the model depend on the hydrodynamic module to perform their functions. Iterations method was applied to solve the mathematical equations, by using the result of the first iteration to solve the second-time step. The following assumptions were used to solve the Saint Venant equations which were; water is incompressible and homogeneous, the wavelengths are large compared with the water depth, the bottom slope is small, and the flow is subcritical. The advection-dispersion equation was solved coupled with the pollutants' first order decays, and a dynamic solution is provided. The model uses the following equations:

The continuity equation;

$$\frac{\partial A}{\partial t} + \frac{\partial Q}{\partial t} = q \tag{2.6}$$

The momentum equation;

$$\frac{\partial Q}{\partial t} + \frac{\partial\left(\alpha \frac{Q^2}{A}\right)}{\partial x} + gA\frac{\partial h}{\partial x} + \frac{gQ}{C^2 AR} = 0 \tag{2.7}$$

Where, Q is the flow rate (m^3/s), α is the momentum coefficient, h is the height (m), q is the lateral inflow (m^2/s), C is the chezy coefficient ($m1/^2/s$), R is the hydraulic radius (m), and A is the area of channel (m^2).

2.2.5.2. Model application

The model has been extensively applied by different researchers to study water parameters of various water bodies. It is an ecological model which can simulate BOD, DO, ammonia, nitrate, and heavy metals. Kazmi and Hansen (1997) applied the model for the evaluation of the water quality conditions and effect of wastewater discharged on the Yamuna River, Northern India. The results showed that the quality of the river is significantly affected by a high eutrophication level released into the river system. MIKE11 was used to simulate DO and BOD in the River Dender in Belgium (Radwan *et al*., 2003). It was also used to investigate the dissolved oxygen level and some water quality parameters in the River Buriganga (Kamal *et al*., 1999). It uses geographical information systems to import and export water quality data.

2.2.5.3. Model limitation

The model can simulate complex water quality scenarios at first-order decay and other factors such as temperature but does not consider denitrification process in its development. The model is difficult to set up without the help of an expert. During the operation of the model, there is a requirement for a lot of information/data which makes it difficult to simulate some parameters if the information is lacking.

2.2.6. SWAT

It is a hydrological and river basin scale model for water resource management which was developed by USDA Agricultural-based Research Service (USDA-ARS) (Neitsch *et al*., 2002; Tolson and Shoemaker, 2007). The model is used to measure the influence of land management practices in a watershed and is free to access by the public (Gassman *et al.*, 2007; Neitsch *et al*., 2011). It can simulate groundwater flow, nutrients, water transportation from channel and reservoirs. Also, it can be used to estimate the impact of nutrients, chemical and sediment adsorption on watershed management.

2.2.6.1. Model system

The model requires accurate information for its operation which includes topography, weather, vegetation, soil properties, and type of water body. It uses daily time step for its operation and performs its simulation by dividing the watershed into a large number of compartments. The compartments are connected in series and further divided into Hydrologic Response Units (HRU). The simulation of water and pollutants from each Hydrologic Response Unit are routed through the stream network to the watershed exit. It can be used to solve various management problems of substantial river basin costs efficiently and also used to study particular processes of pollutants transport.

2.2.6.2. Model application

The model has been broadly utilised by researchers and applied extensively in various applications worldwide. Abbaspour *et al*. (2009) described the impact of future climate in Iran on its water assets using the model, and it was discovered that the wet region of the country would have more precipitation than the dry area. The model was also applied to the Cannonsville reservoir, New York, to calibrate and validate the prediction of flow, nutrients and sediment transport in the area. The model adequately predicted the monthly phosphorus and sediment loading in the reservoir (Tolson and Shoemaker, 2004). This model has been applied to determine the concentration of pesticide at a designated location. SWAT has been used to predict the influence of rural and agricultural management practices on aquatic habitats.

2.2.6.3. Model limitation

The SWAT model uses a relatively simple equation for sediment routing because it does not consider significant sediment transport process such as bottom shear stress in its formulation (Benaman *et al*., 2001). The model uses a daily time step for its operation, however, if a more flexible time increment is used it would be a significant development in the model. It does not accurately evaluate the extreme daily flow occurrence and simulation of runoff yield.

2.2.7. SIMCAT

Simulation catchment (SIMCAT) is one of the available models for simulating water quality parameters such as dissolved oxygen along water bodies. The model is a deterministic model used to predict river quality parameters and flow dynamics along the water column (Cox, 2003). The model was developed by Anglian Water (Warn, 1987) in the United Kingdom, and it has been applied to predict conservative and non-conservative pollutants in the river. It is a stochastic model which utilizes the Monte Carlo simulation approach for its operation and can be used to assess the influence of pollutant discharges on a water body (Warn, 2007).

2.2.7.1. Model system

The model uses the concept of mass balance for its operation and represents the river reaches as continually stirred tank reactors in series (CSTRS) with a steady flow condition. The model can simulate pollutants in fresh water which do not rely on sediment interactions. The flow velocity is obtained from the velocity flow relationship, and it is used to calculate the residence time for each reach. It assumes that pollutant is well mixed throughout each reach of the river (Cox, 2003). The equation presented below describes the mass balance for a reach of the river system:

$$C_o = \frac{C_i Q_i + C_t Q_t + C_e Q_e}{Q_r + Q_t + Q_e} \tag{2.8}$$

Where, Q = flow, (m^3/s); C = pollutant concentration, (mg/l); o = outflow; i = upstream input; t = tributary input; e = effluent discharged, and a = abstractions.

$$v = aQ^b \tag{2.9}$$

$$t = \frac{L}{v} \tag{2.10}$$

Where, v = flow velocity (m/s), Q = flow rate (m^3/s), a, b are constants, t is the residence time (s) and L = length of the reach (m).The solute concentration is first-order decay which will be used to calculate the level of pollutants entering the next reach of the river.

2.2.7.2. Model application

The model requires limited data for its application and is applied at a catchment scale. Jacobs (2007) used the model to the River Dee, Wales to evaluate the potential of water quality influences on the proposed road drainage around the river and its tributaries. Also, the model was used to calculate the pollution level of the area for both the annual average and ninety-five percentile concentration levels for each of the designed drains in the area. It was also used by Crabtree *et al*. (2010) to monitor water quality of the River Ribble catchment, UK by identifying the source of pollution either PS or NPS and predict their impacts on the river quality. The model has been described as an excellent water quality management tool.

2.2.7.3. Model limitation

The model is a simple and flexible model that does not simulate some parameters related to dissolve oxygen concentration. Also, its application to simulation of respiration, photosynthesis, sediment oxygen demand, and reaeration rate is limited in its process.

2.3. General Discussion

In the changing environmental situation, the water quality models are significant in describing the ecological state of different water bodies. It predicts the change in the receiving water when certain boundary or initial conditions are altered. Such changes may be due to morphological modifications to the water body, variations in the source of pollutants and location of pollutant loading into the system and changing trends in climate conditions. Thus, the degree of complexity in describing the ecological state varies in different water quality modeling tools. To choose the type of WQM to be used for various water bodies, it is necessary to investigate the kind of pollutant problem affecting the water system; besides, the cause of the water pollution should be determined to identify the best management solutions. Seven currently available WQM were evaluated for their capabilities and application to different water bodies. The relevant criteria in choosing a water quality model were the easy accessibility of the programme code source and the existence of proper documentation on the model. Evaluation tables were developed to provide more detailed information on the capabilities of each model as presented in Table 2.1. Based on the above criteria as observed from the table it could be seen that CE-QUAL-RIV1 and MIKE II are not readily accessible because they require some cost

in acquiring them while others are user-friendly and easily accessible by the public at a free price via the internet. The level of complexity in the receiving water was evaluated by categorizing AQUATOX, QUAL2E, CEQUALRIV1, SWAT and SIMCAT as a one-dimensional model, where SIMCAT is an over-simplistic model and not useful when simulating photosynthesis, respiration, and sediment oxygen demand. In the application of the models to different water bodies, AQUATOX, WASP, MIKE II, and SWAT could be used; however, each model should be calibrated and validated for a good result and conclusion. Furthermore, in comparing AQUATOX to other WQMs, the prediction of the model appears to be an accurately reflected currently accepted ecological process and behaviour. All the models have been tested for simulating nutrients in different water bodies. However, MIKEII and QUAL2E do not consider denitrification process during its operation. Also, QUAL2E and SIMCAT do not model variable flow conditions because the flow rate is assumed to be a steady state.

The choice of the type of model, suitable for nutrient simulation in receiving water will be subjected to availability of data, model complexity, nature of water body, and the water quality simulation capabilities as presented in Table 2.1. All models reviewed apart from SWAT have the capability of simulating in-stream fate and transport of a wide variety of pollutants. However, the SWAT model can be linked with an in-stream model to give a better result and prediction. The complexity of water quality issues globally should open ways on how to combine different WQMs to simulate some water quality parameters in water bodies, which could solve the problem associated with a single model. A WQM should be flexible and allow for further future improvements and updates based on newly conducted studies and water quality parameters. Critical review of these model shows that most of these models are Fickian based. It is understood from the literatures (Fischer et al., 1979; Chatwin and Allen, 1985; Rutherford, 1994; Ghosh 2001; Ghosh et al 2004; 2008; Kumarasamy et al 2011) that the ADE model has limitations for natural rivers. The HCIS model (Ghosh 2001; Ghosh et al 2004; 2008) has been developed as an alternative model. The previous studies (Ghosh 2001; Ghosh et al 2004; 2008; Kumarasamy 2007; Kumarasamy et al 2011; 2013; Kumarasamy 2015) demonstrated the flexibility of the mixing cells based HCIS model for number of water quality parameters. The water quality model should be chosen according to the basis of the available data to support the model processes. Thus this study focuses on developing three new model components of the HCIS model for simulating nutients concentrations along river reaches.

Table 2.1: Comparison of water quality models

Model	AQUATOX	QUAL2E	WASP	CEQUALRIV1	MIKE II	SWAT	SIMCAT
Model type/Level of complexity	1-D, Dynamic state	1-D, Steady state/Dynamic	1,2,3- D, Dynamic	1-D/ Dynamic	2-D, Steady state, Dynamic	1-D, Quasi - Dynamic	1-D, Steady state
Receiving Water Type	River, Lake, Reservoir	River	River, Lake, Reservoir, Estuary	River	River, Reservoir	River, Lake, Reservoir	River
Modeling approach	Differential equations using 4^{th} and 5^{th} order, Runge-Kutta integration routines	The advection-dispersion-reaction equations, equal river reaches	The advection-dispersion-reaction equations	Continuity equation, Momentum equation, and Constituent fate and transport equation	Implicit finite difference Scheme to solve Saint Venant equation	Mass balance Equation	CSTRS
Model capabilities	DO, CBOD, NH_3, NO_3, OP, PO_4, Temperature, Sediment	DO, BOD, NH_3, NO_3, NO_2, OP, PO_4, Temperature, Coliform Bacteria	DO, CBOD, NH_3, NO_3, NO_2, OP, PO_4, Temperature, Sediment, Metals, Toxics	DO, BOD, NH_3, NO_3, NO_2, OP, PO_4, Temperature, Bacteria, Metals	DO, BOD, temperature, NO_3, NH_3, sediments, coliform bacteria	DO, BOD, NH_3, NO_3, NO_2, OP, PO_4, Temperature, sediment, Toxics, Metal	DO, CBOD, NH_3, PO_4
Special water quality features	Algae, phytoplankton, Periphyton, Planktonic, Benthic algae, Fish	Algae, phytoplankton, Periphyton, Planktonic, Benthic algae	Algae, phytoplankton, Periphyton, Planktonic, pesticides	NIL	phytoplankton, Periphyton, Planktonic, Benthic algae	Surface and groundwater interaction	NIL
Application Considerations	Limited Training/ Public Domain	Limited Training/ Public Domain	Substantial training/ Public Domain	Substantial training/ Limited Distribution	Substantial training/ Significant Cost	Moderate training/ Public Domain	Limited Training/ Public Domain

2.4. Summary

Globally, prediction of changes in pollutant concentration for environmental management and decision making has been made through the development of surface water quality models. This chapter described some of the more frequently used water quality models and their applications to different water bodies. The review has addressed aspects of water quality problems which include; water quality parameters, sediment transport, and hydrodynamics. It also provides the model type which is categorized as steady state, quasi-dynamic and dynamic models. The level of complexity of the model in receiving water such as one, two, three-dimensions, and the governing equation was discussed. It is essential to identify the project goal when developing a water quality modeling tool through discussions with stakeholders, regulating agencies and technical personnel involved in the development. Simulation of water quality parameters in water bodies provides water management guidelines for water sustenance. Also, to choose the best model for the water body, it is vital that the user selects a water quality modeling tool subjected to the modeling objectives and available resources. A list of questions about the water column to be modeled should be adequately addressed with suitable selection criteria. The selected model must be able to simulate different water quality parameters within the water body. Moreover, the user must understand the assumptions used by the model and ensure these assumptions reflect the appearance of the water system to be simulated. There are always uncertainties associated with different models, and these must be figured out to find alternative solution. Water quality models should be flexible and allow for further improvements in the future, and updates based on new studies and water quality parameters. In general, it is best to choose the simplest model that satisfies the project goals. Thus this study demonstrates the further development of the HCIS model and its capability to simulate nutrients pollutant concentrations along river reaches.

CHAPTER 3: A MATHEMATICAL MODEL DEVELOPMENT FOR SIMULATING AMMONIA POLLUTANT TRANSPORT ALONG A RIVER

3.1. Overview

The chapter focuses on developing an analytical solution for the pollutant transport of the ammonia concentration through the plug flow, the first and second well-mixed cells of the HCIS model. The HCIS model coupled with the first order kinetic equation for ammonia nutrient is developed to simulate the ammonia pollutant concentration in the water column. The first order kinetic equations for ammonia includes the effects of the transformation of ammonia to nitrite, the uptake of ammonia by the algae, the respiration rate of the algae and the input of benthic source to the ammonia concentration in the water column. The proposed model is tested using hypothetical data, and the results are compared with the numerical solution of the Fickian-based advection-dispersion equation (ADE) model coupled with a first-order kinetic equation for ammonia nutrient.

3.2. Introduction

The majority of world's population mostly depend on streams and rivers for domestic and industrial usage. Streams are an essential part of the ecosystem, which provides shelter for aquatic organisms, and that needs to be protected from all sources of pollution. The discharge of organic waste into streams and rivers has resulted in an increase in water pollution with a deteriorating effect on the aquatic habitat. Research has shown that the rise in urban and industrial activities has mainly contributed to the water pollution and ecosystem degradation (Alam, 2007; Anyadike *et al*., 2013; Wadi *et al.*, 2014; Liangliang and Daoliang, 2015). The stream water quality is affected by both point and non-point source pollution (Gao *et al*., 2015), that have resulted in significant water quality problems such as eutrophication (María Elena Pérez *et al.*, 2013; Yang *et al.,* 2008). The eutrophication in waterbodies supports the excessive growth of phytoplankton and other photosynthetic plants that results in the depletion of dissolved oxygen (DO) levels within the water body (Kuo *et al.,* 2006; Conley *et al.*, 2009; Rabalais *et al.*, 2009; Seibel, 2011). The level of DO concentration in waterways is a fundamental measure of water quality used to assess the level of pollution of rivers and streams. Polluted streams have a profoundly destructive impact on the ecosystems because of a critical drop in DO concentration levels, which hurts the aquatic animals in water columns (Cox, 2003; Seibel, 2011; Rakib, 2015). The decreased DO levels in the water bodies leads to significant impairment in water quality and increases the mortality rate of the aquatic habitat (Kannel *et al.,* 2011). Ammonia nutrients, which is one of the principal sources of nutrients in the water, is essential

for aquatic plant growth (Aliverdi *et al*., 2014; Zhu et *al.,* 2015). However, a high content of ammonia nutrients results in a significant increase of algae, which affects water quality and diminishes the oxygen level required for aquatic animals to survive (Kamer *et al.,* 2004). Consequently, this results in serious environmental and health issues.

Presently, there has been an increment in pollutant loading in rivers and streams, which calls for the continuous development and improvement of current water quality models. It is essential to know the rate at which the streams are capable of dispersing or transporting the pollutants they receive by using a useful evaluation tool for water quality management. Hence, the study of pollutant transport in different water bodies is essential to correctly evaluate the fate and threat of nutrient pollution in rivers and streams. Due to the high concentration of ammonia pollutants entering the water bodies, there is a need to make the water safe and clean for human consumption and use by aquatic animals. Therefore, the development of water quality models (WQM) is essential to predict the fate of a pollutant in the water bodies for the better management of surface water (Chapra, 2008; Sharma and Kansal, 2013; Wang *et al*., 2013; Parsaie and Haghiabi, 2015). Besides, it is a vital tool for maintaining appropriate water nutrient standards for human consumption, aquatic organisms' survival, water sustainability and water quantity for future use (Cosgrove and Rijsberman, 2000; Rahaman and Varis, 2005).

The use of mathematical techniques to develop a water quality model for predicting water pollution status is one of the objectives of water pollution studies. It represents a physical mechanism that decides the position and momentum of pollutants in water bodies, which is utilized for analyzing and predicting the fate and transport of contaminants in water systems. Different scholars like Thomann and Mueller (1987); Gotovtsev (2010); Genuchten *et al.* (2013); Wadi *et al*. (2014); Shao-Chen *et al.* (2014); Parsaie and Haghiabi (2015) and Szomorová and Halaj (2015); have used mathematical concepts to study pollutant transport in different water bodies. Their approaches assume that pollutants discharged in water columns decay according to first order reaction and they demonstrate the use of mathematical models for water quality assessment in water bodies. Also, numerous researchers have studied the fate of ammonia pollutant transport and its effects on the aquatic environment. Tufford and McKellar (1999) use the Wasp 5 modeling system to simulate the ammonia nutrient in Lake Marion. Rode *et al.* (2008) also focus on nutrient management in surface water by using the SWAT model to simulate the nitrogen transport in the Weibe Elster River. Schütze *et al*. (2011) use the SWQM model to assess urban discharges into receiving water and describe the process of ammonia pollutant loading in the river. Jha and Gu (2010) use QUAL2E

to evaluate the allowable contaminant loads under both the seasonal and non-seasonal discharge control programme in the Des Moines River. Ani *et al*. (2010) use the ADE models to simulate the ammonia pollutant transport of different types of waste discharged in the River Swale, England. Lin and Webster (2012) developed a model to simulate nutrient uptake in the Snake River, Wyoming, USA. The model was used to assess the sensitivity of the pulse nutrition addition (PNA) to the water columns. Most models are based on an advection-dispersion equation (ADE) model. However, the ADE model has a limitation in simulating the observed behaviour of natural river adequately due to constraints in the assumption used for the model derivation and difficulties in its parameter estimations (Fischer *et al.,* 1979; Ghosh *et al.,* 2004; Neuman and Tartakovsky, 2009; Kumarasamy *et al.,* 2013). Alternatively, other models namely the Cell-in-Series (CIS) model (Banks, 1974; Bear, 1972) and the Aggregated Dead Zone (ADZ) model (Beer and Young, 1983) were developed. Ghosh *et al.* (2008); Kumarasamy, (2015) describe the difficulty in estimating the first arrival time of pollutants downstream as the limitation of the CIS model. Furthermore, the CIS model considers each cell to be thoroughly mixed as it does not predict the advection component effectively but simulates the dispersion component. Additionally, ADZ has difficulty in estimating the model coefficients (Kumarasamy, 2015).

Ghosh (2001) developed the hybrid cells in series (HCIS) model for advection-dispersion pollutant transport and addressed the limitations of ADE, CIS, and ADZ models. Ghosh *et al*. (2008); Kumarasamy *et al*. (2013), and Kumarasamy (2015) highlight some of the advantages of the HCIS model over ADE and CIS models which includes, conversion of the second order partial differential equation of the ADE model to first order ordinary differential equation which makes it simple to solve analytically, even for additional water quality parameters. The HCIS model consists of a plug flow component that simulates the advection component of solute transport which overcomes the difficulty associated with the CIS model. Kumarasamy *et al*. (2011), Kumarasamy *et al.* (2013), and Kumarasamy (2015) use the HCIS model to simulate the dissolved oxygen concentration, decay process and pollutant sorption process in rivers. The HCIS model is therefore considered as an alternative model for solute transport studies in natural streams and consequently a motive for this present study to develop a model component coupled with a first-order kinetic equation of ammonia along with advection and dispersion processes for simulating the spatial and temporal variations of ammonia pollutant concentration in natural rivers and streams. The proposed model was applied to assess the ammonia nutrient status of the uMgeni River.

3.3. The Model Development

The research aims to develop a model component for the HCIS model to study the fate and transport of the ammonia pollutants' concentration at various points along a river reach. The sources of ammonia concentration in the model are from agricultural leaching, industrial effluent, respiration of algae and benthic release of ammonia nutrients. Besides, nitrification and the uptake of ammonia for growth by algae are considered as the sink of the ammonia in the river system. The water quality mass balance equation was formulated for the ammonia concentration in the component of the HCIS model under steady-state conditions. The following differential equation describes the first order kinetic equation of ammonia concentration (Brown and Barnwell, 1987):

$$\frac{\partial C_a(x,t)}{\partial t} = -k_a C_a(x,t) + \left[(\rho) - (F\mu)\right]\alpha A_g(t) + \frac{\delta_3}{d} \tag{3.1}$$

where x is the distance along the river (m), t is time (Sec), C_a is the concentration of ammonia (mg/l), k_a is the ammonia oxidation rate coefficient (day^{-1}) which is temperature dependent, F is the fraction of algal nitrogen uptake from the ammonia pool, $A_g(t)$ is the algal biomass concentration (mg/l), μ is the algal growth rate coefficient (day^{-1}), δ_3 is the Benthic release of ammonia nitrogen (mg- N/m^2 – day), d is the mean stream depth (m),α is the nitrogen fraction of algae biomass and ρ is the algae respiration rate coefficient ($day^{-1)}$ which increases the ammonia nutrient in the water column. The first term on the right side in Eq. (3.1) describes the nitrification, which causes ammonia to be transferred to nitrite. The second term represents the input of ammonia nutrient due to algae respiration and the algae uptake of the ammonia nutrient. The third term describes the input due to the benthic release of ammonia nutrient. The rate of change of algae biomass can be written as the difference between the growth rate of algae and their respiration. The differential equation that defines the rate of change of algae biomass is formulated according to (Brown and Barnwell 1987) which is described by the following equation:

$$\frac{\partial A_g(t)}{\partial t} = (\mu - \rho) A_g(t) \tag{3.2}$$

The algal growth is the one process to be considered when modelling nutrients. In this model chlorophyll A (CHL-a), which is a green pigment in the water systems, is used to estimate the mass of algae within the water column. It also measures the level of phytoplankton activity within the river (Gregor and Maršálek, 2004). The increment in algae concentration is stated by utilising the growth rate (μ) which is a function of nutrient, light and temperature and is formulated according to Liebig's law (Brown and Barnwell, 1987):

$$\mu = \mu_{\max} \theta_{\max} (FL)(FN) \tag{3.3}$$

Where, $\mu_{\max}$ is the maximum algae growth rate (day^{-1}) which is dependent on temperature, FL and FN are the limitations due to light intensity and nitrogen availability, respectively. The death of algae occurs primarily through respiration whose rate (day^{-1}) varies from 0.01 to 0.05 (Benedini and Tsakiris, 2013). It is temperature dependent and is the opposite process of photosynthesis. F is the fraction of algae nutrient from the ammonia pool, which is expressed as:

$$F = \frac{P_n C_a(t)}{P_n C_a(t) - (1 - P_n) C_c(t)} \tag{3.4}$$

The development of the model began by considering a river reach, which is conceptually made up of a series of hybrid components. Each element is presumed to be made of a plug flow and two well-mixed cells with different residence times, connected in series as shown in Figure 3.1. The boundary concentration of ammonia pollutant at time t = 0 varies from zero to C_R. The replacement of the plume in the plug flow cell takes place over a period (T_1) which can be expressed as the ratio of the volume of the plug flow cell to the flow rate. The ammonia pollutant losses a fraction of its concentration due to the decay during downstream transport because of the nitrification of ammonia to nitrate and ammonia uptake by algae. The residence time of the first mixed cell is (T_2), and the fluid is well-mixed before entering the second well-mixed cell, which has a residence time (T_3). A plug flow cell is conceptualized to have a series of compartments of length (Δx), in which the ammonia pollutant is transported downstream through those compartments and undergoes first order reactions. The contaminant injected in the system, which is also known as a plume, will remain in the compartment for a time interval (Δt) before it moves to the next compartment, and is then replaced by the incoming plume. There will be no mixing of pollutants in the former and the subsequent chambers because the replacement of the plume in the entire compartment will occur concurrently. In the plug flow cell, the effect of dispersion when compared with advection is assumed insignificant, but in the two well-mixed cells, advection-dispersion occurs. To predict the concentration of ammonia pollutant in the river reaches, the water system is assumed to consist of a series of hybrid cells.

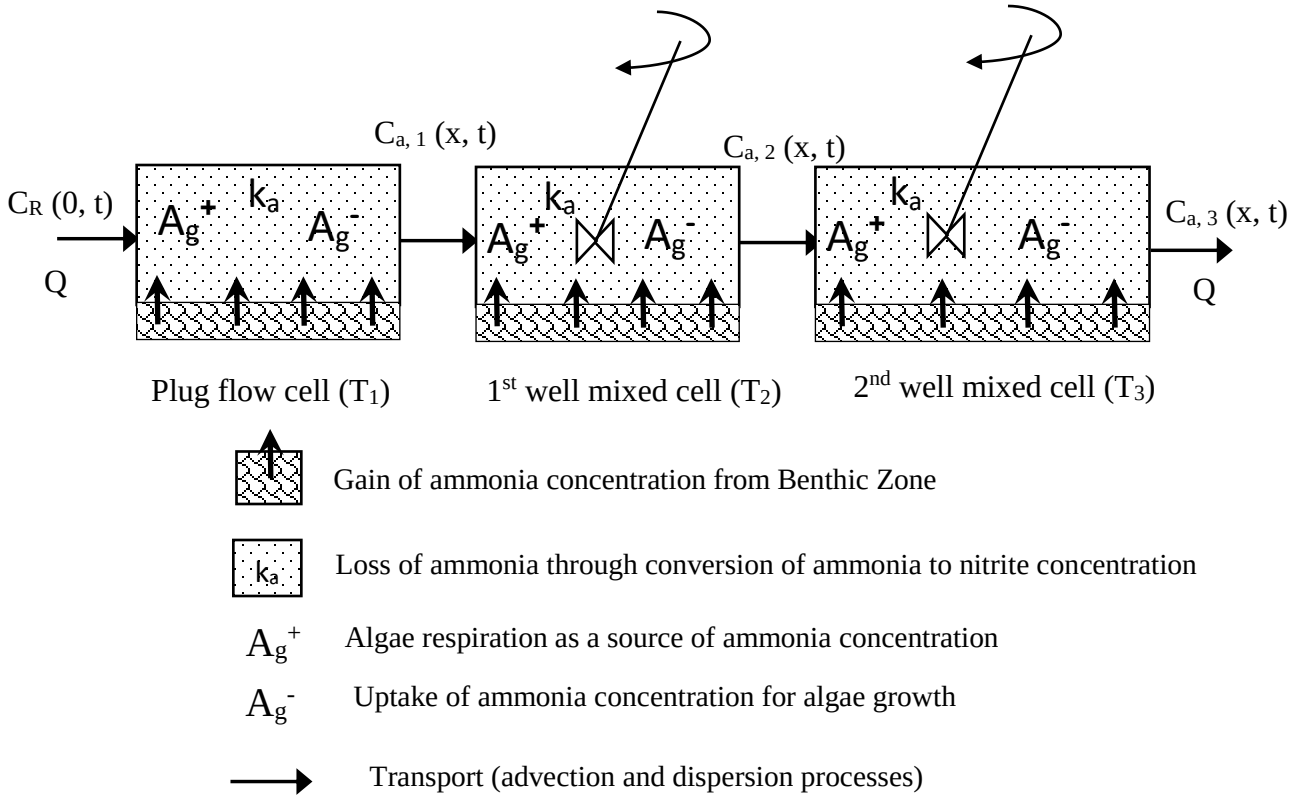

Figure 3.1: The process of ammonia pollutant concentration through a hybrid unit

3.3.1. Formulation of ammonia concentration in the plug flow cell

A control volume (V) was considered as presented in Figure 3.2 which consists of a water column through which a non-conservative ammonia pollutant is transported downstream within the plug flow cell. The ammonia pollutant solute in the plug flow cell undergoes a pure translation without any change in its concentration. The concentration of ammonia contaminant in the water column is designated as C_a (x, t). A fraction of the ammonia pollutant concentration is lost due to the nitrification of ammonia to nitrite and the consumption by algae at minor intervals (Δt). Also, the respiration of algae and the benthic rate of ammonia nutrients contribute to the source of ammonia in the water bodies. The remaining pollutant moves forward to the next control volume. The increment in algae biomass consumes the dissolved oxygen from the water system. A second order partial differential equation was formulated for a mass balance for the ammonia pollutant concentration in a steady-state flow condition. At the effluent of the plug flow cell, the level of the ammonia pollutant is determined. The rates of change of the concentration of ammonia contaminants with position x and time t are expressed as:

$$\frac{\partial C_a(x,t)}{\partial t}+\frac{u\partial C_a(x,t)}{\partial x}=-k_a C_a(x,t)+\left[(\rho)-(F\mu)\right]\alpha A_g(t)+\frac{\delta_3}{d} \tag{3.5}$$

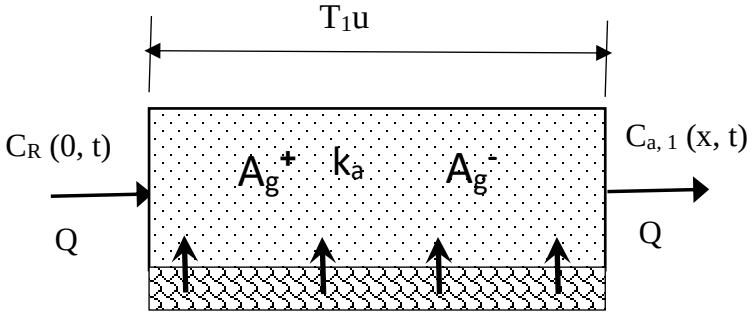

Figure 3.2: The process of concentration of ammonia pollutant though a plug flow cell

Eq. (3.5) is solved with the initial and boundary conditions such as $C_a(x,0) = 0$ for $x>0$; $C_a(0, t) = C_R$ for $t\geq 0$; $C_a(T_1u, t)=0$ for $0<t<T_1$.

The algae biomass equation in Eq. (3.2) has a solution shown below.

$$A_g(t)=A_o e^{(\mu-\rho)t} \tag{3.6}$$

The above equation can be modified to express $A_g(x, t)$ for a constant initial (A_0) at a distance of x to a control volume within the plug flow cell.

$$A_g(x,t)=A_o e^{(\mu-\rho)\left(t-\frac{x}{u}\right)} \tag{3.7}$$

Taking Laplace transform of each term in Eq. (3.5) and rearranging

$$\frac{\partial C_a^*}{\partial x}=\frac{-(s+k_a)C_a^*}{u}+\frac{\left[(\rho)-(F\mu)\right]\alpha A_o e^{-(\mu-\rho)\frac{x}{u}}}{(s-\mu+\rho)u}+\frac{\delta_3}{du} \tag{3.8}$$

Solving Eq. (3.8)

$$C_{a,1}^*=\left[\begin{array}{l}\left\{\left[\frac{\rho\alpha A_o}{[s-(\mu-\rho)]}-\frac{F\mu\alpha A_o}{[s-(\mu-\rho)]}\right]\left(\frac{e^{(\rho-\mu)\frac{x}{u}}}{[s+k_a+\rho-\mu]}\right)\right\}+\left\{\frac{\delta_3}{d(s+k_a)}\right\} \\ +\left\{\frac{C_R}{S}e^{\frac{-(s+k_a)x}{u}}\right\}-\left\{\left[\frac{\rho\alpha A_o}{[s-(\mu-\rho)]}-\frac{F\mu\alpha A_o}{[s-(\mu-\rho)]}\right]\left(\frac{1}{[s+k_a+\rho-\mu]}\right)e^{\frac{-(s+k_a)x}{u}}\right\}-\left\{\frac{\delta_3}{d(s+k_a)}e^{\frac{-(s+k_a)x}{u}}\right\}\end{array}\right] \tag{3.9}$$

The concentration of ammonia pollutant at the end of plug flow cell is obtained as below by solving Eq. (3.9) using inverse Laplace transform and is valid for $t \geq T_1$.

$$C_{a,1}(T_1u,t) = C_R U(t-T_1)e^{-k_aT_1} - \left[\frac{\rho\alpha A_o - F\alpha\mu A_o}{ka} U(t-T_1)e^{-k_aT_1} - 1\right]\left(e^{-(\rho-\mu)(t-T_1)}\right) - \frac{\delta_3 e^{-k_a t}}{d.k_a}\left[\left(U(t-T_1)-1\right)\right] \quad (3.10)$$

where U (t-T_1) is the step function.

3.3.2. Formulation of ammonia concentration in the first thoroughly mixed cell

Pollutants enter the first well-mixed cell from the plug flow cell after traveling a distance (T_1u) as shown in Figure 3.3. The first well-mixed cell is assumed to have a filling time (T_2) that is equal to the fraction of the volume (V_2) of the well-mixed cell to the flow rate (Q). In this cell, the decay of ammonia pollutant takes place, which allows a fraction of the ammonia concentration to be lost due to the nitrification of ammonia to nitrite and due to the consumption by algae. Also, the respiration of algae and the benthic release of ammonia nutrients contribute to the source of ammonia concentration in the water body. The mass balance of ammonia pollutant concentration in the first well-mixed cell has been formulated as follows:

$$C_{a,1}uA\Delta t - C_{a,2}uA\Delta t - k_aV_2C_{a,2}\Delta t + \left[(\rho)-(F\mu)\right]\alpha A_g(t)V_2\Delta t + \frac{\delta_3}{d}V_2\Delta t = V_2\Delta C_{a,2} \quad (3.11)$$

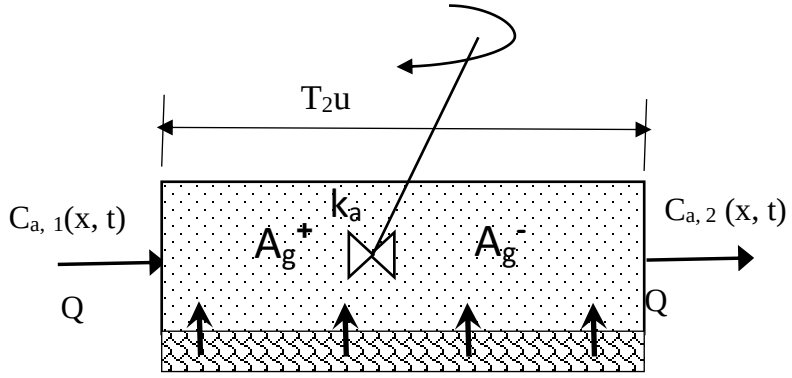

Figure 3.3: The process of concentration of ammonia pollutant though the first well – mixed cell

On the left-hand side, the first term represents the effluent mass from the plug flow cell. The second term is the mass leaving the cell, the third term is the nitrification of ammonia to nitrite. The fourth term represents the input of ammonia nutrient due to algae respiration and the algae uptake of ammonia nutrient. The fifth term describes the benthic release of ammonia nitrogen. The right-hand term describes

the change of mass within the cell. Eq. (3.11) is rewritten in differential form as expressed in Eq. (3.12) and solved which gives ammonia concentration at the end of first well-mixed cell in Eq. (3.13).

$$\frac{dC_{a,2}}{dt}+\frac{\left(1+k_aT_2\right)C_{a,2}}{T_2}=\frac{C_{a,1}}{T_2}+\left[\left(\rho\right)-\left(F\mu\right)\right]\alpha A_g\left(t\right)+\frac{\delta_3}{d} \tag{3.12}$$

$$\begin{aligned}
C_{a,2}=\Bigg[&\left\{\frac{C_RU\left(t-T_1\right)e^{-k_aT_1}}{1+k_aT_2}\right\}-\left\{\frac{\left(\rho\alpha A_o-F\mu\alpha A_o\right)U\left(t-T_1\right)e^{T_1(\rho-\mu-k_a)}e^{-(\rho-\mu)t}}{k_a\left(1+k_aT_2+\mu T_2-\rho T_2\right)}\right\}\\
&+\left\{\frac{\left(\rho\alpha A_o-F\mu\alpha A_o\right)e^{T_1(\rho-\mu)}e^{-(\rho-\mu)t}}{k_a\left(1+k_aT_2+\mu T_2-\rho T_2\right)}\right\}-\left\{\frac{\delta_3U\left(t-T_1\right)e^{-k_at}}{dk_a}\right\}+\left\{\frac{\delta_3e^{-k_at}}{dk_a}\right\}\\
&+\left\{\frac{\left[\left(\rho\right)-\left(F\mu\right)\right]\alpha A_oT_2e^{-(\rho-\mu)t}}{\left(1+k_aT_2+\mu T_2-\rho T_2\right)}\right\}+\left\{\frac{\delta_3T_2}{d\left(1+k_aT_2\right)}\right\}-\left\{\frac{C_RU\left(t-T_1\right)e^{T_1\left(\frac{1}{T_2}\right)}e^{\frac{-(1+k_aT_2)t}{T_2}}}{1+k_aT_2}\right\}\\
&+\left\{\frac{\left(\rho\alpha A_o-F\mu\alpha A_o\right)U\left(t-T_1\right)e^{T_1\left(\frac{1}{T_2}\right)}e^{\frac{-(1+k_aT_2)t}{T_2}}}{k_a\left(1+k_aT_2+\mu T_2-\rho T_2\right)}\right\}-\left\{\frac{\left(\rho\alpha A_o-F\mu\alpha A_o\right)e^{\frac{(1+k_aT_2)(T_1-t)}{T_2}}}{k_a\left(1+k_aT_2+\mu T_2-\rho T_2\right)}\right\}\\
&+\left\{\frac{\delta_3U\left(t-T_1\right)e^{T_1\left(\frac{1}{T_2}\right)}e^{\frac{-(1+k_aT_2)t}{T_2}}}{dk_a}\right\}-\left\{\frac{\delta_3e^{T_1\left(\frac{1}{T_2}\right)}e^{\frac{-(1+k_aT_2)t}{T_2}}}{dk_a}\right\}\\
&-\left\{\frac{\left[\left(\rho\right)-\left(F\mu\right)\right]\alpha A_oT_2e^{\frac{(1+k_aT_2+\mu T_2-\rho T_2)T_1}{T_2}}e^{\frac{-(1+k_aT_2)t}{T_2}}}{\left(1+k_aT_2+\mu T_2-\rho T_2\right)}\right\}-\left\{\frac{\delta_3T_2e^{\left(\frac{1+k_aT_2}{T_2}\right)(T_1-t)}}{d\left(1+k_aT_2\right)}\right\}\Bigg]
\end{aligned} \tag{3.13}$$

3.3.3. Formulation of ammonia concentration in the second thoroughly mixed cell

It is considered that the second mixed cell has a filling time of (T_3) as shown in Figure 3.4. The outflow from the first well-mixed cell is the inflow to the second well-mixed cell. The decay of ammonia pollutant and the addition of ammonia concentration take place in this cell as well. The mass balance in the second mixed cell is shown below:

$$C_{a,2}uA\Delta t-C_{a,3}uA\Delta t-k_aV_3C_{a,3}\Delta t+\left[\left(\rho\right)-\left(F\mu\right)\right]\alpha A_g\left(t\right)V_3\Delta t+\frac{\delta_3}{d}V_3\Delta t=V_3\Delta C_{a,3} \tag{3.14}$$

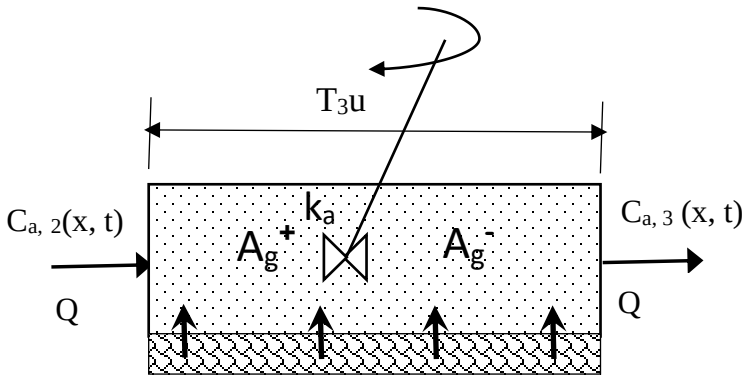

Figure 3.4: The process of concentration of ammonia pollutant though the second well – mixed cell

The first term on the left side is the mass entering the cell, the second is the mass leaving the cell, and the third term is the mass due to the death and respiration of algae. The last term on the left side is mass due to the benthic release of ammonia in the water column.

Eq. (3.14) is written in first order differential form as expressed in Eq. (3.15) and solved to determine the step response function for ammonia concentration at the end of the first hybrid unit

$$\frac{dC_{a,3}}{dt}+\frac{\left(1+k_aT_3\right)C_{a,3}}{T_3}=\frac{C_{a,2}}{T_3}+\left[\left(\rho\right)-\left(F\mu\right)\right]\alpha A_g\left(t\right)+\frac{\delta_3}{d} \tag{3.15}$$

Eq. (3.13) was substituted to Eq. (3.15) and solved with integration method to determine the step response function for ammonia concentration at the end of the first hybrid unit.

$$\begin{aligned}C_{a,3}=&\left[\frac{C_RU\left(t-T_1\right)e^{-k_aT_1}}{\left(1+k_aT_2\right)\left(1+k_aT_3\right)}\left\{1-e^{-\left(\frac{1+k_aT_3}{T_3}\right)\left(t-T_1\right)}\right\}\right]-\left[\frac{C_RU\left(t-T_1\right)e^{-\left(\frac{1+k_aT_3}{T_3}\right)\left(t-T_1\right)}T_2}{\left(T_2-T_3\right)}\left\{A\right\}\right]\\&-\left[\frac{\left(\rho\alpha A_0-F\alpha\mu A_0\right)U\left(t-T_1\right)}{k_a\left(1+k_aT_2+\mu T_2-\rho T_2\right)}\left\{B\right\}\right]+\left[\frac{\left(\rho\alpha A_0-F\alpha\mu A_0\right)}{\left(1+k_aT_2+\mu T_2-\rho T_2\right)}\left\{G\right\}\right]-\left[\frac{\delta_3U\left(t-T_1\right)e^{-k_at}}{d.k_a}\left\{D\right\}\right]\\&+\left[\frac{\delta_3e^{-k_at}}{d.k_a}\left\{D\right\}\right]+\left[\frac{\delta_3T_2}{d.\left(1+k_aT_2\right)}\left\{E\right\}\right]+\left[\frac{\delta_3T_3}{d.\left(1+k_aT_3\right)}\left\{1-e^{-\left(\frac{1+k_aT_3}{T_3}\right)\left(t-T_1\right)}\right\}\right]\end{aligned} \tag{3.16}$$

where,

$$A=\left\{\frac{e^{t\left(\frac{1}{T_3}-\frac{1}{T_2}\right)}e^{\left(\frac{T_1}{T_2}\right)}}{(1+k_aT_2)}-e^{\left(\frac{T_1}{T_3}\right)}\right\}$$

$$B=\left\{\frac{e^{-T_1(k_a-\rho+\mu)}e^{-t(\rho+\mu)}}{(1+k_aT_3+\mu T_3-\rho T_3)}-\frac{T_2e^{\left(\frac{T_1}{T_3}\right)}e^{-t\left(\frac{1+k_aT_3}{T_3}\right)}}{(T_2-T_3)}-\frac{e^{\left(\frac{T_1}{T_3}\right)}e^{-t\left(\frac{1+k_aT_3}{T_3}\right)}}{(1+k_aT_3+\mu T_3-\rho T_3)}-\frac{T_2e^{t\left(\frac{1}{T_3}-\frac{1}{T_2}\right)}e^{\left(\frac{T_1}{T_2}\right)}e^{-t\left(\frac{1+k_aT_3}{T_3}\right)}}{(T_2-T_3)}\right\}$$

$$G=\left\{\begin{array}{l}\frac{e^{-(\rho-\mu)(t-T_1)}}{k_a(1+k_aT_3+\mu T_3-\rho T_3)}-\frac{T_2e^{t\left(\frac{1}{T_3}-\frac{1}{T_2}\right)}e^{-t\left(\frac{1+k_aT_3}{T_3}\right)}e^{T_1\left(\frac{1+k_aT_2}{T_2}\right)}}{k_a(T_2-T_3)}-\frac{T_2e^{-T_1(\rho-\mu)}e^{-\left(\frac{1+k_aT_3}{T_3}\right)(t-T_1)}}{(1+k_aT_3)}+\frac{T_2e^{-t(\rho-\mu)}e^{-\left(\frac{1+k_aT_3}{T_3}\right)(t-T_1)}}{(1+k_aT_3+\mu T_3-\rho T_3)}\\ -\frac{e^{-\left(\frac{1+k_aT_3}{T_3}\right)(t-T_1)}}{k_a(1+k_aT_3+\mu T_3-\rho T_3)}+\frac{T_2e^{-\left(\frac{1+k_aT_3}{T_3}\right)(t-T_1)}}{k_a(T_2-T_3)}+\frac{T_2e^{-T_1(\rho-\mu)}e^{-\left(\frac{1+k_aT_3}{T_3}\right)(t-T_1)}}{(1+k_aT_3)}-\frac{T_2e^{-T_1(\rho-\mu)}e^{-\left(\frac{1+k_aT_3}{T_3}\right)(t-T_1)}}{(1+k_aT_3+\mu T_3-\rho T_3)}\end{array}\right\}$$

$$D=\left\{1-\frac{T_2e^{-\left(\frac{t-T_1}{T_2}\right)}}{(T_2-T_3)}-e^{\left(\frac{t-T_1}{T_3}\right)}+\frac{T_2e^{-\left(\frac{t-T_1}{T_2}\right)}}{(T_2-T_3)}\right\}$$

$$F=\left\{\frac{1}{(1+k_aT_3)}-\frac{e^{-k_a(t-T_1)}e^{-\left(\frac{t-T_1}{T_3}\right)}}{(T_2-T_3)}-\frac{e^{-\left(\frac{1+k_aT_3}{T_3}\right)(t-T_1)}}{(1+k_aT_3)}+\frac{T_2e^{-\left(\frac{1+k_aT_3}{T_3}\right)(t-T_1)}}{(T_2-T_3)}\right\}$$

Eq. (3.16) is used to predict the fate of the ammonia pollutants' transport due to the oxidation of ammonia to nitrite, the algae process and the benthic release of ammonia nitrogen. The unit pulse response function $\delta_{HCIS\text{-}NH3}(n,\Delta t)$ is obtained numerically by differentiating the unit step response functions with respect to 't' as shown below:

Eq. (3.17) is used to predict the fate of the ammonia pollutants' transport due to the oxidation of ammonia to nitrite, the algae process and the benthic release of ammonia nitrogen. The unit pulse response function $\delta_{HCIS\text{-}NH3}(n,\Delta t)$ is obtained numerically by differentiating the unit step response functions with respect to 't' as shown below:

$$\delta_{HCIS-NH_3}(n,\Delta t)=\frac{K_{HCIS-NH_3}(n\Delta t)-K_{HCIS-NH_3}\left((n-1)\Delta t\right)}{\Delta t} \tag{3.17}$$

Where, $K_{HCIS\text{-}NH3}$ is the step response of the first hybrid unit.

The Impulse response function for ammonia concentration at the end of the first hybrid unit is presented in Eq. (3.18) by differentiating Eq. (3.16) with respect to t,

$$\frac{dC_{a,3}}{dt}=\left(\begin{array}{l}\left[\frac{C_R U(t-T_1)e^{-k_aT_1}}{(1+k_aT_2)(1+k_aT_3)}\left\{1+\frac{(1+k_aT_3)e^{-\left(\frac{1+k_aT_3}{T_3}\right)(t-T_1)}}{T_3}\right\}\right]+\left[\frac{C_R U(t-T_1)(1+k_aT_3)e^{-\left(\frac{1+k_aT_3}{T_3}\right)(t-T_1)}}{T_3(T_2-T_3)}\{\Im\}\right]\\ -\left[\frac{(\rho\alpha A_o-F\alpha\mu A_o)U(t-T_1)}{k_a(1+k_aT_2+\mu T_2-\rho T_2)}\{\Re\}\right]+\left[\frac{(\rho\alpha A_o-F\alpha\mu A_o)}{(1+k_aT_2+\mu T_2-\rho T_2)}\{\mathrm{E}\}\right]+\left[\frac{\delta_3 U(t-T_1)e^{-k_at}}{d}\{\Pi\}\right]\\ -\left[\frac{\delta_3 e^{-k_at}}{d}\{\Pi\}\right]+\left[\frac{\delta_3 T_2}{d(1+k_aT_2)}\{\exists\}\right]+\left[\frac{\delta_3 T_3}{d(1+k_aT_3)}\left\{1+\frac{(1+k_aT_3)e^{-\left(\frac{1+k_aT_3}{T_3}\right)(t-T_1)}}{T_3}\right\}\right]\end{array}\right) \tag{3.18}$$

where, $$\Im=\left[\left\{\frac{(T_2-T_3)e^{t\left(\frac{1}{T_3}-\frac{1}{T_2}\right)}e^{\left(\frac{T_1}{T_2}\right)}}{(T_3T_2)(1+k_aT_2)}\right\}-\left\{e^{\left(\frac{T_1}{T_3}\right)}\right\}\right]$$

$$\Re=\left[\begin{array}{l}-\left\{\frac{(\rho+\mu)e^{-k_aT_1}e^{-(\rho+\mu)(t-T_1)}}{(1+k_aT_3+\mu T_3-\rho T_3)}\right\}+\left\{\frac{T_2e^{\left(\frac{T_1}{T_3}\right)}(1+k_aT_3)e^{-t\left(\frac{1+k_aT_3}{T_3}\right)}}{T_3(T_2-T_3)}\right\}\\ +\left\{\frac{e^{\left(\frac{T_1}{T_3}\right)}(1+k_aT_3)e^{-t\left(\frac{1+k_aT_3}{T_3}\right)}}{T_3(1+k_aT_3+\mu T_3-\rho T_3)}\right\}+\left\{\frac{T_2(1+k_aT_2)e^{\left(\frac{T_1}{T_2}\right)}e^{-t\left(\frac{1+k_aT_2}{T_2}\right)}}{T_2(T_2-T_3)}\right\}\end{array}\right]$$

$$E = \left[\begin{array}{l} -\left\{ \dfrac{(\rho-\mu)e^{-(\rho-\mu)(t-T_1)}}{k_a(1+k_aT_3+\mu T_3-\rho T_3)} \right\} + \left\{ \dfrac{T_2(1+k_aT_2)e^{-\left(\frac{1+k_aT_2}{T_2}\right)(t-T_1)}}{k_aT_2(T_2-T_3)} \right\} + \left\{ \dfrac{T_2(1+k_aT_3)e^{-\left(\frac{1+k_aT_3}{T_3}\right)(t-T_1)}}{T_3(T_2-T_3)} \right\} \\ -\left\{ \dfrac{T_2(1+k_aT_3+\rho T_3-\mu T_3)e^{(1+k_aT_3+\rho T_3-\mu T_3)t}e^{\left(\frac{1+k_aT_3}{T_3}\right)T_1}}{T_3(1+k_aT_3+\mu T_3-\rho T_3)} \right\} + \left\{ \dfrac{(1+k_aT_3)e^{-\left(\frac{1+k_aT_3}{T_3}\right)(t-T_1)}}{k_aT_3(1+k_aT_3+\mu T_3-\rho T_3)} \right\} \\ -\left\{ \dfrac{T_2(1+k_aT_3)e^{-\left(\frac{1+k_aT_3}{T_3}\right)(t-T_1)}}{k_aT_3(T_2-T_3)} \right\} - \left\{ \dfrac{T_2e^{-T_1(\rho-\mu)}(1+k_aT_3)e^{-\left(\frac{1+k_aT_3}{T_3}\right)(t-T_1)}}{T_3(1+k_aT_3)} \right\} + \left\{ \dfrac{T_2e^{-T_1(\rho-\mu)}(1+k_aT_3)e^{-\left(\frac{1+k_aT_3}{T_3}\right)(t-T_1)}}{T_3(1+k_aT_3+\mu T_3-\rho T_3)} \right\} \end{array} \right]$$

$$\prod = \left[1 + \left\{ \frac{e^{-\left(\frac{t-T_1}{T_2}\right)}}{(T_2-T_3)} \right\} - \left\{ \frac{e^{\left(\frac{t-T_1}{T_3}\right)}}{T_3} \right\} + \left\{ \frac{e^{-\left(\frac{t-T_1}{T_2}\right)}}{(T_2-T_3)} \right\} \right]$$

$$\exists = \left[\begin{array}{l} \left\{ \dfrac{1}{(1+k_aT_3)} \right\} + \left\{ \dfrac{(1+k_aT_3)e^{-\left(\frac{1+k_aT_3}{T_3}\right)(t-T_1)}}{T_3(T_2-T_3)} \right\} + \left\{ \dfrac{(1+k_aT_3)e^{-\left(\frac{1+k_aT_3}{T_3}\right)(t-T_1)}}{T_3(1+k_aT_3)} \right\} \\ -\left\{ \dfrac{T_2(1+k_aT_3)e^{-\left(\frac{1+k_aT_3}{T_3}\right)(t-T_1)}}{T_3(T_2-T_3)} \right\} \end{array} \right]$$

3.3.4. Estimation of Ammonia Pollutant Concentration using the Convolution Technique

The concentration of ammonia pollutant at any downstream location was determined using the convolution technique. The process was done by considering the river reach to be composed of a series of equal size hybrid units, where the effluent from the previous hybrid unit is the input to the subsequent hybrid unit as shown in Figure 3.5. Hence, the exchange of the ammonia pollutant concentration takes place in all the hybrid units. The response of the n^{th} hybrid unit when $n \geq 2$ as expressed by Kumarasamy *et al*. (2011).

$$C(i\Delta x, n\Delta t) = \sum_{\gamma=1}^{n} C\left[(i-1)\Delta x, \gamma\right] \delta_{HCIS-NH_3}\left[n-\gamma+1, \Delta t\right] \tag{3.19}$$

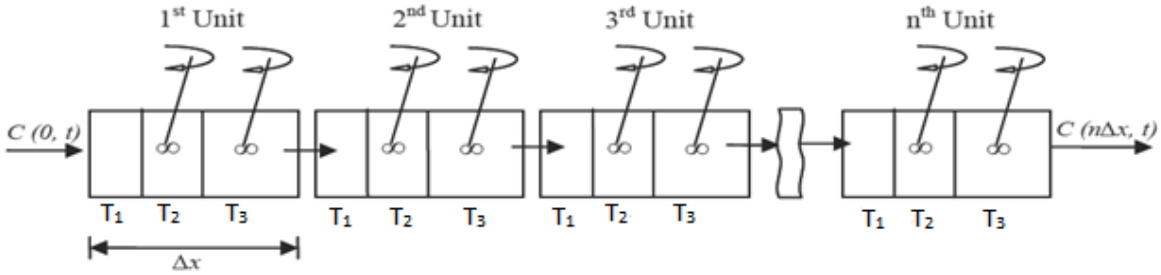

Figure 3.5: Series of hybrid units representing a river reach of nΔx length (Kumarasamy et al. 2013)

3.3.5. Model Parameters

The model parameters, T_1,T_2 and T_3 which are the residence times of pollutant in the hybrid unit of the proposed model can be determined (Ghosh, 2001; Ghosh et al., 2008). It has been estimated that the parameters satisfy the Peclet number ($P_e = \Delta x u / D_L \geq 4$). The model parameters depend on the dispersion coefficient and the size of the hybrid unit and which are calculated as:

$$T_1 = \frac{0.04\Delta x^2}{D_L} \quad , \tag{3.20}$$

$$T_2 = \frac{0.05\Delta x^2}{D_L} \tag{3.21}$$

$$T_3 = \frac{\Delta x}{u} - \frac{0.09\Delta x^2}{D_L} \tag{3.22}$$

3.4. Model Verification using a Numerical Approach

In showing the possibility of a clear trend in the concentration–time profile of the HCIS-NH_3 with the ADE-NH_3 model, it is essential to compare the results of HCIS-NH_3 with the ADE-NH_3 model. The partial differential equation describing the advection–dispersion equation for one–dimensional flow can be described as:

$$\frac{\partial C_a(x,t)}{\partial t} = -u\frac{\partial C_a(x,t)}{\partial x} + D_L\frac{\partial^2 C_a(x,t)}{\partial x^2} - k_a C_a(x,t) + \left[(\rho) - (F\mu)\right]\alpha A_g(t) + \frac{\delta_3}{d} \tag{3.23}$$

where, C_a is the concentration of ammonia pollutant (mg/l), k_a is the ammonia oxidation rate coefficient (day^{-1}); F is the fraction of algal nitrogen uptake from the ammonia pool; Ag(t) is the algal biomass concentration (mgA/l); μ is the algal growth rate coefficient (day^{-1}); and δ_3 is the benthic release of ammonia nitrogen (mg- N/m^2 – day); d is the mean stream depth (m); α is the nitrogen fraction of algal biomass; and ρ is the algae respiration rate coefficient (day^{-1}) which increases the ammonia nutrient in the water column. Furthermore, u is the flow velocity (m/min) and D_L is the longitudinal dispersion coefficient (m^2/min).

The ADE-NH_3 model equation was solved numerically using the explicit finite difference method, which satisfies the initial and boundary condition used for the HCIS-NH_3 model equation. The explicit finite difference scheme is used to estimate the approximate values of the unknown function at some grid points in the domain when the initial and boundary conditions are known. The explicit forward difference is used in determining the time derivative, and central difference approximations are utilized for the space derivatives as shown below.

$$\frac{\partial C_a(x,t)}{\partial t} = \frac{C_a(x,t+\Delta t) - C_a(x,t)}{\Delta t} \tag{3.24}$$

$$\frac{\partial C_a(x,t)}{\partial x} = \frac{C_a(x+\Delta x,t) - C_a(x-\Delta x,t)}{2\Delta x} \tag{3.25}$$

$$\frac{\partial^2 C_a(x,t)}{\partial x^2} = \frac{C_a(x+\Delta x,t) - 2C_a(x,t) + C_a(x-\Delta x,t)}{\Delta x^2} \tag{3.26}$$

Eq. (3.24 - 3.26) were substituted into Eq. (3.23) and solved to obtain the step response function as expressed below.

$$C_a(x,t+\Delta t) = \left\{ \begin{array}{l} C_a(x,t)\left[1 - \left(\frac{2D_L\Delta t}{(\Delta x)^2}\right) - k_a\Delta t\right] - C_a(x+\Delta x,t)\left[\left(\frac{u\Delta t}{2\Delta x}\right) - \left(\frac{D_L\Delta t}{(\Delta x)^2}\right)\right] \\ + C_a(x-\Delta x,t)\left[\left(\frac{u\Delta t}{2\Delta x}\right) + \left(\frac{D_L\Delta t}{(\Delta x)^2}\right)\right] + \left[\left[(\rho) - (F\mu)\right]\alpha A_o e^{(\mu-\rho)t} + \frac{\delta_3}{d}\right]\Delta t \end{array} \right\} \tag{3.27}$$

The stability of the numerical scheme depends on a small value of the Courant number which must be less than or equal to one. To reduce oscillation, it is necessary to choose a time step and grid space using the Courant formula. The time step and grid space are taken to be Δt = 1min and Δx =100m, respectively

in such a way that $(u\Delta t/\Delta x) \leq 1$. In addition, the values of the dispersion coefficient and flow velocity were chosen as 1000m^2/min and 20m/min respectively.

3.5. Results and Discussion

3.5.1. Simulation and testing of Ammonia transport with synthetic data

The proposed model was first verified by using synthetic data to study the responses of the HCIS-NH_3 model for a selected data set. Some approximate kinetic and chemical parameters were taken from the literature Brown and Barnwell (1987); Slaughter (2011) and their values are given in Table 3.1. The model parameters (T_1, T_2, and T_3) were determined by using the empirical equations for a given value of u and D_L which satisfies the Peclet number Pe $\geq$ 4 (Ghosh, 2001). Therefore, the values of T_1, T_2, and T_3 were 1.7min, 2.3min and 6.0min respectively with Δx = 200m, u and D_L to be 20m/min and 1000m^2/min respectively. The ammonia pollutant in the river at various points along the flow direction was simulated using the developed HCIS-NH_3 model by considering the effects of the transformation of ammonia to nitrite, the uptake of ammonia by algae and the respiration rate of algae. Furthermore, the impact of the benthic release of ammonia concentration was considered. The response of the unit step function at the end of the first hybrid unit as computed from Eq. (3.16) is presented in Figure 3.6. The figure shows the result of the ammonia concentration over time for different values of ammonia oxidation rate (ka) (0.001 and 0.005 per min) with all other parameters constant. It can be noted that the variation in the ammonia oxidation rate (ka) affects the rate of transport of the ammonia pollutants in the water body as it moves downstream. Also, the effluent from the lower value of ka reaches the boundary concentration faster than the higher value of ka. Figure 3.7 shows the response of the unit impulse function at the end of the first hybrid unit for the same set of parameters and k_a values. It can be seen from the figure that a reduction occurs in the peak concentration as there was an increase in the ammonia oxidation rate (k_a) in the water column. There was a decrease of 2.73 percent from the peak concentration when ka = 0.005 per min compared to when ka = 0.001 per min.

Table 3.1: The selected parameters used in the model simulation

Notation	Description	values	Units
K_a	Rate constant for the biological oxidation	0.001 & 0.005	min-^{1}
μ	Algal growth rate	0.005	min-^{1}
ρ	Algal respiration rate	0.0002	min-^{1}
δ_3	Benthos source rate for ammonia nitrogen	0.00004	mg-O_2/m^2-min-^{1}
α	Fraction of algal biomass that is Nitrogen	0.0004	mg-N/mgA
PN	Algal preference factor for ammonia	0.5	

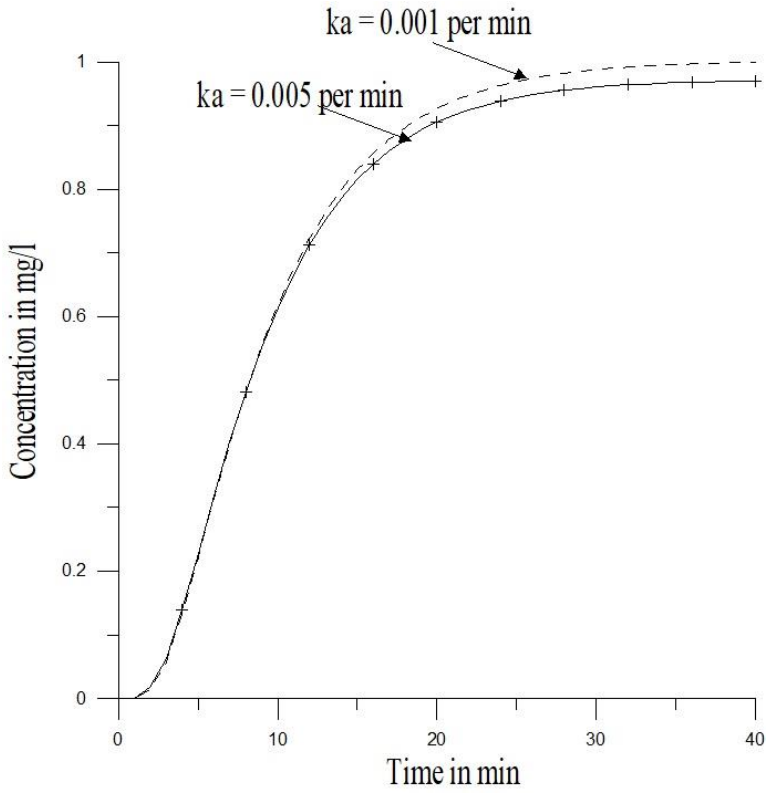

Figure 3.6: Unit step responses of the HCIS–NH_3 model, with decay rate coefficient, K_a = 0.001 per min and 0.005 per min at the end of first hybrid units for T_1 = 1.7 min, T_2 = 2.3 min, T_3= 6.0min, u = 20 m/min and Δx = 200 m

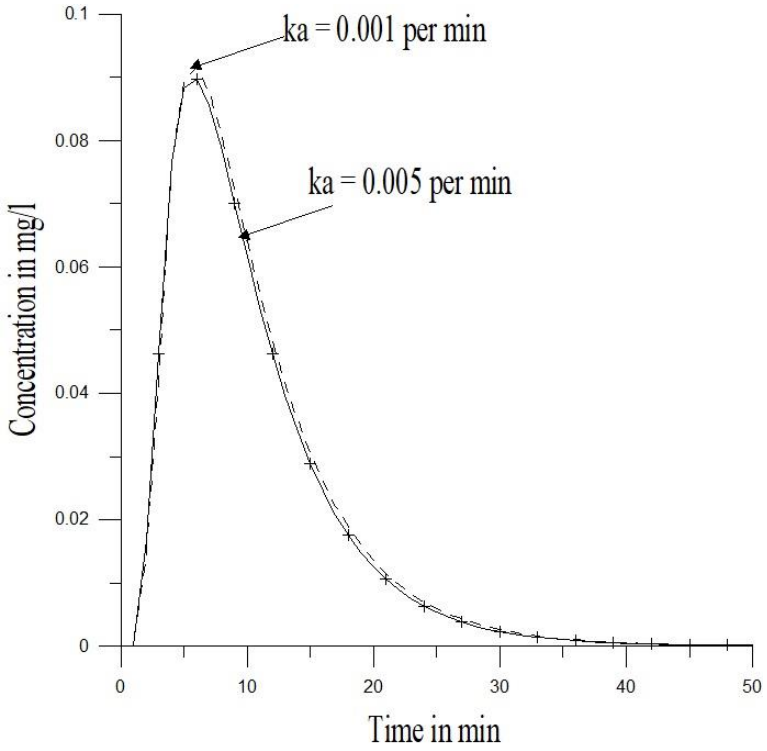

Figure 3.7: Unit impulse responses of the HCIS–NH_3 model, with decay rate coefficient, k_a = 0.001 per min and 0.005 per min at the end of first hybrid units for T_1 = 1.7 min, T_2 = 2.3 min, T_3= 6.0min, u = 20 m/min and Δx = 200 m

The unit impulse responses of the HCIS-NH_3 model at the end of 1st, 2nd, 4th and the 8th hybrid unit for different ammonia oxidation rates (0.001and 0.005per min) are simulated using Eq. (3.19) and are presented in Figure 3.8. It can be observed that there was a reduction in the peak concentration and the time to peak as the number of hybrid units increased. Furthermore, the ammonia pollutant concentration decreased as it moved downstream in the river system. The C-t distribution also showed a longer tail in the falling limb with an increase in the number of hybrid units. The proposed hybrid model can make a reasonable prediction of the peak concentration value and time to peak. The C-t profile approached a bell-shaped distribution as it moved downstream due to the high rate of spread out of the ammonia concentration in the water column.

Eq. (3.23) has been solved to obtain the step response for a downstream location. The impulse response of the ADE-NH_3 model was obtained by differentiating Eq. (3.27) with respect to time (t) numerically.

Having finite difference grid sizes Δt = 1min and Δx =100m, flow velocity and dispersion u=20m/s and D_L=1000m^2/s, numerical convolution has been adopted for simulating ammonia concentration along the river reach (at x=200m, 400m, 800m and 1200m) `as shown in Figure 3.9. The responses at the same locations (first hybrid unit: n=1, second: n=2, fourth: n=4 and sixth: n=6) were simulated using HCIS-NH_3 and shown in Figure 3.9. It is noted from Figure 3.9 that both models adequately reproduced the overall shape and the peak of the concentration-time profile. There was a slight difference in peak concentrations in the impulse response functions of the HCIS-NH_3 and the numerical solution of ADE because of the difference in space discretization in the hybrid model. It can be observed that HCIS is an adequate model to simulate ammonia concentration pollutants in the water column and is easy to solve analytically when compared to the Fickian-based ADE model.

The unit step response and impulse response functions of the HCIS-NH_3 model have been simulated with synthetic data using an analytical solution obtained from the hybrid models. It was observed that the response of the model with its parameters (T_1, T_2, and T_3) for a step and instantaneous input is nearly identical to the response generated by the ADE-NH_3 model which has two parameters (u, DL) when the peclet number (Pe = Δxu / DL) is greater or equal to 4. The inclusion of kinetics reaction of ammonia with an advection-dispersion process reduced the peak concentration and elongated the falling limb of the C-t profile. The first hybrid unit in Figure 3.8 slightly predicted the peak concentration, but at the remaining hybrid units, it captured it very well. Moreover, it was noted that a right-skewed C-t distribution was observed in the first hybrid, which tends to a normal distribution as the number of hybrid units increased. Thus, these characteristics of the C-t profiles for a stream with a kinetics reaction of ammonia component give an acceptable and expected result. Furthermore, it could be observed that the influence of a high nitrification rate, which constitutes as one of the essential sinks of ammonia in the river, leads to a decrease in concentration of ammonia pollutant as it moves downstream. Consequently, the concentration of ammonia pollutants decreased along the course of the river as it transformed into nitrite in the presence of dissolved oxygen. Furthermore, increases in algae concentration in the river will also reduce the ammonia concentration in the water body. The performance assessment between the HCIS-NH_3 and the ADE-NH_3 models was tested using quantitative statistical methods based on the coefficient of determination (R^2), root mean square error (RMSE), Nash-Sutcliffe efficiency coefficient (NSE) and RMSE observations standard deviation ratio (RSR). The C-t profile presented in Figure 3.9 was used for the statistical analysis, and it could be observed from Table 3.2 that RMSE and RSR were closer to zero and had minimal value. Also, the NSE and R^2 were higher than 0.5 and close to unity. Therefore, the

results of the statistical analysis indicate a good correlation between both models. Hence, the HCIS model could be used for predicting pollutant transport in a water body.

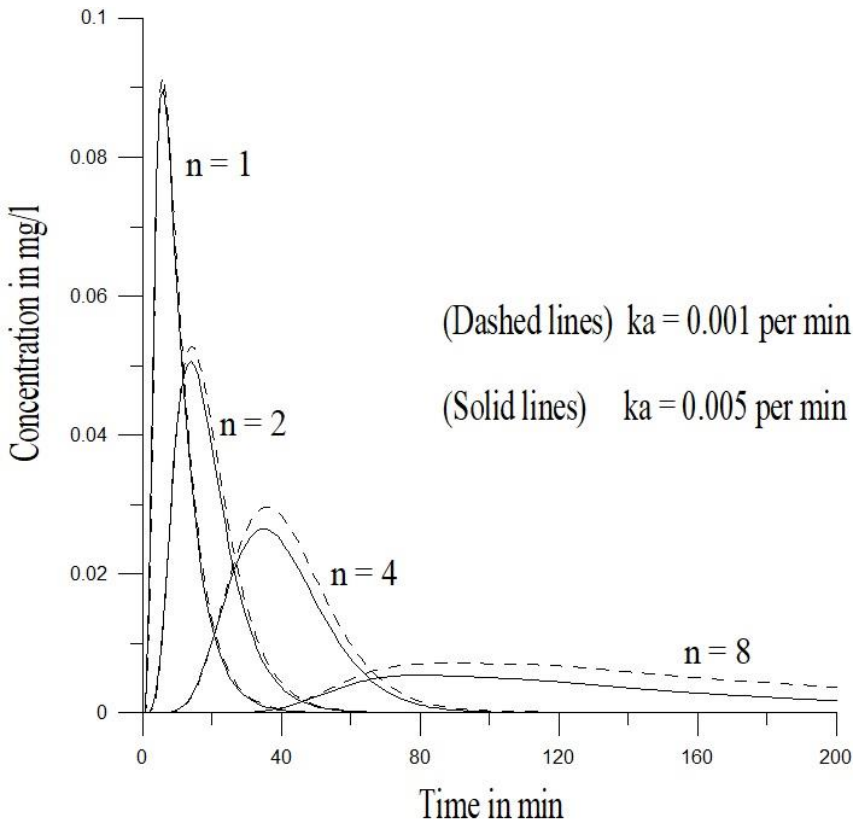

Figure 3.8: Unit impulse responses of the HCIS–NH_3 model, with decay rate coefficient, k_a = 0.001 per min and 0.005 per min, at the end of first at the end of first (n = 1), second (n = 2), fourth (n = 4) and eighth (n = 8) hybrid units T_1 = 1.7 min, T_2 = 2.3 min, T_3= 6.0min, u = 20 m/min and Δx = 200 m

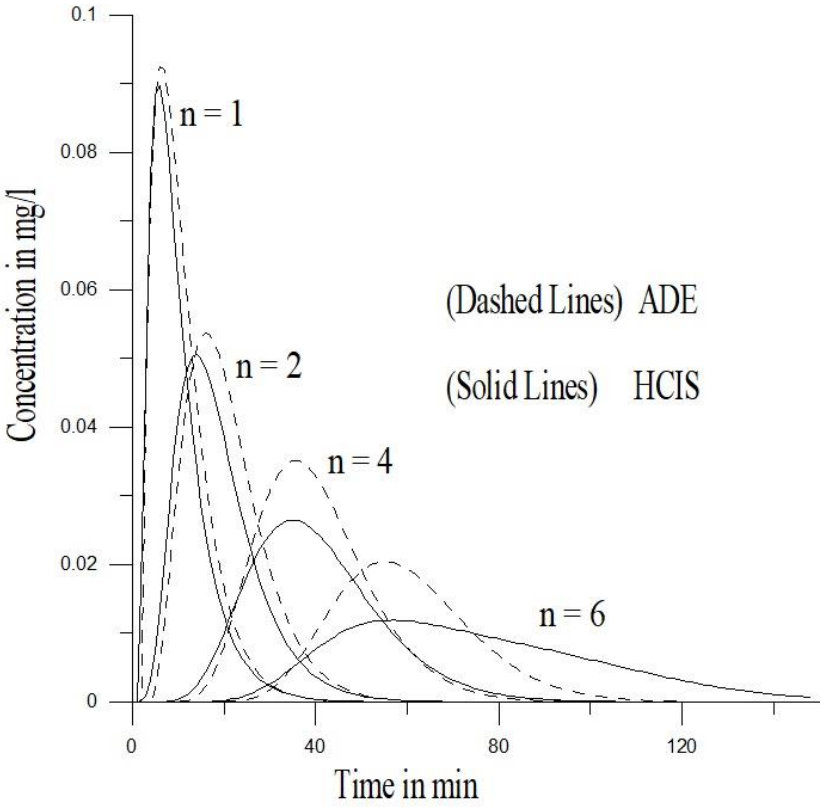

Figure 3.9: Unit pulse responses of ADE model (u = 20 m/min; D_L = 1000 m^2/min and at 200, 400, 800 and 1200m) and HCIS-NH_3 model at the end of first (n = 1), second (n = 2), fourth (n = 4) and sixth (n = 6) hybrid units T_1 = 1.7 min, T_2 = 2.3 min, T_3= 6.0min, Δ x = 200 m, with decay rate coefficient k_a = 0.005 per min

Table 3.2: Correlation between ADE-NH_3 and HCIS – NH_3 models

Unit	R^2	RMSE	NSE	RSR
First	0.984	0.0023	0.975	0.0062
Second	0.955	0.0027	0.950	0.0091
Fourth	0.987	0.0021	0.941	0.0084
Sixth	0.767	0.0031	0.722	0.0231

3.6. Summary

In this chapter, a component of the HCIS model was developed by coupling a first-order kinetic equation of ammonia concentration with advection and dispersion of pollutant transport processes The HCIS model, which consists of a plug flow cell and two unequal well-mixed cells all connected in series, was used to simulate the temporal and spatial variations of a non-conservative ammonia pollutant concentration in a river system. An analytical solution was developed for the pollutant transport of the ammonia concentration through the plug flow, the first and second well-mixed cells of the HCIS model. A C# programming language code was used to compute the analytical solution. The measured flow velocity and estimated longitudinal dispersion coefficient were used to determine the model parameters which are the residence times of the hybrid unit. However, the HCIS model parameters could be determined from observed concentration profiles at any river using the optimization method. Furthermore, other kinetic rate parameters could be estimated from the laboratory experiments. The HCIS-NH_3 model results were compared to the numerical solution of ADE-NH_3, and it showed that they followed the same trend and were in good agreement with the ADE model's C-t profile. Consequently, the model has demonstrated its capability of simulating ammonia nutrient pollution in rivers during non-monsoon periods and thus is a suitable tool for decision making relating to water quality problem. Therefore, the simplicity in solving the HCIS model and its application to a natural stream makes advantageous over other existing water quality models.

CHAPTER 4: A MATHEMATICAL MODEL DEVELOPMENT FOR SIMULATING NITRITE POLLUTANT TRANSPORT ALONG A RIVER

4.1. Overview

The chapter focuses on formulating a mathematical model to simulate the spatial and temporal variation of nitrite concentration for river system. The HCIS model coupled with the first order kinetic equation for nitrite nutrient is developed to simulate the nitrite pollutant concentration in the water column. The proposed model considers the transformation of nitrite to nitrate and oxidation of ammonia to nitrite due to nitrification process. The model is tested using hypothetical data. And results are compared with the numerical solution of the Fickian-based advection-dispersion equation (ADE) model coupled with the first-order kinetic equation for nitrite nutrient.

4.2. Introduction

Increase in pollution caused by industrialization, urbanization, and agriculture has resulted in impacting river ecosystem health. Different studies have been carried out on water bodies which indicate that one of the primary pollutant threats to the river health is the high influx of nutrients in the surface water (Nyenje *et al*., 2010; Varol and Sen, 2012; Kiedrzyńska *et al*., 2014; Gavrilescu *et al*., 2015). Eutrophication occurs when surface water is enriched with a high quantity of nutrients that stimulate algae growth and results in the reduction of dissolved oxygen (DO) concentration (Smith and Schindler, 2009; Lewis *et al*., 2011; Zamparas and Zacharias, 2014) that prompts a further decline in the water quality. The adequate evaluation of DO and nutrients in the water column is essential for the existence of aquatic habitats and to sustain a healthy aquatic ecosystem. Hence, it is necessary to evaluate some nutrients being discharged into the surface water (Peredes *et al*., 2010; Kannel *et al*., 2011). Nitrite nutrients are one of the critical parameters for ascertaining the suitability of water for drinking purposes and use by aquatic animals. Nitrites form mostly due to oxidation of ammonia in water bodies, and other sources which include fertilizer, animal waste, and human waste discharged into the rivers and streams (Raimonet *et al*., 2015). Liu *et al*. (2005) describe nitrification of ammonia as a two-step biochemical process through which ammonia is reduced to nitrite and also, nitrite is converted to nitrate. Most potential health effects of nitrites are seen in infants between the ages of 0-6 months which is responsible for a temporary blood disorder called Methaemoglobinaemia (Samatya *et al*., 2006).

Restoring the quality of water bodies to an acceptable level requires effective management of these pollutants through rigorous water quality monitoring and modeling. The application of different water quality modelling (WQM) tools are often demonstrated as an effective and cheaper method for water quality assessment. Different WQM tools were applied in many studies to determine the effect of nutrient pollutants transport in surface water. Yuceer *et al.* (2016) used a continuous stirred tank reactor (CSTR) method to simulate water quality constituent which includes nitrite concentration in the Beylerderesi River, Turkey. They applied the optimisation technique to estimate the model parameters by using the sequential Quadratic programming (SQP) method. Their results agreed with the measured data of nitrite concentration in the water body. Oliveira *et al.* (2012) discovered significant nutrient enrichment in the Certima River, Portugal by using the QUAL2KW model to evaluate the response of different loads of nutrients in the river. They identified domestic and diffuse source of contamination as the main cause of nitrogen nutrient in surface water. The model adequately described the measured data of nutrients satisfactorily. Silva *et al*. (2015) used a statistical analysis to assess the temporal and spatial distribution of nitrite concentration in the Cachoeira River, Brazil, where a low nitrite concentration was detected in the river. Vonder Wiesche *et al*. (1998) highlighted how environmental factors and inorganic nitrogen affect the variation of nitrite concentration in Lahn River, Germany. They stated that the increase in nitrite concentration in the river was because of high water temperature and a high level of ammonia concentration in the river. Corriveau *et al*. (2010) reported the effect of an agricultural watershed on the influx of nutrients in the Brasdhenri River, Quebec. They observed that there was an increase in nitrite concentration in the river during summer period with a low flow. Furthermore, Mirbagheri *et al*. (2009) developed a model to evaluate some parameters such as DO, BOD, ammonia, nitrites, and nitrates for the Jajrood River, Iran. They used implicit finite difference scheme to solve their model equations. Additionally, their model results could describe the parameters in the river effectively. Wang *et al*. (2011) presented an application of the MIKE II model on the effect of nutrients transport of the lower and middle reaches of the Hanshui River. They developed a rainfall-runoff model to estimate the amount of discharged nutrient pollutant into the river from the catchment. The results of their study show a good simulation of the river nutrients when compared to the observed data.

Different methods were used to solve solute transport in a water body which includes the finite difference scheme and analytical methods. The Fickian-based ADE equation was numerically solved by the finite difference scheme and has been a popular method for solving pollutants transport in rivers and streams. One of the limitations of the ADE model is its ineffectiveness in practical applications (Ghosh *et al*., 2008;

Neuman and Tartakovsky, 2009). The cell-in-series (CIS) model was developed to serve as an alternative model to the ADE model to simulate pollutant transport in a water body (Banks, 1974; Wang and Chen, 1996). However, the limitation of the CIS model is its deficiency in simulating the advection component effectively, where the river reach is assumed to be a thoroughly mixed cell (Kumarasamy, 2015). The HCIS model was developed to solve solute pollutant transports in surface water and to resolve the limitation associated with the existing models (Kumarasamy *et al.*, 2011). The new model applied ordinary differential equation that can be analytically solved and makes it advantageous over the ADE model. Additionally, the ability to simulate the advection component with the new model tackles the limitation related to the CIS model (Kumarasamy *et al.*, 2013). In this study, an analytical solution was developed for a hybrid mixing cells model that incorporates the kinetic reaction of nitrite coupled with ADE processes. The HCIS-NO_2 model was used to evaluate the nitrite concentration of the uMgeni River. Additionally, this study also illustrates the numerical solution for a Fickian-based ADE model coupled with the first-order reaction of nitrite processes. The results of both models were compared.

4.3. The Model Development

A river reach is divided into series of conceptual hybrid units. The hybrid unit is comprised of a plug cell and two mixed cells as presented in Figure 4.1. The first cell has a residence time (T_1), and the other two cells have unequal residence time (T_2 and T_3) which are the model parameters. Where the concentrations of nitrite pollutants C_b (x, t) vary with time (t) along the length of the river reach which is affected by a point source pollutant. The conversion of ammonia to nitrite through the action of nitrosomonas bacteria, agricultural and industrial wastes were assumed to be the sources of nitrite in the system. Furthermore, oxidation of nitrite through the action of Nitrobacter bacteria was considered as a sink of nitrite in the river system. Sakalauskienė (2001) presented the first-order kinetic equation of nitrite as expressed in Eq. (4.1).

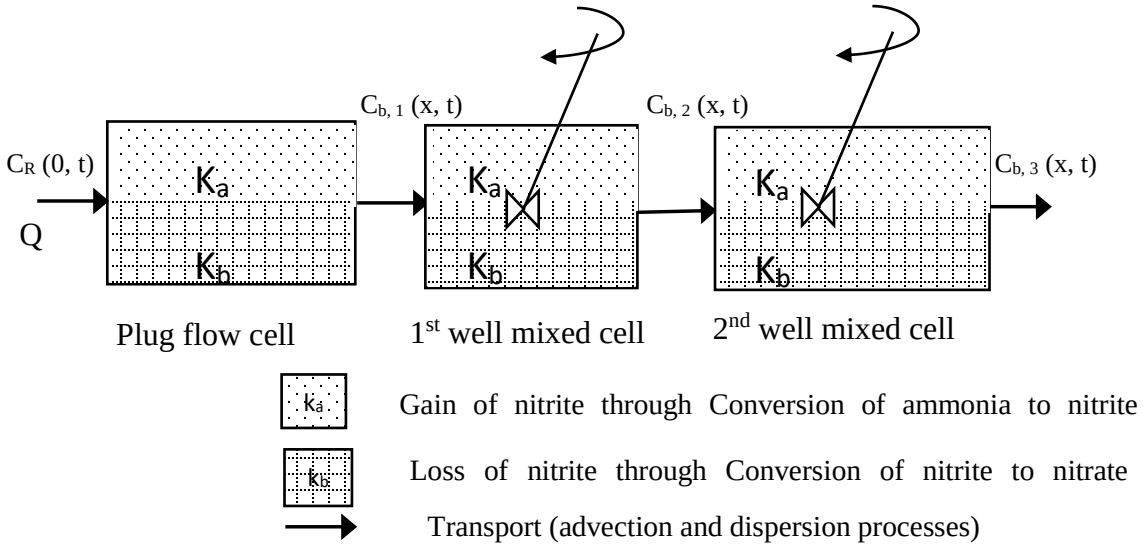

Figure 4. 1: The process of nitrite pollutant concentration through a hybrid unit

$$\frac{\partial C_b(x,t)}{\partial t} = k_a C_a(x,t) - k_b C_b(x,t) \tag{4.1}$$

Where, C_a signifies ammonia concentration in the river (mg/l), (k_a) represents oxidation rate of ammonia (day-^{1}), C_b is nitrite concentration (mg/l) and k_b (day-^{1}) is the oxidation rate of nitrite. The first term on the right side defines the procedure by which nitrite is produced through oxidation of ammonia, the other term describes the means through which nitrite is reduced in the system.

The process of the HCIS model begins in the plug flow cell, where the nitrite concentration ensures a transformation without a variation in its concentration. The effluents from the first cell pass into the next cell where it gets thoroughly mixed for a period and later enters the third cell. Thus, it can be concluded that the transport of nitrite solute in the first cell signifies pure advection. Moreover, the advection-dispersion process takes in the two mixing cells. We assumed that the initial quantity of nitrite pollutant in the entire cell is zero and the boundary conditions change from 0 to C_R. The nitrification processes occur in all three cells as the nitrite pollutant travels downstream. We considered the flow rate Q (m^3/s) to be in a steady condition for the river flow. In this study, the HCIS model will be used to predict nitrite concentration in the river reach using Laplace transform techniques, mass balance method and convolution techniques at the end of successive units.

4.3.1. Formulation of Nitrite Concentration in the Plug Flow Cell.

A plug flow cell was assumed to have control volume (V) and a length (Δx) and was considered to transport a concentration of nitrite pollutants C_b (x, t) downstream. The plug flow cell consists of a series of compartments which contain a plume of water. T_1 is the time required for the fluid to stay in the plug flow before it gets to be replaced. A little time interval (Δt) was considered where some portion of nitrite (NO_2) pollutant concentration is transformed to nitrate (NO_3). Also, ammonia (NH_3) concentration is being converted to nitrite during the oxidation process within the system. After the nitrification and oxidation process, the nitrite solute in the river will move to the next control volume.

The following partial differential equation was formulated as expressed:

$$\frac{\partial C_b(x,t)}{\partial t} + \frac{u\partial C_b(x,t)}{\partial x} = k_a C_a(x,t) - k_b C_b(x,t) \tag{4.2}$$

The solution of the above equation was attained with the following boundary and initial conditions such as:

C_b (x, 0) = 0 for x > 0;

C_b (0, t) = C_R for t ≥ 0;

C_b (T_1u, t) = 0 for 0 < t < T_1.

Eq. (4.2) was solved using Laplace transform; integration method and inverse Laplace transform techniques to obtain:

$$C_{b,1}(x,t) = \left[C_R U(t-T_1) e^{-k_b T_1} \right] + \left[\frac{k_a C_{a,1}(x,t)}{k_b} \left\{ e^{-k_b t} - U(t-T_1) e^{-k_b T_1} e^{-k_b (t-T_1)} \right\} \right] \tag{4.3}$$

The nitrite concentration at the end of the plug flow cell was presented in Eq. (4.3) and is effective for t ≥ T_1. Thus, U (t – T_1) is a step function, and $C_{a,1}$(x, t) is the ammonia concentration in the plug flow cell (Olowe and Kumarasamy, 2017).

4.3.2. Formulation of the Concentration of Nitrite in the First Well-Mixed Cell.

Nitrite concentration at the end of the previous cell will be the source of nitrite in the first thoroughly mixed cell. The residence time required for the first thoroughly mixed cell is $T_2 = V_2/Q$. Where V_2

represents the volume of the first mixed cell and Q signifies the flow rate of the cell. Hence, the mass balance of the concentration of nitrite pollutant in the second cell is presented in Eq. (4.4)

$$C_{b,1}Q\Delta t - C_{b,2}Q\Delta t + k_a C_{a,2}V_2\Delta t - k_b C_{b,2}V_2\Delta t = V_2\Delta C_{b,2} \tag{4.4}$$

The first and second terms indicate the mass of nitrite concentration pollutant entering and leaving the first mixed cell. While the third represents the conversion the nitrification processes, and the last term signifies the biochemical reduction of nitrite concentration in the river. Furthermore, the right term describes the change of mass within the first mixed cell. Eq. (4.4) is described in the ordinary differential form as expressed in Eq. (4.5), which was solved to give the nitrite concentration at the end of the cell which is illustrated in Eq. (4.6).

$$\frac{dC_{b,2}}{dt} + \frac{\left(1+k_bT_2\right)C_{b,2}}{T_2} = \frac{C_{b,1}}{T_2} + k_aC_{a,2} \tag{4.5}$$

$$C_{b,2} = \begin{pmatrix} \dfrac{C_R U\left(t-T_1\right)}{\left(1+k_bT_2\right)}\left[e^{-k_bT_1} - e^{-k_bT_2}e^{\left(\frac{1}{T_2}\right)(T_1-t)}\right] + \dfrac{k_aC_{a,1}}{k_b}\left[e^{k_bt} - e^{-k_bt}e^{\left(\frac{1}{T_2}\right)(T_1-t)}\right] \\ -\dfrac{k_aC_{a,1}U\left(t-T_1\right)}{k_b}\left[e^{k_bt} - e^{-k_bt}e^{\left(\frac{1}{T_2}\right)(T_1-t)}\right] + \dfrac{k_aC_{a,2}T_2}{\left(1+k_bT_2\right)}\left[1-e^{\left(\frac{1+k_bT_2}{T_2}\right)(T_1-t)}\right] \end{pmatrix} \tag{4.6}$$

4.3.3. Formulation of Nitrite Concentration in the Second Well-Mixed Cell.

The cell was considered to have a residence time $T_3 = V_3/Q$. The nitrite pollutant from the first mixing cell will move to the second mixing cell. In the cell, concentration of nitrite will decay to nitrate pollutant and an accumulation of nitrite will occur due to nitrification of ammonia concentration. Therefore, the equation below represents the mass balance in the cell.

$$C_{b,2}Q\Delta t - C_{b,3}Q\Delta t + k_aC_{a,3}V_3\Delta t - k_bC_{b,3}V_3\Delta t = V_3\Delta C_{b,3} \tag{4.7}$$

The first and second terms indicate the mass of nitrite concentration pollutant entering and leaving the second mixed cell. While, the third represents the conversion of the nitrification processes and the last term signifies the biochemical reduction of nitrite concentration in the river. Furthermore, the right term describes the change of mass within the second mixed cell. Eq. (4.7) is described in the ordinary differential form and resolved to estimate the step response function of concentration of nitrite for a hybrid unit.

$$\frac{dC_{b,3}}{dt}+\frac{\left(1+k_bT_3\right)C_{b,3}}{T_3}=\frac{C_{b,2}}{T_3}+k_aC_{a,3} \tag{4.8}$$

Eq. (4.6) was substituted into Eq. (4.8) and multiplied by $e^{\left(\frac{1+k_bT_3}{T_3}\right)t}$ to yield

$$dC_{b,3}e^{\left(\frac{1+k_bT_2}{T_2}\right)t}=\left[\begin{array}{l}\left\{\frac{C_RU\left(t-T_1\right)e^{-k_bT_1}e^{\left(\frac{1+k_bT_3}{T_3}\right)t}}{T_3\left(1+k_bT_2\right)}\right\}-\left\{\frac{C_RU\left(t-T_1\right)e^{-k_bT_2}e^{\left(\frac{1+k_bT_3}{T_3}\right)t}e^{\left(\frac{1}{T_2}\right)\left(T_1-t\right)}}{T_3\left(1+k_bT_2\right)}\right\}\\+\left\{\frac{k_aC_{a,1}}{T_3k_b}e^{\left(\frac{1+k_bT_3}{T_3}\right)t}\right\}-\left\{\frac{k_aC_{a,1}e^{\left(\frac{1}{T_2}\right)T_1}e^{\left(\frac{1}{T_3}-\frac{1}{T_2}\right)t}}{T_3k_b}\right\}-\left\{\frac{k_aC_{a,1}U\left(t-T_1\right)}{T_3k_b}e^{\left(\frac{1+k_bT_3}{T_3}\right)t}\right\}\\+\left\{\frac{k_aC_{a,1}U\left(t-T_1\right)e^{\left(\frac{1}{T_2}\right)T_1}e^{\left(\frac{1}{T_3}-\frac{1}{T_2}\right)t}}{T_3k_b}\right\}+\left\{\frac{k_aC_{a,2}T_2e^{\left(\frac{1+k_bT_3}{T_3}\right)t}}{T_3\left(1+k_bT_2\right)}\right\}-\left\{\frac{k_aC_{a,2}T_2e^{\left(\frac{1+k_bT_2}{T_2}\right)T_1}e^{\left(\frac{1}{T_3}-\frac{1}{T_2}\right)t}}{T_3k_b}\right\}\\+\left\{k_aC_{a,3}e^{\left(\frac{1+k_bT_3}{T_3}\right)t}\right\}\end{array}\right] \tag{4.9}$$

Solving Eq. (4.9) with the integration method to estimate the step response function for the nitrite concentration at a hybrid unit.

$$C_{b,3}=\left[\begin{array}{l}\left(\frac{C_RU\left(t-T_1\right)}{\left(1+k_bT_2\right)\left(1+k_bT_3\right)}\left\{A\right\}\right)-\left(\frac{C_RU\left(t-T_1\right)T_2e^{-k_bT_2}}{\left(1+k_bT_2\right)\left(T_2-T_3+k_bT_2T_3\right)}\left\{B\right\}\right)\\+\left(\frac{k_aC_{a,1}}{k_b}\left\{D\right\}-\frac{k_aC_{a,1}U\left(t-T_1\right)}{k_b}\left\{N\right\}\right)+\left(\frac{T_2k_aC_{a,2}}{\left(1+k_bT_2\right)}\left\{\Phi\right\}+\frac{T_3k_aC_{a,3}}{\left(1+k_bT_3\right)}\left\{\Omega\right\}\right)\end{array}\right] \tag{4.10}$$

where,

$$A=\left\{\left(e^{-k_bT_1}\right)-\left(e^{\left(1/T_3\right)\left[T_1-t\right]}e^{-k_bt}\right)\right\},\ B=\left\{\left(e^{\left(1/T_2\right)\left[T_1-t\right]}\right)-\left(e^{\left(\frac{1+k_bT_3}{T_3}\right)\left[T_1-t\right]}\right)\right\}$$

$$N = \left\{ \left(\frac{e^{k_b t}}{(2T_3 k_b + 1)} \right) - \left(\frac{T_2 e^{\left(1/T_2\right)T_1} e^{-\left(\frac{1+k_b T_2}{T_2}\right)t}}{(T_2 - T_3)} \right) - \left(\frac{e^{k_b T_1} e^{\left(\frac{1+k_b T_3}{T_3}\right)(T_1 - t)}}{(2T_3 k_b + 1)} \right) + \left(\frac{T_2 e^{\left(1/T_3\right)T_1} e^{-\left(\frac{1+k_b T_3}{T3}\right)t}}{(T_2 - T_3)} \right) \right\}$$

$$D = \left\{ \left(\frac{e^{k_b t}}{(2T_3 k_b + 1)} \right) - \left(\frac{T_2 e^{\left(1/T_2\right)T_1} e^{-\left(\frac{1+k_b T_2}{T_2}\right)t}}{(T_2 - T_3)} \right) - \left(\frac{e^{k_b T_1} e^{\left(\frac{1+k_b T_3}{T_3}\right)(T_1 - t)}}{(2T_3 k_b + 1)} \right) + \left(\frac{T_2 e^{\left(1/T_3\right)T_1} e^{-\left(\frac{1+k_b T_3}{T_3}\right)t}}{(T_2 - T_3)} \right) \right\}$$

$$\Phi = \left\{ \left(\frac{1}{(1 + k_b T_3)} \right) - \left(\frac{T_2 e^{\left(\frac{1+k_b T_2}{T_2}\right)(T_1 - t)}}{(T_2 - T_3)} \right) - \left(\frac{e^{\left(\frac{1+k_b T_3}{T_3}\right)(T_1 - t)}}{(1 + k_b T_3)} \right) + \left(\frac{T_2 e^{\left(\frac{1+k_b T_3}{T_3}\right)(T_1 - t)}}{(T_2 - T_3)} \right) \right\}, \qquad \Omega = \left\{ 1 - e^{\left(\frac{1+k_b T_3}{T_3}\right)(T_1 - t)} \right\}$$

Eq. (4.10) simulates the concentration of nitrite at the close of a unit which represents the step response of the first unit. Where $C_{b,3}$ [mg/l] signifies the amount of nitrite solute at the end of a unit; $C_{a,2}$ and $C_{a,3}$ (mg/l) evaluate the level of ammonia in both mixed cells respectively (Olowe and Kumarasamy, 2017). The impulse response function $\delta_{HCIS\text{-}NO2}(n, \Delta t)$ was estimated by differentiating Eq. (4.10) with respect to (t) as described:

$$\delta_{HCIS-NO_2}(n, \Delta t) = \frac{K_{HCIS-NO_2}(n\Delta t) - K_{HCIS-NO2}((n-1)\Delta t)}{\Delta t} \tag{4.11}$$

The Impulse response function for the concentration of nitrite at the end of a hybrid unit is presented in Eq. (4.12).

$$C_{b,3}=\left[\begin{array}{l}\left(\dfrac{C_R U(t-T_1)}{(1+k_bT_2)(1+k_bT_3)}\{B1\}\right)-\left(\dfrac{C_R U(t-T_1)T_2 e^{-k_bT_2}}{(1+k_bT_2)(T_2-T_3+k_bT_2T_3)}\{B2\}\right)\\ +\left(\dfrac{k_aC_{a,1}}{k_b}\{B3\}-\dfrac{k_aC_{a,1}U(t-T_1)}{k_b}\{B4\}\right)+\left(\dfrac{T_2k_aC_{a,2}}{(1+k_bT_2)}\{B5\}+\dfrac{T_3k_aC_{a,3}}{(1+k_bT_3)}\{B6\}\right)\end{array}\right] \quad (4.12)$$

$$B1=\left\{\left(e^{-k_bT_1}\right)-\left(e^{\left(1/T_3\right)T_1}\frac{1+k_bT_3}{T_3}e^{-\left(\frac{1+k_bT_3}{T_3}\right)t}\right)\right\},$$

$$B2=\left\{\frac{1}{T_2}\left(e^{\left(1/T_2\right)[T_1-t]}\right)-\frac{1+k_bT_3}{T_3}\left(e^{\left(\frac{1+k_bT_3}{T_3}\right)[T_1-t]}\right)\right\}$$

$$B3=\left\{\begin{array}{l}\left(\dfrac{k_be^{k_bt}}{(2T_3k_b+1)}\right)-\left(\dfrac{e^{\left(1/T_2\right)T_1}1+k_bT_2e^{-\left(\frac{1+k_bT_2}{T_2}\right)t}}{(T_2-T_3)}\right)\\ -\left(\dfrac{1+k_bT_3e^{k_bT_1}e^{\left(\frac{1+k_bT_3}{T_3}\right)(T_1-t)}}{T_3(2T_3k_b+1)}\right)+\left(\dfrac{T_2e^{\left(1/T_3\right)T_1}1+k_bT_3e^{-\left(\frac{1+k_bT_3}{T_3}\right)t}}{T_3(T_2-T_3)}\right)\end{array}\right\}$$

$$B4=\left\{\begin{array}{l}\left(\dfrac{k_be^{k_bt}}{(2T_3k_b+1)}\right)-\left(\dfrac{e^{\left(1/T_2\right)T_1}1+k_bT_2e^{-\left(\frac{1+k_bT_2}{T_2}\right)t}}{(T_2-T_3)}\right)\\ -\left(\dfrac{1+k_bT_3e^{k_bT_1}e^{\left(\frac{1+k_bT_3}{T_3}\right)(T_1-t)}}{T_3(2T_3k_b+1)}\right)+\left(\dfrac{T_2e^{\left(1/T_3\right)T_1}1+k_bT_3e^{-\left(\frac{1+k_bT_3}{T_3}\right)t}}{T_3(T_2-T_3)}\right)\end{array}\right\}$$

$$B5 = \left\{ \begin{array}{l} \left(\dfrac{1}{\left(1+k_b T_3\right)} \right) - \left(\dfrac{\left(1+k_b T_2\right) e^{\left(\frac{1+k_b T_2}{T_2}\right)(T_1 - t)}}{\left(T_2 - T_3\right)} \right) \\ - \left(\dfrac{\left(1+k_b T_3\right) e^{\left(\frac{1+k_b T_3}{T_3}\right)(T_1 - t)}}{T_3\left(1+k_b T_3\right)} \right) + \left(\dfrac{T_2\left(1+k_b T_3\right) e^{\left(\frac{1+k_b T_3}{T_3}\right)(T_1 - t)}}{T_3\left(T_2 - T_3\right)} \right) \end{array} \right\},$$

$$B6 = \left\{ 1 - \left(\frac{1+k_b T_3}{T_3} \right) e^{\left(\frac{1+k_b T_3}{T_3}\right)(T_1 - t)} \right\}$$

Eqs. (4.10) and (4.12) are useable when $t \geq T_1$ and signify the step and impulse response of a unit.

Eq. (4.13) presents a convolution technique to determine the nitrite concentration at a downstream location along the river. The process considered a river to consist of a series of hybrid units where the concentration of nitrite pollutants from one hybrid unit will be the influent to the next unit as presented in Figure 3.5. In addition, Eqs. (3.20 – 3.22) were used to estimate the model parameters (T_1, T_2, and T_3)

$$C(i\Delta x, n\Delta t) = \sum_{\gamma=1}^{n} C[(i-1)\Delta x, \gamma]\delta_{HCIS-NO_3}(n-\gamma+1, \Delta t) \tag{4.13}$$

4.4. Model Verification using a Numerical Approach

The capability of HCIS-NO_2 model was verified by comparing with the Fickian-based ADE-NO_2 model. The second order differential equation of ADE along with the kinetic reaction of nitrite for a one-dimensional flow is given:

$$\frac{\partial C_b(x,t)}{\partial t} = -u\frac{\partial C_b(x,t)}{\partial x} + D_L\frac{\partial^2 C_b(x,t)}{\partial x} + k_a C_a(x,t) - k_b C_b(x,t) \tag{4.14}$$

Where, C_b and C_a illustrate the nitrite and ammonia concentration (mg/l) respectively; K_b [day-^{1}] signifies the oxidation rate of nitrite which is temperature dependent; Ka [day-^{1}] is the rate of oxidation of ammonia.

The conditions used for Eq. (4.2) were used to solve Eq. (4.14) by applying an explicit finite difference scheme. The process considered the forward difference in time, backward upwind for the advection term, and the central difference in space for the dispersion term which yields the solution described in Eq. (4.18) and the result was compared with the HCIS-NO_2 model. A small courant number was used, which must be less than or equal to one, for the numerical solution to be correct. The time step and grid space were chosen as Δt = 1min and Δx =100m, respectively

$$\frac{\partial C_b(x,t)}{\partial t} = \frac{C_b(x,t+\Delta t) - C_b(x,t)}{\Delta t} \tag{4.15}$$

$$\frac{\partial C_b(x,t)}{\partial x} = \frac{C_b(x+\Delta x,t) - C_b(x-\Delta x,t)}{2\Delta x} \tag{4.16}$$

$$\frac{\partial^2 C_b(x,t)}{\partial x^2} = \frac{C_b(x+\Delta x,t) - 2C_b(x,t) + C_b(x-\Delta x,t)}{\Delta x^2} \tag{4.17}$$

Eqs. (4.15 – 4.17) were substituted into Eq. (4.14) and solved to obtain the step response function as expressed below.

$$C(x,t+\Delta t) = \left[\begin{array}{l} \left(C(x,t)\left[1 - \frac{2D_L\Delta t}{(\Delta x)^2} - k_b\Delta t\right]\right) - \left(C(x+\Delta x,t)\left[\frac{u\Delta t}{2\Delta x} - \frac{D_L\Delta t}{(\Delta x)^2}\right]\right) \\ + \left(C(x-\Delta x,t)\left[\frac{u\Delta t}{2\Delta x} + \frac{D_L\Delta t}{(\Delta x)^2}\right]\right) + C_a(x,t)(k_a\Delta t) \end{array} \right] \tag{4.18}$$

4.5. Results and Discussions

4.5.1. Simulation and testing of Nitrite transport with synthetic data

Spatial and temporal variation of NO_2 was simulated in a river to validate the potential of the new model where a synthetic data set was generated for the stream. The parameters T_1, T_2, and T_3 of the HCIS-NO_2 model were estimated as 1.70 min, 2.30 min, and 6.0 min respectively by considering a river with an estimated value for u and D_L. The value of u and D_L was given as 20m/min and 1000m^2/min respectively and the size of hybrid unit Δx = 200m was determined satisfying the peclet number condition. The transformation of NH_3 to NO_2 and conversion of NO_2 to NO_3 through the nitrification process were considered in the model simulation. Considering the estimated model parameters (T_1, T_2, and T_3) and

different values of k_b (= 0.002 and 0.005 per min) the unit step and impulse responses of the first unit as computed with Eqs. (4.10) and (4.12), are presented in Figures 4.2 and 4.3. The step responses of the nitrite concentration with respect to time for different oxidation rates of nitrite k_b (= 0.002 and 0.005 per min) and keeping the NH_3 oxidation rate (k_a) constant is presented in Figure 4.2. From the figure, it was observed that the concentration of nitrite increases as the time increases until it reaches the boundary concentration where it remains constant. Also, it was observed that the effluent of the lower value of k_b attains boundary concentration earlier than the effluent from the higher value of k_b. The impulse responses described in Figure 4.3 shows a reduction in the peak concentration as the value of k_b increases in the water body. Thus, the variation in the nitrification rate (k_b) affects the nitrite pollutants as it moves downstream and makes it more attenuated within the water body.

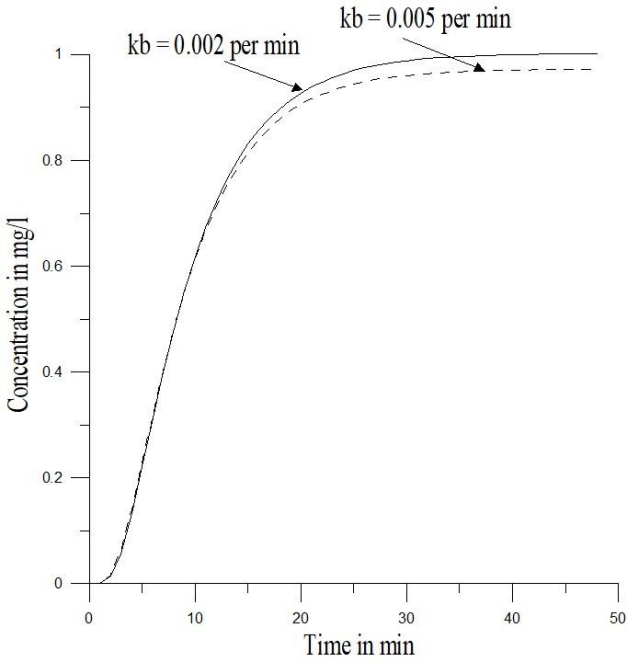

Figure 4.2: Unit step responses of the HCIS-NO_2 model, for nitrification coefficient, K_b= (0.005 and 0.002 per min) at Δx = 200m and (T_1 = 1.7 min, T_2 = 2.3 min, and T_3 = 6.0min)

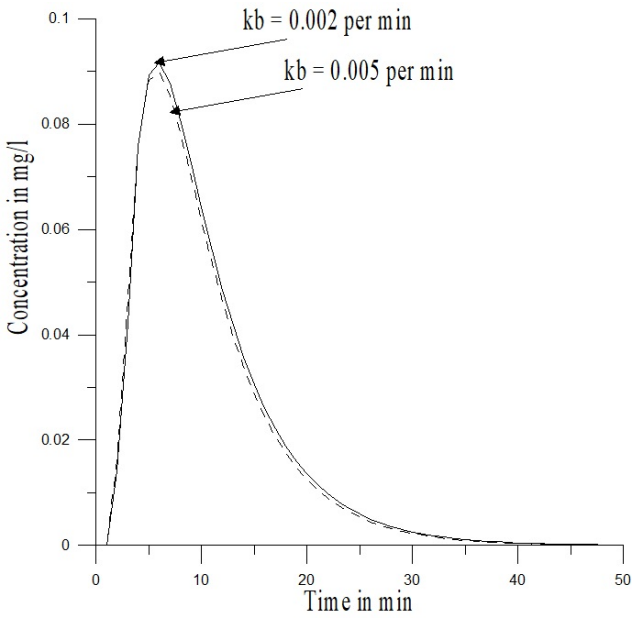

Figure 4.3: Unit impulse responses of the HCIS–NO_2 model, for nitrification coefficient, K_b= (0.005 and 0.002 per min) at Δx = 200m and (T_1 = 1.7 min, T_2 = 2.3 min, and T_3 = 6.0min)

Furthermore, the impulse response functions were generated at the end of first, second, fourth and eighth hybrid unit using the nitrite oxidation rates k_b (= 0.002 and 0.005 per min) and keeping the ammonia oxidation rate (k_a) constant as shown in Figure 4.4. It could be observed that as the nitrite pollutants move downstream, the C-t distribution get more attenuated and the peak concentration reduced as the hybrid units increase. Furthermore, the time to peak decreases as hybrid units increases. Therefore, it can be observed that the reduction in nitrite pollutants as it travels downstream in the river was due to the nitrification process which converts the nitrite to nitrate concentration. Figure 4.5 was used to demonstrate the influence of ammonia oxidation rate on the variation of nitrite pollutant as it travels downstream within the river, where values of k_a (=0.002 and 0.005 per min) were used and kept (k_b) constant. It can be observed that the higher value of k_a leads to an increment in the nitrite concentration in the river when compared to the lower value of ka. Besides, a bell-shaped distribution was observed in the profile as the nitrite pollutant travels downstream, the peak concentration reduces and falling limb is elongated as the number of units increases.

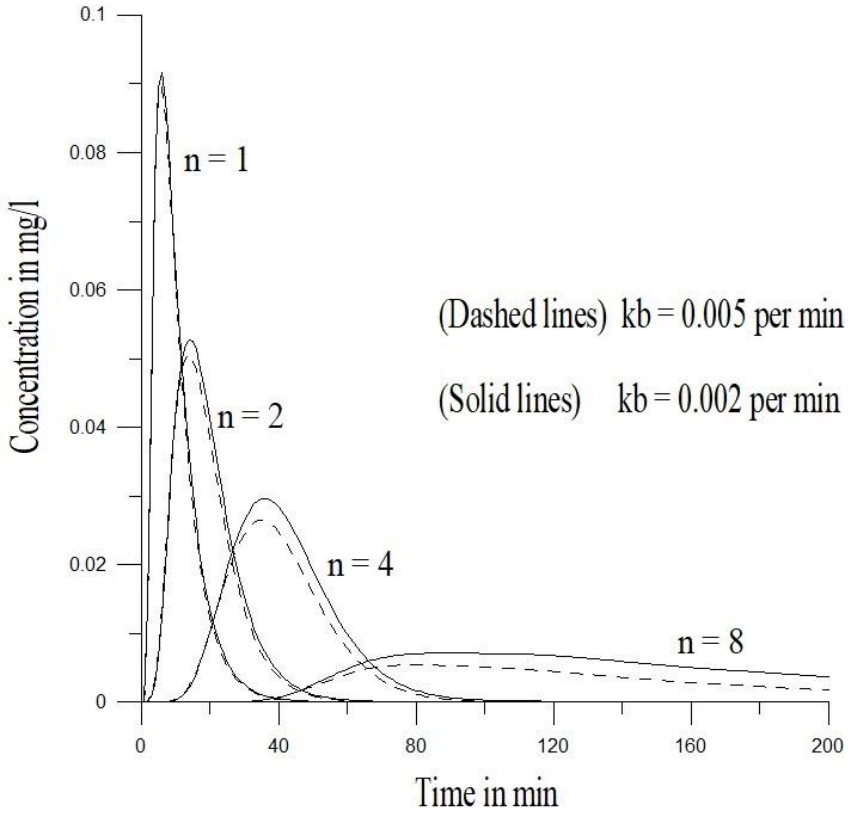

Figure 4.4: Unit impulse responses of the HCIS–NO_2 model, for nitrification coefficient, K_b = (0.005 and 0.002 per min), at Δx (= 200m, 400m, 800m, and 1600m) and (T_1 = 1.7 min, T_2 = 2.3 min, and T_3 = 6.0min)

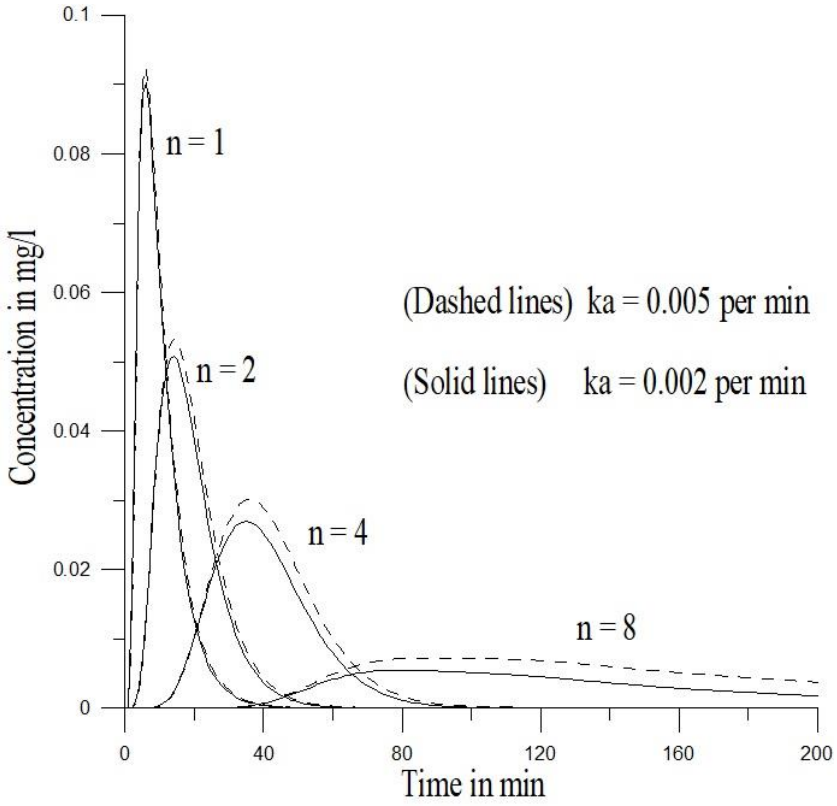

Figure 4.5: Unit impulse responses of the HCIS–NO_2 model, for NH_3 oxidation coefficient, K_a = (0.005 and 0.002 per min), at Δx (= 200m, 400m, 800m, and 1600m) and (T_1 = 1.7 min, T_2 = 2.3 min, and T_3 = 6.0min)

The new model was validated with the impulse response functions of the numerical solution of the Fickian-based ADE-NO_2 model as shown in Figure 4.6. Eq. (4.15) was numerically differentiated with respect to time in order to determine the impulse response of the ADE-NO_2 model. The following data set were used for the simulation of the ADE-NO_2 model: Δt = 1min, Δx =100m, flows velocity (u) = 20m/min and dispersion coefficient D_L = 1000m^2/min. The impulse response at the point when (X = 200m) and also, when (X = 400m, 800m and 1600m) from the point of injection were described in Figure 4.6. Numerical convolution was used to determine the concentration of nitrite pollutant downstream. The impulse responses were generated at the same location for the hybrid units when Δx (= 200m, 400m, 800m, and 1600m) as presented in Figure 4.6. It could be observed that the concentration-time profiles agreed with each other and showed similar conditions as the nitrite pollutant moves downstream. Moreover, the peak and the shape of the C- t profile was satisfactorily produced by both models. However, marginal differences in the peak concentration were observed in the profile due to the difference in space

discretization. Also, the truncation procedure followed in solving the ADE model using a numerical method was another reason for the differences. It could be seen that the HCIS-NO_2 model agreed with the numerical solution of the ADE-NO_2 model. The quantitative measures presented in Table 4.1, describe the coefficient of Nash-Sutcliffe efficiency coefficient (NSE), RMSE observations standard deviation ratio, and coefficient of determination (R^2) which were applied to evaluate the performance of the HCIS-NO_2 model. Figure 4.6 was used for the quantitative measures and it was observed from the table that the value for NSE and R^2 were closer to unity. Furthermore, RMSE and RSR have a minimum value. Consequently, the results of the quantitative measures signify an excellent correlation between both models.

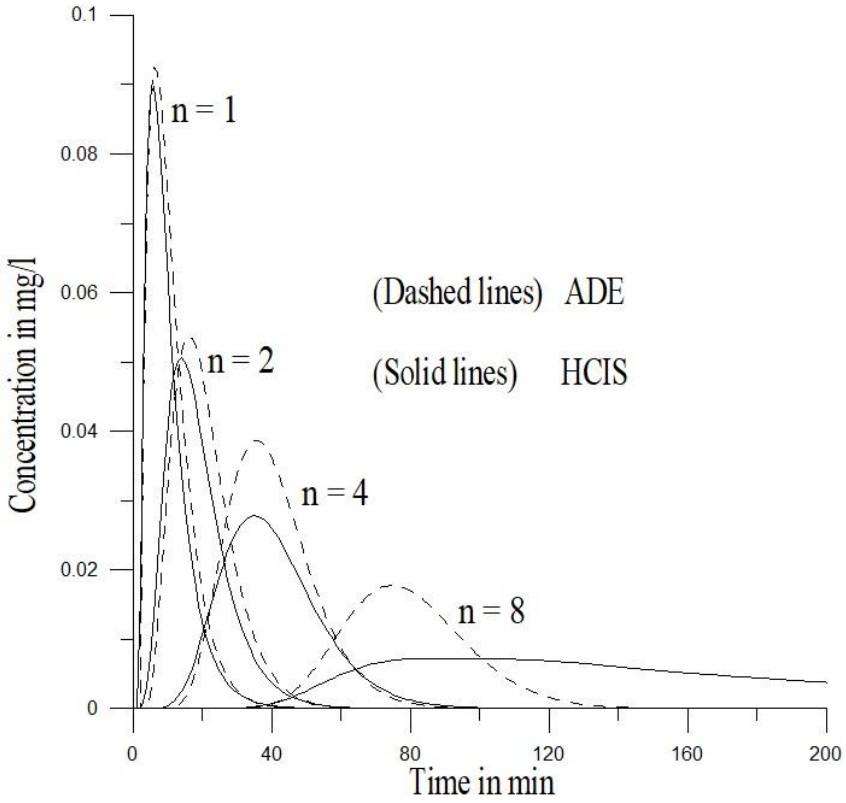

Figure 4. 6: Evaluation of unit impulse responses of the HCIS-NO_2 model with the ADE-NO_2 model at X = (200, 400, 800 and 1600m) for nitrification coefficient, k_b = 0.005 per min

Table 4. 1: The quantitative measures between the HCIS-NO_2 and ADE–NO_2 models

Unit	R^2	NSE	RMSE	RSR
1^{st}	0.980	0.972	0.0028	0.0073
2^{nd}	0.964	0.942	0.0022	0.0082
4^{th}	0.952	0.931	0.0025	0.0085
8^{th}	0.754	0.711	0.0034	0.0242

4.6. Summary

This section described the formulation and application of a hybrid model for a non-conservative transport of nitrite solute in a natural river. In this chapter, the advection-dispersion equation with first order kinetic reaction of nitrite was solved analytically using the concept of a hybrid model. The developed model was derived to evaluate the spatiotemporal variation of nitrite pollutant in a natural water body. The model parameters were estimated using the flow characteristics and longitudinal dispersion coefficient of the water body when the Peclet number condition is satisfied ($Pe \geq 4$). An analytical solution for the HCIS-NO_2 model was obtained in the cells using the principle of Laplace transform technique. The performance of the HCIS-NO_2 model solution was verified through comparison of the results of the Fickian-based ADE model. It was noticed that the results of the new model having parameters (T_1, T_2, and T_3) is almost matching to the response of the ADE-NO_2 model with two parameters (u and D_L). Very high NSE and R^2 value were obtained in the statistical analysis which indicates a good agreement between the HCIS-NO_2 model and ADE- NO_2 model. The HCIS-NO_2 model has demonstrated to be a valuable and successful tool for simulating solute transport in a natural river.

CHAPTER 5: A MATHEMATICAL MODEL DEVELOPMENT FOR SIMULATING NITRATE POLLUTANT TRANSPORT ALONG A RIVER

5.1. Overview

In this chapter, a simplified mathematical model, i.e., the hybrid cells in series model (HCIS) is developed to simulate the spatial and temporal variation of nitrate concentration along a river reach. The study is aimed to derive analytical solutions for the first order reaction kinetics of nitrate with the advection and dispersion process to simulate nitrate nutrients along a river reach using Laplace transformation technique. The model simulates the fate and transport of nitrate along a river reach by considering various processes such as the transformation of nitrite to nitrate through nitrification process, the uptake of nitrate by algae for its growth and conversion of nitrate to nitrogen gas due to denitrification along with advection and dispersion pollutant transport processes. The model is tested using hypothetical data, and the results are compared with the numerical solution of the Fickian-based advection-dispersion equation (ADE) model coupled with a first-order kinetic equation for nitrate nutrient.

5.2. Introduction

Enrichment of water bodies with nitrate nutrients is increasing worldwide because of anthropogenic impact on the environment, which is very harmful to humans and aquatic animals. Excess concentration of nitrates in water bodies promotes the overgrowth of phytoplankton which results in a low level DO concentration in the surface water (Valent *et al*., 2011; Atashgahi *et al*., 2015; Rusanov and Khromov, 2016). However, one of the parameters used to measure the pollution level in a natural river and stream is the amount of DO concentration in the system, which must be adequately monitored (Seibel, 2011; Tyagi *et al.*, 2012). A substantial rise in the number of algae in the surface water causes degradation of the stream water quality and decreases the DO concentration on which fish and other aquatic life depend (Bailey and Ahmadi, 2014). Algae blooms in surface water are very dangerous to human health because they produce bacteria which have an adverse effect on humans. Also, drinking water which contains a high concentration of nitrates also influences on human health. The presence of excessive nitrate concentration in drinking water leads to methaemoglobinaemia which results in the inability of the vein to convey oxygen within the human body (Fewtrell, 2004).

Kannel *et al*. (2007) described some water quality parameters which ensure excellent river health such as dissolved oxygen (DO), carbonaceous biological oxygen demand (CBOD), total phosphorus (TP), pH,

temperature, and total nitrogen (TN). They are the factors that must be considered when assessing the quality of water in the aquatic system. These parameters must meet standard criteria before the aquatic ecosystem can be regarded as healthy water for human consumption and use by aquatic organisms. There are many sources of nitrate nutrients in the surface water which includes anthropogenic sources due to domestic sewage, industrial waste and fertilizer discharged into water bodies. Also, it can be formed by oxidation of nitrites through the process of nitrification. Nitrification is the process through which ammonia nutrients are consecutively oxidised to nitrite and nitrate nutrient under aerobic conditions (Aissa-Grouz *et al.*, 2015). The autotrophic bacteria which are accountable for the transformation of nitrite to nitrate nutrient in the river system is known as Nitrobacter (Cebron and Garnier, 2005).

Different models have been used in many studies to monitor nitrate concentration in different water bodies. Donner *et al.* (2002) used two physical based models to evaluate the nitrate concentration in the Mississippi River. It was observed that the increment in the concentration of nitrate in the river was as a result of an increase in runoff from the catchment areas. Multivariate statistics were used by Tisseuil *et al*. (2008) to model the level of nitrate in the Garonne River, southwest France. It was discovered that a diffuse source of agricultural inputs caused the high impact of nitrate in the river. Pohlert *et al.* (2005) applied the SWAT model to simulate nitrate concentration in the Dill River, Germany, and it was observed from their results that the model could reproduce the seasonal change in nitrate loading in the river adequately. Sui and Frankenberger (2008) presented the application of the SWAT model to simulate the monthly nitrate concentration for the sugar creek watershed, central Indiana. It was observed from their results that the model could predict the concentration of nitrate accurately. Another study was carried out by Oeurng *et al*. (2016) to assess the variation of nitrate level in the Sesan, Sekong, and Srepok Rivers, Cambodia. The results of their study revealed a substantial amount of nitrate concentration in the rivers during the monsoon season. Yin *et al.* (2016) employed a hydrological catchment (HYPE) model to simulate different nutrient loads in the Hong-Ru River. The model could simulate the temporal and spatial variation of nitrate concentration effectively when compared with the measured values. Lam *et al.* (2010) described the influence of different causes of pollution on the concentration of nitrate in the Kielstau River, Germany, by using the SWAT model. Based on their study, it was found that diffuse sources of pollution contributed to a greater quantity of nitrate in the river.

To control the nitrate levels in the water bodies, additional research is needed to monitor its concentration in the water system which will lead to the best management practices. It is significant to manage the river

quality and estimate the influence of nitrate pollutants as it affects the water body. The nitrate pollutant load discharged into water bodies should be adequately maintained so that it does not change the surface water. Water pollution has now become an essential study for scientists in environmental engineering, hydrology, chemical engineering, and mathematics to find the best management policies to the pollution problem (Wadi *et al*., 2014). The investigation on the transport of nitrate nutrients in surface water is vital for better assessment and restoration of the water body. Also, the study is necessary to suitably evaluate the fate and the level of pollution caused by nitrate nutrients in the water column. Furthermore, it will make the water safe for aquatic habitat usage and human consumption.

The impact of pollution incidents on rivers and streams could be predicted using water quality modeling tools. The process of applying mathematical techniques in solving solute transport in a water system yields a good result in the management process of the receiving water. Thus, modeling in the form of mathematical solutions is becoming more useful and forming a fundamental part of the water body management. An effective method of controlling and predicting water pollution is the use of mathematical models. There are numerous methods of solving solute transport problems in a natural river such as the ADE model, the CIS model, and the ADZ model. However, some issues are associated with the existing methods, which were described in Kumarasamy (2015), and Olowe and Kumarasamy (2017). Ghosh (2001) developed a new method recognized as the hybrid cell-in-series (HCIS) model techniques used to solve pollutant transport problems in rivers and streams. It was observed that the HCIS model overcomes the limitation associated with existing methods of solving solute transport in surface water. This study focused on developing an analytical solution for the hybrid cells-in-series method along with the kinetic reaction of nitrate (HCIS-NO_3). The solution obtained for the HCIS-NO_3 model was applied to monitor the variation of nitrate concentration in the uMgeni River. Also, the results of the HCIS-NO_3 model was verified in comparison with the results obtained for the numerical solution of the Fickian ADE equation solved with explicit finite difference scheme. This research will allow the useful contribution to understanding the effect of nitrate pollutant transport problems in surface water.

5.3. The Model Development

The section focused on developing a hybrid model component to study the effect of nitrate nutrients in surface water by monitoring its concentration along the river reach. The flow and transport of nitrate pollutants within the water column was assumed to be one-dimensional. The concentration of nitrate

pollutant Cc (x, t) in mg/l was presumed to fluctuate with time (t) in minutes along the length (x) in m of the river reach which is affected by a point source of organic waste. Also, the flow of the river was described as a steady state condition. The sources of nitrate in the water bodies were due to nitrification of nitrite to nitrate through the action of nitrobacter bacteria under aerobic conditions and from agricultural and industrial waste. Denitrification of nitrate to nitrogen gas was considered as a source of removal of nitrate in the river which takes place under anaerobic conditions (Boyer *et al.*, 2006) and uptake by aquatic plants such as algae. The HCIS model is typically based on analytical methods that incorporate a combination of plug flow and a two well-mixed cells reactor approach for pollutant transport.

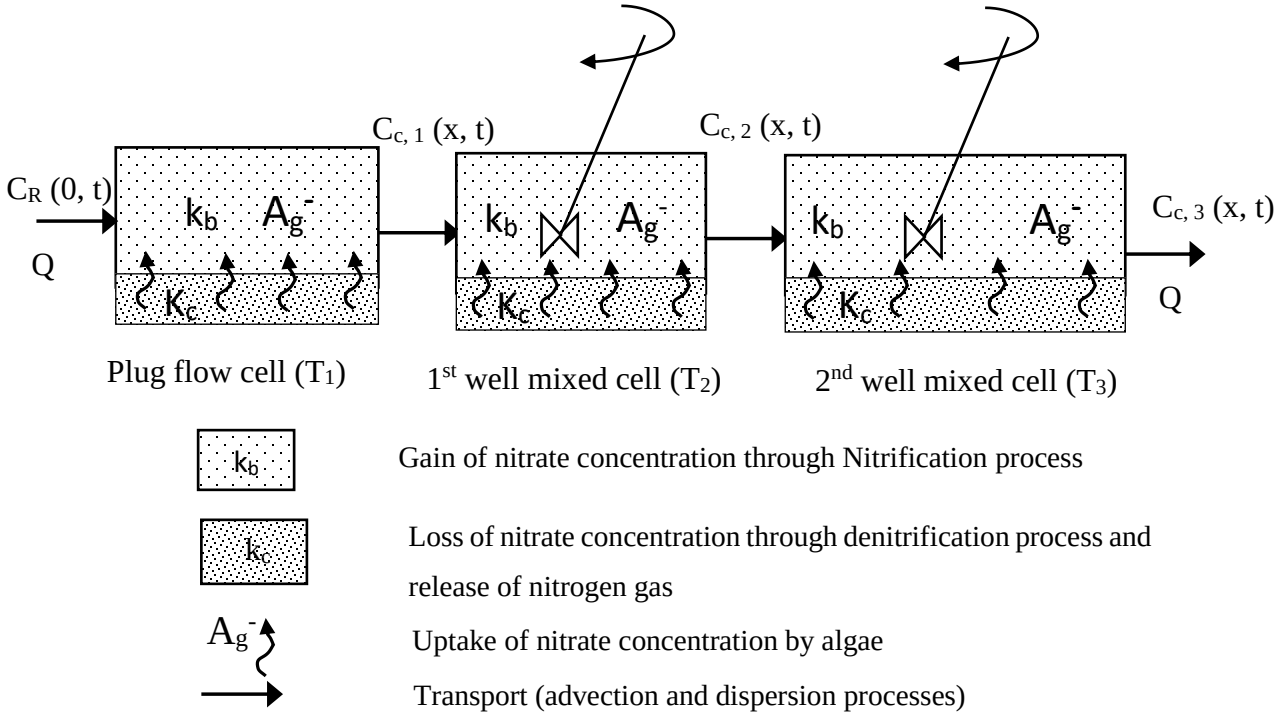

Figure 5. 1: The process of nitrate pollutant concentration though a hybrid unit cell

A river reach is divided into a series of conceptual hybrid units. The hybrid unit is comprised of a plug cell and two thoroughly mixed cells as presented in Figure 5.1. It was assumed that the nitrate concentration has an initial value of zero in each cell. Also, the boundary concentration varies from zero to C_R when the time is equal to zero. Where C_R is the nitrate pollutant concentration at the inlet boundary. Nitrification and denitrification processes were considered in all the cells of the hybrid units as the pollutant travels downstream. Furthermore, consumption of nitrate for algae growth also takes place in all the cells. Effluent from the plug flow will enter the first mixing cell where it gets thoroughly mixed

for a period and later enters the second mixing cell and is carefully mixed. Thus, it can be concluded that the transport of nitrate in the plug flow cell signifies the advection process and also, an advection and dispersion process take in the two-mixing cells. In this study, the analytical solution was derived using Laplace transform techniques and a mass balance concept. Convolution techniques were used to determine the nitrate pollutant at the end of subsequent hybrid units. The nitrate-nutrient undergoes kinetic reactions based on nitrification rate, denitrification rate, nitrate uptake by biomass and algae. Kinnunen *et al.* (1982) expressed the first order kinetic equation of nitrate concentration as presented below:

$$\frac{\partial C_c(x,t)}{\partial t} = k_b C_b(x,t) - (1 - F(t))\alpha\mu A_g(t) - k_c C_c(x,t) \tag{5.1}$$

Where, C_c and C_b signify the concentration of nitrate and nitrite in mg/l respectively, and the rate of oxidation of nitrite is represented as K_b in day-^{1}. In addition, the portion of algae nitrogen from ammonia is represented as F, the portion of algae biomass is α in mg-N/mg-A. Ag [mg-A/l] is the algae biomass concentration, μ [day-^{1}] represents the growth rate of algae, K_c signifies the denitrification rate coefficient [day-^{1}]. From the equation, the right-hand side indicates the source of nitrate concentration and the uptake of nitrate by algae is represented by the second term. In addition, the last term designates denitrification of nitrate to nitrogen gas which depends on temperature.

The rate of loss of nitrate concentration in the model formulation was assumed to be due to denitrification and algae consumption. Denitrification takes place in the sediment part of the river body where the oxygen levels are depleted. Furthermore, conversion of nitrite to nitrate also contributes to additional nitrate concentration in the water column. Nitrification occurs in the upper oxic layer of the sediment while denitrification arises under this layer (Marchant *et al.*, 2016). A factor that influences the rate of denitrification in water bodies is the level of nitrate concentration in surface water. Hence, it could be described that the rate of denitrification in the water column is proportional to nitrate concentration. The mathematical expression for the denitrification rate is presented in Eq. (5.2) as described in Wool *et al.* (2006):

$$k_c = k_c \theta^{(T-20)} \frac{DO}{K_{nit} + DO} C_c \tag{5.2}$$

Where, DO signifies dissolved oxygen [mg/l], kc [day-1] represents the denitrification rate coefficient at 20^{o}C, K_{nit} is the oxygen half saturation constant [mg/l].

The algae biomass concentration can be expressed by the differential equation below as described by Brown and Barnwell (1987).

$$\frac{\partial A_g(t)}{\partial t} = (\mu - \rho) A_g(t) \tag{5.3}$$

Where, Ag [mg-A/l] is the algae biomass concentration; μ [day-^{1}] signifies the algae growth coefficient; ρ [day-^{1}] signifies the algae respiration rate coefficients which are also temperature dependent. The algae growth and respiration are the one process to be considered when modeling nitrate nutrient in water bodies.

Integrating Eq. (5.3) with respect to time to yield the solution shown below:

$$A_g(t) = A_o e^{(\mu-\rho)t} \tag{5.4}$$

Eq. (5.4) was modified as:

$$A_g(x,t) = A_o e^{(\mu-\rho)\left(t-\frac{x}{u}\right)} \tag{5.5}$$

The above equation was solved by Laplace transform technique to yield:

$$A_g^* = \frac{A_o e^{-(\mu-\rho)\frac{x}{u}}}{[s-(\mu-\rho)]} \tag{5.6}$$

5.3.1. Formulation of nitrate concentration in the plug flow cell

A plug flow cell was assumed to have control volume (V) and was considered to transport a concentration of nitrate pollutants downstream. It has a length (Δx) which is considered to have a series of sections that contain a plume of water. (T_1) is the time required for the fluid to stay in the cell before it is replaced. The residence time (T_1) describes the relation between V and Q. Nitrate concentration in the cell is represented as Cc (x, t). A time interval (Δt) was considered where a fraction of the nitrate concentration is transformed to nitrogen gas through the process of denitrification and the consumption of nitrate by an algae biomass. In addition, the nitrification process takes place within the cell. After the nitrification and denitrification process has taken place within the cell, the remaining nitrate pollutant in the cell will move to the next control volume. Thus, a partial differential equation is formulated as:

$$\frac{\partial C_c(x,t)}{\partial t} + u\frac{\partial C_c(x,t)}{\partial x} = k_b C_b(x,t) - (1-F(t))\alpha\mu A_g(t) - k_c C_c(x,t) \tag{5.7}$$

Where, C_c (x, t) [mg-A/l] represents the nitrate concentration in the cell and C_b (x, t) [mg-A/l] indicates the nitrite concentration within the cell.

The initial and boundary condition used to solve equation (5.7) is stated below:

$C_c(x,0) = 0$ x>0; t =0

$C_c(0,t) = C_R$ t≥0; x = 0

$C_c(T_1 u, t) = 0$ 0<t<T_1

Applying Laplace transformations to Eq. (7), we have:

$$sC_c^* + u\frac{dC_c^*}{dx} = k_b C_b^* - (1-F)\alpha\mu A_g^* - k_c C_c^* \tag{5.8}$$

Re-arranging Eq. (8) and substitute Eq. (6) to yield:

$$\frac{dC_c{}^*}{dx} = \left[-\left(\frac{s+k_c}{u}\right) C_c{}^* + \left(\frac{k_b C_b{}^*}{u}\right) - \left(\frac{(1-F)\alpha A_o e^{-(\mu-\rho)\frac{x}{u}}}{(s-\mu+\rho)u}\right)\right] \tag{5.9}$$

The nitrate concentration at the end of the cell is described in Eq. (5.10) by solving Eq. (5.9) using the integration method and applying the boundary and initial conditions which is valid for t ≥ T1.

$$C_C(x,t) = \left[\begin{array}{l} \left(C_R U(t-T_1)e^{-k_c T_1}\right) + \left(\frac{k_b c_{b,1}(x,t)}{k_c}\left\{e^{-k_c t} - e^{-k_c T_1}U(t-T_1)e^{-k_c(t-T_1)}\right\}\right) \\ -\left(\frac{(1-F)\alpha\mu A_o e^{(\rho-\mu)T_1}}{k_c}\left\{e^{-(\rho-\mu)t} - e^{(k_c+\rho-\mu)t}\right\}\right) \\ +\left(\frac{(1-F)\alpha\mu A_o}{k_c}e^{-k_c T_1}U(t-T_1)\left\{e^{-(\rho-\mu)(t-T_1)} - e^{(k_c+\rho-\mu)(t-T_1)}\right\}\right) \end{array}\right] \tag{5.10}$$

Where,C_c (x, t) indicates the quantity of nitrate at the end of the cell in mg/l, $C_{b,1}$ is the nitrite concentration in the plug flow, U (t – T1) is a step function.

5.3.2. Formulation of nitrate concentration in the first thoroughly mixed cell

The amount of nitrate solute from the previous cell will be the influent to the first mixed cell. The process that takes place within the first mixing cell includes the nitrification and denitrification processes. In addition, consumption of nitrate concentration for algae growth also takes place within the cell. Let the residence time of the cell represent $T_2 = V_2/Q$. The following mass balance was formulated in the cell:

$$C_{c,1}Q\Delta t - C_{c,2}Q\Delta t + k_b C_{b,2}V_2\Delta t - (1-F)\alpha\mu A_g(t)V_2\Delta t - k_c C_{c,2}V_2\Delta t = V_2\Delta C_{c,2} \tag{5.11}$$

The first and second term indicate the mass of nitrate pollutant flowing into and leaving the cell respectively. In addition, the mass due to nitrite concentration is represented by the third term which indicate a source of nitrate, the fourth term is due to algae growth. The last term is the conversion of nitrate to nitrogen gas due to the denitrification process. The right-hand side is the change in mass of nitrate concentration within the cell. Eq. (5.11) was expressed in an ordinary differential form, then solved to estimate the nitrate concentration at the end of the cell to yield the following solution:

$$C_{c,2} = \left[\begin{array}{l} \left(\frac{C_R U(t-T_1)}{(1+k_cT_2)}\left\{e^{-k_cT_1} - e^{\left(\frac{1}{T_2}\right)[T_1-t]}e^{-k_ct}\right\}\right) + \left(\frac{k_bC_{b,1}e^{-\left(\frac{1+k_cT_2}{T_2}\right)t}}{k_c}\{A\}\right) \\ -\left(\frac{k_bC_{b,1}}{k_c}\{B\}\right) - \left(\frac{(1-F)\alpha\mu A_o e^{(\rho-\mu)T_1}}{k_c}\{D\}\right) + \left(\frac{(1-F)U(t-T_1)\alpha\mu A_o}{k_c}\{E\}\right) \\ +\left(\frac{k_bC_{b,2}T_2}{(1+k_cT_2)}\{G\}\right) - \left(\frac{(1-F)\alpha\mu A_o T_2}{(T_2\mu - T_2\rho + 1 + T_2k_c)}\{J\}\right) \end{array}\right] \tag{5.12}$$

where,

$$A = \left\{e^{\left(\frac{1}{T_2}\right)t} - U(t-T_1)e^{\left(\frac{1}{T_2}\right)t}\right\}; \qquad B = \left\{e^{\left(\frac{1}{T_2}\right)T_1} - U(t-T_1)e^{\left(\frac{1}{T_2}\right)T_1}\right\}$$

$$D=\left\{\begin{array}{l}\dfrac{e^{-(\rho-\mu)t}}{\left(T_2\rho-T_2\mu-1-T_2k_c\right)}-\dfrac{e^{(k_c+\rho-\mu)t}}{\left(2k_cT_2+\rho T_2-\mu T_2+1\right)}\\ -\dfrac{e^{-(\rho-\mu)T_1}e^{\left(\frac{1}{T_2}\right)[T_1-t]}e^{k_c(T_1-t)}}{\left(T_2\rho-T_2\mu-1-T_2k_c\right)}+\dfrac{e^{(k_c+\rho-\mu T_1)t}e^{\left(\frac{1+k_cT_2}{T_2}\right)[T_1-t]}}{\left(2k_cT_2+\rho T_2-\mu T_2+1\right)}\end{array}\right\}$$

$$E=\left\{\begin{array}{l}\dfrac{e^{-\left(\frac{1+k_cT_2}{T_2}\right)t}e^{(\rho-\mu)T_1}e^{\left(\rho-\mu-k_c-\frac{1}{T_2}\right)t}}{\left(T_2\rho-T_2\mu-1-T_2k_c\right)}-\dfrac{e^{(k_c+\rho-\mu)[t-T_1]}}{\left(2k_cT_2+\rho T_2-\mu T_2+1\right)}\\ -\dfrac{e^{-\left(\frac{1+k_cT_2}{T_2}\right)[T_1+t]}}{\left(T_2\rho-T_2\mu-1-T_2k_c\right)}-\dfrac{e^{\left(\frac{1+k_cT_2}{T_2}\right)[T_1-t]}}{\left(2k_cT_2+\rho T_2-\mu T_2+1\right)}\end{array}\right\}$$

$$G=\left\{1-e^{\left(\frac{1+k_cT_2}{T_2}\right)[T_1-t]}\right\};\qquad J=\left\{e^{(\mu-\rho)t}-e^{(\mu-\rho)T_1}e^{\left(\frac{1+k_cT_2}{T_2}\right)[T_1-t]}\right\}$$

The concentration of nitrate at the end of the zone is represented in Eq. (5.12). Where, $C_{b,1}$ and $C_{b,2}$ (mg/l) evaluate the quantity of nitrite at the end of plug flow and first mixed cell respectively.

5.3.3. Formulation of nitrate concentration in the second thoroughly mixed cell

T_3 represents the residence time of the cell, where effluent from the previous cell is the inflow into the cell. Consequently, nitrification, denitrification, and consumption of nitrate concentration for algae growth take place within the cell. Carrying out the mass balance in the cell as described in Eq. (5.13).

$$C_{c,2}Q\Delta t-C_{c,3}Q\Delta t+k_bC_{b,3}V_3\Delta t-(1-F)\alpha\mu A_g(t)V_3\Delta t-k_cC_{c,3}V_3\Delta t=V_3\Delta C_{c,3} \tag{5.13}$$

The first and second term indicate the mass of nitrate pollutant flowing into and leaving the cell respectively. In addition, the mass due to nitrite concentration is represented by the third term which indicates a source of nitrate, the fourth term is due to algae growth. The last term is the conversion of nitrate to nitrogen gas due to the denitrification process. The right-hand side is the change in mass of nitrate concentration within the cell. The following ordinary differential equation was formulated from Eq. (5.13):

$$\frac{dC_{c,3}}{dt}+\left(\frac{1+k_cT_3}{T_3}\right)C_{c,3}=\frac{C_{c,2}}{T_3}+k_bC_{b,3}-(1-F)\alpha\mu A_o e^{(\mu-\rho)t} \tag{5.14}$$

Insert Eq. (5.12) into Eq. (5.14) and solved by method of integration to determine the concentration of nitrate at the end of a hybrid unit which yields:

$$C_{c,3}=\left[\begin{array}{l}\left(\frac{C_RU(t-T_1)}{(1+k_cT_2)}\{\varpi\}\right)-\left(\frac{(1-F)\alpha\mu A_o e^{(\rho-\mu)T_1}}{k_c}\{\theta\}\right)+\left(\frac{(1-F)U(t-T_1)\alpha\mu A_o}{k_c}\{\vartheta\}\right)\\+\left(\frac{T_2k_bC_{b,2}}{(1+k_cT_2)(1+k_cT_3)}\{\chi\}\right)-\left(\frac{(1-F)\alpha\mu A_oT_2}{(T_2\mu-T_2\rho+1+T_2k_c)}\{\gamma\}\right)+\left(\frac{T_3k_bC_{b,3}}{(1+k_cT_3)}\{\varepsilon\}\right)\\-\left(\frac{(1-F)\alpha\mu A_o e^{-(\rho-\mu)t}T_3}{(T_2\mu-T_2\rho+1+T_3k_c)}\{\eta\}\right)\end{array}\right] \tag{5.15}$$

$$K_{HCIS-NO_3}=\left[\begin{array}{l}\left(\frac{U(t-T_1)}{(1+k_cT_2)}\{\varpi\}\right)-\left(\frac{(1-F)\alpha\mu A_o e^{(\rho-\mu)T_1}}{k_c}\{\theta\}\right)+\left(\frac{(1-F)U(t-T_1)\alpha\mu A_o}{k_c}\{\vartheta\}\right)\\\left(+\frac{T_2k_bC_{b,2}}{(1+k_cT_2)(1+k_cT_3)}\{\chi\}\right)-\left(\frac{(1-F)\alpha\mu A_oT_2}{(T_2\mu-T_2\rho+1+T_2k_c)}\{\gamma\}\right)+\left(\frac{T_3k_bC_{b,3}}{(1+k_cT_3)}\{\varepsilon\}\right)\\\left(-\frac{(1-F)\alpha\mu A_o e^{-(\rho-\mu)t}T_3}{(T_2\mu-T_2\rho+1+T_3k_c)}\{\eta\}\right)\end{array}\right] \tag{5.16}$$

where, $\varpi=\left\{\frac{e^{-k_cT_1}}{(1+k_cT_3)}-e^{\left(\frac{1}{T_2}\right)[T_1-t]}e^{-k_ct}-\frac{e^{-k_ct}e^{\left(\frac{1}{T_3}\right)[T_1-t]}}{(1+k_cT_3)}+e^{\left(\frac{1}{T_2}\right)[T_1-t]}e^{-k_ct}e^{\left(\frac{1}{T_3}\right)[T_1-t]}\right\}$

$$\theta=\left\{\begin{array}{l}\dfrac{e^{-(\rho-\mu)t}}{\left(T_2\rho-T_2\mu-1-T_2k_c\right)\left(T_3\rho-T_3\mu-1-T_3k_c\right)}-\dfrac{e^{(k_c+\rho-\mu)t}}{\left(2T_2k_c+T_2\rho-T_2\mu+1\right)\left(2T_3k_c+T_3\rho-T_3\mu+1\right)}\\ -\dfrac{e^{-(\rho-\mu)T_1}e^{\left(\frac{1+k_cT_2}{T_2}\right)[T_1-t]}}{\left(T_2\rho-T_2\mu-1-T_2k_c\right)\left(1+k_cT_3\right)}+\dfrac{e^{(k_c+\rho-\mu)t}e^{\left(\frac{1+k_cT_2}{T_2}\right)[T_1-t]}}{\left(2T_2k_c+T_2\rho-T_2\mu+1\right)\left(2T_3k_c+T_3\rho-T_3\mu+1\right)}\\ -\dfrac{e^{-(\rho-\mu)T_1}e^{-\left(\frac{1+k_cT_3}{T_3}\right)[T_1+t]}}{\left(T_2\rho-T_2\mu-1-T_2k_c\right)\left(T_3\rho-T_3\mu-1-T_3k_c\right)}+\dfrac{e^{(k_c+\rho-\mu)T_1}e^{\left(\frac{1+k_cT_3}{T_3}\right)[T_1-t]}}{\left(2T_2k_c+T_2\rho-T_2\mu+1\right)\left(2T_3k_c+T_3\rho-T_3\mu+1\right)}\\ +\dfrac{e^{-(\rho-\mu)T_1}e^{\left(\frac{1+k_cT_2}{T_2}\right)[T_1-t]}e^{\left(\frac{1+k_cT_3}{T_3}\right)[T_1-t]}}{\left(T_2\rho-T_2\mu-1-T_2k_c\right)\left(1+k_cT_3\right)}-\dfrac{e^{(k_c+\rho-\mu)T_1}e^{\left(\frac{1+k_cT_3}{T_3}\right)[T_1-t]}e^{\left(\frac{1+k_cT_2}{T_2}\right)[T_1-t]}}{\left(2T_2k_c+T_2\rho-T_2\mu+1\right)\left(2T_3k_c+T_3\rho-T_3\mu+1\right)}\end{array}\right\}$$

$$\vartheta=\left\{\begin{array}{l}\dfrac{e^{(\rho-\mu)[T_1+t]}}{\left(T_2\rho-T_2\mu-1-T_2k_c\right)\left(T_3\rho-T_3\mu+1+T_3k_c\right)}-\dfrac{e^{(k_c+\rho-\mu)[t-T_1]}}{\left(2T_2k_c+T_2\rho-T_2\mu+1\right)\left(1+k_cT_3\right)}\\ -\dfrac{e^{-\left(\frac{1+k_cT_3}{T_3}\right)[T_1+t]}}{\left(T_2\rho-T_2\mu-1-T_2k_c\right)\left(1+k_cT_3\right)}-\dfrac{e^{\left(\frac{1+k_cT_2}{T_2}\right)[T_1-t]}}{\left(2T_2k_c+T_2\rho-T_2\mu+1\right)\left(1+k_cT_3\right)}\\ -\dfrac{e^{\left(\frac{1+k_cT_3}{T_3}\right)[T_1-t]}}{\left(T_2\rho-T_2\mu-1-T_2k_c\right)\left(T_3\rho-T_3\mu+1+T_3k_c\right)}+\dfrac{e^{(k_c+\rho-\mu)[t-T_1]}e^{\left(\frac{1+k_cT_3}{T_3}\right)[T_1-t]}}{\left(2T_2k_c+T_2\rho-T_2\mu+1\right)\left(1+k_cT_3\right)}\\ +\dfrac{e^{-\left(\frac{1+k_cT_3}{T_3}\right)[T_1+t]}}{\left(T_2\rho-T_2\mu-1-T_2k_c\right)\left(1+k_cT_3\right)}+\dfrac{e^{\left(\frac{1+k_cT_2}{T_2}\right)[T_1-t]}}{\left(2T_2k_c+T_2\rho-T_2\mu+1\right)\left(1+k_cT_3\right)}\end{array}\right\}$$

$$\chi=\left\{1-e^{\left(\frac{1+k_cT_2}{T_2}\right)[T_1-t]}-e^{\left(\frac{1+k_cT_3}{T_3}\right)[T_1-t]}+e^{\left(\frac{1+k_cT_2}{T_2}\right)[T_1-t]}e^{\left(\frac{1+k_cT_3}{T_3}\right)[T_1-t]}\right\}$$

$$\gamma=\left\{\begin{array}{l}\dfrac{e^{(\mu-\rho)t}}{\left(T_3\mu-T_3\rho+1+T_3k_c\right)}-\dfrac{e^{(\mu-\rho)T_1}e^{\left(\frac{1+k_cT_2}{T_2}\right)[T_1-t]}}{\left(1+k_cT_3\right)}\\ -\dfrac{e^{(\mu-\rho)T_1}e^{\left(\frac{1+k_cT_3}{T_3}\right)[T_1-t]}}{\left(T_3\mu-T_3\rho+1+T_3k_c\right)}+\dfrac{e^{(\mu-\rho)T_1}e^{\left(\frac{1+k_cT_2}{T_2}\right)[T_1-t]}e^{\left(\frac{1+k_cT_3}{T_3}\right)[T_1-t]}}{\left(1+k_cT_3\right)}\end{array}\right\}$$

$$\varepsilon = \left\{1 - e^{\left(\frac{1+k_c T_3}{T_3}\right)[T_1 - t]}\right\} \qquad \eta = \left\{1 - e^{(\mu-\rho)T_1} e^{\left(\frac{1+k_c T_3}{T_3}\right)[T_1 - t]}\right\}$$

The concentration of nitrate at the end of a unit is represented in Eq. (5.15). For a unit step input, i.e. C_R = 1 which is injected, Eq. (5.16) predicts the nitrate pollutants at the end of a unit. $K_{HCIS-NO3}$ designates the step response function. In Eq. (5.15), $C_{c,3}$ [mg/l] is the concentration of nitrate pollutant at the end of a hybrid unit. $C_{b,2}$ and $C_{b,3}$ (mg/l) are nitrite concentrations at the first and second mixed cells respectively.

The unit impulse response function $\delta_{HCIS-NO3}$ (n,Δt) was estimated using:

$$\delta_{HCIS-NO_3}(n, \Delta t) = \frac{K_{HCIS-NO_3}(n\Delta t) - K_{HCIS-NO_3}((n-1)\Delta t)}{\Delta t} \tag{5.17}$$

$$C_{c,3} = \left[\begin{array}{l} \left(\frac{C_R U(t-T_1)}{(1+k_c T_2)}\{D1\}\right) - \left(\frac{(1-F)\alpha\mu A_o e^{(\rho-\mu)T_1}}{k_c}\{D2\}\right) + \left(\frac{(1-F)U(t-T_1)\alpha\mu A_o}{k_c}\{D3\}\right) \\ + \left(\frac{T_2 k_b C_{b,2}}{(1+k_c T_2)(1+k_c T_3)}\{D4\}\right) - \left(\frac{(1-F)\alpha\mu A_o T_2}{(T_2\mu - T_2\rho + 1 + T_2 k_c)}\{D5\}\right) + \left(\frac{T_3 k_b C_{b,3}}{(1+k_c T_3)}\{D6\}\right) \\ - \left(\frac{(1-F)\alpha\mu A_o e^{-(\rho-\mu)t} T_3}{(T_2\mu - T_2\rho + 1 + T_3 k_c)}\{D7\}\right) \end{array}\right] \tag{5.18}$$

$$D1 = \left\{\begin{array}{l} \frac{e^{-k_c T_1}}{(1+k_c T_3)} + \frac{(1+k_c T_2) e^{\left(\frac{1+k_c T_2}{T_2}\right)t} e^{\left(\frac{1}{T_2}\right)T_1}}{T_2} + \frac{(1+k_c T_3) e^{\left(\frac{1+k_c T_3}{T_3}\right)t} e^{\left(\frac{1}{T_3}\right)T_1}}{T_3(1+k_c T_3)} \\ - \frac{(T_3 + k_c T_2 T_3 + T_2) e^{-t\left(\frac{T_3 + k_c T_2 T_3 + T_2}{T_2 T_3}\right)} e^{\left(\frac{T_3+T_2}{T_2 T_3}\right)T_1}}{T_2 T_3} \end{array}\right\}$$

$$D2=\left\{\begin{array}{l}
-\dfrac{(\rho-\mu)e^{-(\rho-\mu)t}}{(T_2\rho-T_2\mu-1-T_2k_c)(T_3\rho-T_3\mu-1-T_3k_c)}-\dfrac{(k_c+\rho-\mu)e^{(k_c+\rho-\mu)t}}{(2T_2k_c+T_2\rho-T_2\mu+1)(2T_3k_c+T_3\rho-T_3\mu+1)} \\
+\dfrac{(1+k_cT_2)e^{-(\rho-\mu)T_1}e^{\left(\frac{1+k_cT_2}{T_2}\right)[T_1-t]}}{T_2(T_2\rho-T_2\mu-1-T_2k_c)(1+k_cT_3)}+\dfrac{(\rho-\mu-1)e^{\left(\frac{\rho-\mu-1}{T_2}\right)t}e^{\left(\frac{1+k_cT_2}{T_2}\right)T_1}}{T_2(2T_2k_c+T_2\rho-T_2\mu+1)(2T_3k_c+T_3\rho-T_3\mu+1)} \\
+\dfrac{(1+k_cT_3)e^{-(\rho-\mu)T_1}e^{-\left(\frac{1+k_cT_3}{T_3}\right)[T_1+t]}}{T_3(T_2\rho-T_2\mu-1-T_2k_c)(T_3\rho-T_3\mu-1-T_3k_c)}+\dfrac{(1+k_cT_3)e^{(k_c+\rho-\mu)T_1}e^{\left(\frac{1+k_cT_3}{T_3}\right)[T_1-t]}}{T_3(2T_2k_c+T_2\rho-T_2\mu+1)(2T_3k_c+T_3\rho-T_3\mu+1)} \\
+\dfrac{(1+k_cT_2)(1+k_cT_3)e^{-(\rho-\mu)T_1}e^{\left(\frac{1+k_cT_2}{T_2}\right)[T_1-t]}e^{\left(\frac{1+k_cT_3}{T_3}\right)[T_1-t]}}{T_2T_3(T_2\rho-T_2\mu-1-T_2k_c)(1+k_cT_3)}-\dfrac{(1+k_cT_2)(1+k_cT_3)e^{(k_c+\rho-\mu)T_1}e^{\left(\frac{1+k_cT_3}{T_3}\right)[T_1-t]}e^{\left(\frac{1+k_cT_2}{T_2}\right)[T_1-t]}}{T_2T_3(2T_2k_c+T_2\rho-T_2\mu+1)(2T_3k_c+T_3\rho-T_3\mu+1)}
\end{array}\right\}$$

$$D3=\left\{\begin{array}{l}
\dfrac{(\rho-\mu)e^{(\rho-\mu)[T_1+t]}}{(T_2\rho-T_2\mu-1-T_2k_c)(T_3\rho-T_3\mu+1+T_3k_c)}-\dfrac{(k_c+\rho-\mu)e^{(k_c+\rho-\mu)[t-T_1]}}{(2T_2k_c+T_2\rho-T_2\mu+1)(1+k_cT_3)} \\
+\dfrac{(1+k_cT_3)e^{-\left(\frac{1+k_cT_3}{T_3}\right)[T_1+t]}}{T_3(T_2\rho-T_2\mu-1-T_2k_c)(1+k_cT_3)}+\dfrac{(1+k_cT_2)e^{\left(\frac{1+k_cT_2}{T_2}\right)[T_1-t]}}{T_2(2T_2k_c+T_2\rho-T_2\mu+1)(1+k_cT_3)} \\
+\dfrac{(1+k_cT_3)e^{\left(\frac{1+k_cT_3}{T_3}\right)[T_1-t]}}{T_3(T_2\rho-T_2\mu-1-T_2k_c)(T_3\rho-T_3\mu+1+T_3k_c)}-\dfrac{(1+k_cT_3)e^{(k_c+\rho-\mu)[t-T_1]}e^{\left(\frac{1+k_cT_3}{T_3}\right)[T_1-t]}}{T_3(2T_2k_c+T_2\rho-T_2\mu+1)(1+k_cT_3)} \\
-\dfrac{(1+k_cT_3)e^{-\left(\frac{1+k_cT_3}{T_3}\right)[T_1+t]}}{T_3(T_2\rho-T_2\mu-1-T_2k_c)(1+k_cT_3)}-\dfrac{(1+k_cT_2)e^{\left(\frac{1+k_cT_2}{T_2}\right)[T_1-t]}}{T_2(2T_2k_c+T_2\rho-T_2\mu+1)(1+k_cT_3)}
\end{array}\right\}$$

$$D4=\left\{1+\frac{(1+k_cT_2)e^{\left(\frac{1+k_cT_2}{T_2}\right)[T_1-t]}}{T_2}+\frac{(1+k_cT_3)e^{\left(\frac{1+k_cT_3}{T_3}\right)[T_1-t]}}{T_3}+\frac{(1+k_cT_2)(1+k_cT_3)e^{\left(\frac{1+k_cT_2}{T_2}\right)[T_1-t]}e^{\left(\frac{1+k_cT_3}{T_3}\right)[T_1-t]}}{T_2T_3}\right\}$$

$$D5=\left\{\begin{array}{l}
\dfrac{(\mu-\rho)e^{(\mu-\rho)t}}{(T_3\mu-T_3\rho+1+T_3k_c)}+\dfrac{(1+k_cT_2)e^{(\mu-\rho)T_1}e^{\left(\frac{1+k_cT_2}{T_2}\right)[T_1-t]}}{T_2(1+k_cT_3)} \\
+\dfrac{(1+k_cT_3)e^{(\mu-\rho)T_1}e^{\left(\frac{1+k_cT_3}{T_3}\right)[T_1-t]}}{T_3(T_3\mu-T_3\rho+1+T_3k_c)}+\dfrac{(1+k_cT_2)(1+k_cT_3)e^{(\mu-\rho)T_1}e^{\left(\frac{1+k_cT_2}{T_2}\right)[T_1-t]}e^{\left(\frac{1+k_cT_3}{T_3}\right)[T_1-t]}}{T_2T_3(1+k_cT_3)}
\end{array}\right\}$$

$$D6 = \left\{ 1 + \frac{(1 + k_c T_3) e^{\left(\frac{1+k_c T_3}{T_3}\right)[T_1 - t]}}{T_3} \right\}, \qquad D7 = \left\{ 1 + \frac{(1 + k_c T_3) e^{(\mu-\rho)T_1} e^{\left(\frac{1+k_c T_3}{T_3}\right)[T_1 - t]}}{T_3} \right\}$$

Eq. (5.15) and (5.18) illustrate the unit step and impulse response functions at the end of a unit.

The nitrate concentration at subsequent units was estimated by applying the convolution technique by considering a river reach which consists of a series of hybrid units having a size (Δx) as presented in Figure 3.5.

5.4. Model Verification using a Numerical Approach

The potential of the HCIS-NO_3 model was demonstrated by comparing with the performance of the Fickian-based model. Therefore, the ADE-NO_3 model was formulated as:

$$\frac{\partial C_c(x,t)}{\partial t} = -u \frac{\partial C_c(x,t)}{\partial x} + D_L \frac{\partial^2 C_c(x,t)}{\partial x} + k_b C_b(x,t) - (1 - F)\alpha\mu A_g - k_c C_c(x,t) \tag{5.19}$$

Where, C_c and C_b signify the concentration of nitrate and nitrite respectively, the rate of oxidation of nitrite is represented as K_b in day-^{1}. In addition, the portion of algae nitrogen from ammonia is represented as F, the portion of algal biomass is α in mg-N/mg-A. A_g signifies the algae concentration [mg-A/l], μ [day-^{1}] indicates the algae growth rate, K_c is the rate of denitrification coefficient [day-^{1}].

The explicit finite difference method was used to resolve the numerical equations of the ADE-NO_3 model. The boundary and initial condition applied for the HCIS-NO_3 model equation was used in solving Eq. (5.19). The approximate value of the unknown at some grid points were determined by using the scheme when the boundary and initial conditions were known.

$$\frac{\partial C_c(x,t)}{\partial t} = \frac{C_c(x,t+\Delta t) - C_c(x,t)}{\Delta t} \tag{5.20}$$

$$\frac{\partial C_c(x,t)}{\partial x} = \frac{C_c(x+\Delta x,t) - C_c(x-\Delta x,t)}{2\Delta x} \tag{5.21}$$

$$\frac{\partial^2 C_c(x,t)}{\partial x^2} = \frac{C_c(x+\Delta x,t) - 2C_c(x,t) + C_c(x-\Delta x,t)}{\Delta x^2} \tag{5.22}$$

Eq. (5.20) – (5.22) were substituted into Eq. (5.19) and solved to obtain the step response function as expressed below:

$$C(x,t+\Delta t)=\begin{bmatrix}\left(C(x,t)\left[1-\frac{2D_L\Delta t}{(\Delta x)^2}-k_c\Delta t\right]\right)-\left(C(x+\Delta x,t)\left[\frac{u\Delta t}{2\Delta x}-\frac{D_L\Delta t}{(\Delta x)^2}\right]\right)\\+\left(C(x-\Delta x,t)\left[\frac{u\Delta t}{2\Delta x}+\frac{D_L\Delta t}{(\Delta x)^2}\right]\right)+\left(k_bC_b(x,t)-(1-F)\alpha\mu A_o e^{(\mu-\rho)t}\right)\Delta t\end{bmatrix} \quad (5.23)$$

The stability of the solution can generally be found for a small Courant number ($C_r = u\Delta t/\Delta x$). However, for a large Courant number the solution exhibits an oscillatory performance. Thus, the time step and grid space were chosen as Δt = 1min and Δx =100m, respectively hence ($u\Delta t/\Delta x \leq 1$).

5.5. Results and Discussion

5.5.1. Simulation and testing of Nitrate transport with synthetic data

In this section, hypothetical data sets were used to understand the capabilities of the analytical solution obtained in this research. The model parameters were determined using Eq. (3.20) – (3.22) with known dispersion coefficient (D_L), flow velocity (u), and the hybrid unit's size (Δx). Consequently, the properties chosen for the river reach were u = 20m/min, D_L = 1000m^2/min, and Δx = 200m having satisfied the peclet number condition (Pe $\geq$ 4) (Ghosh, 2001). Thus, the three-time model parameters T_1, T_2, and T_3 were 1.70min, 2.3min, and 6.0min respectively. In addition, the kinetics parameters used for this model were presented in Table 5.1. Hypothetical data sets were applied to the HCIS-NO_3 model to simulate the nitrate pollutant concentration along the river downstream. The effects of nitrate loss due to denitrification, which depends on temperature, was considered in the simulation. In addition, the uptake of nitrate for algae growth and nitrification of nitrites, as a source of nitrate in the river were considered. To illustrate the denitrification process within the hybrid units, the estimated parameters (T_1, T_2, and T_3) were used to determine the unit impulse and step response functions of a unit by means of Eq. (5.15) and (5.18). The denitrification rate factor k_c = (0.005 and 0.002 per min) were compared keeping other parameters constant and a nitrification rate k_b of 0.001 per min was used for the simulation. Figures 5.2 and 5.3 show the unit step and impulse function responses for a hybrid unit. Figure 5.2 shows that the concentration of nitrate pollutant increases as time increases until it attains the boundary condition. Furthermore, it was noticed that the nitrate concentration obtained from the smaller value of denitrification rate (k_c) attains the boundary concentration faster than the larger value of k_c. Thus as denitrification rate (k_c) increases,

the reach concentration decreases which attributes to the first order decay process which occurred in the river reach. The impulse response presented in Figure 5.3 indicates a decrease in the peak value of the nitrate concentration with an increase in the denitrification rate (k_c) in the river. The figure illustrates the changes in concentration of nitrate as a function of time. It was observed from the figures that the difference in k_c values affects the rate of movement of nitrate pollutants in the river as it travels downstream. The unit impulse responses were generated for denitrification rate (k_c= 0.005 and 0.002 per min) when Δx (= 200m, 400m, 800m, and 1600m) by applying Eq. (5.19) and presented in Figure 5.4.

It was observed from Figure 5.4 that as the denitrification rate increases, the peak concentration decreases and the elongation of falling limb exists. Furthermore, it was illustrated from the figure that as the quantity of hybrid units increases, the peak value of nitrate concentration decreases at successive hybrid units. The solute plumes were gradually spreading out because of dispersion process in the river. Moreover, as there were increases in hybrid units, there were delays in the occurrence of the rising limbs observed from the profile. A bell-shaped distribution was noticed from the C-t profile as the solute moved downstream because of first-order decay of nitrate concentration in the river. The C-t profile of the 8^{th} hybrid unit could be associated with the long distance between the point of injection of the nitrate pollutant and its position. It can be concluded that there was a reduction in nitrate concentration in the river as the solute moved downstream because of the denitrification process and phytoplankton effect.

Table 5.1: The calibration parameters for the model simulation

Notation	Parameters	Units	values
K_b	Nitrite oxidation rate	min^{-1}	0.002 and 0.005
K_c	Denitrification rate at 20°C	min^{-1}	0.002 and 0.005
μ	Algal growth rate	min^{-1}	0.005
ρ	Algal respiration rate	min^{-1}	0.0002
α	Fraction of algal biomass that is Nitrogen	mg-N/mg A	0.0006

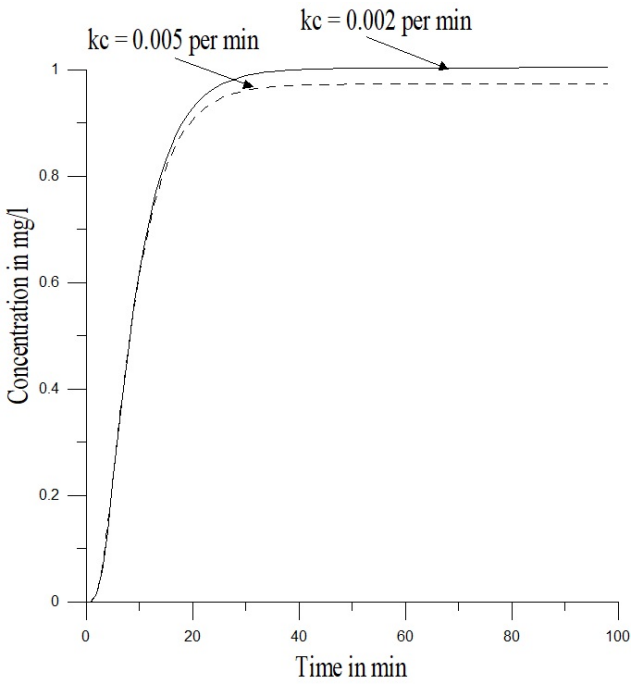

Figure 5.2: Unit step responses of the HCIS-NO_3 model, for denitrification coefficient, K_c= (0.005 and 0.002 per min) at Δx = 200m and (T_1 = 1.7 min, T_2 = 2.3 min, and T_3 = 6.0min)

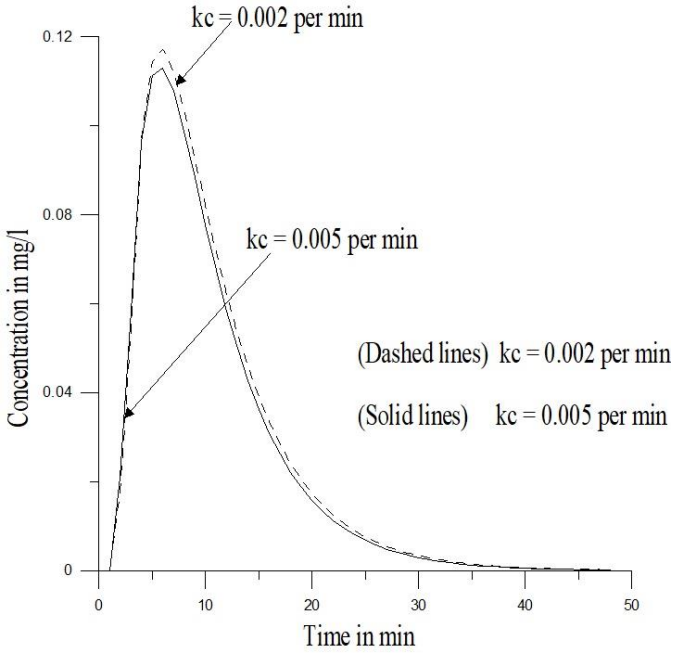

Figure 5.3: Unit impulse responses of the HCIS-NO_3 model for a denitrification rate coefficient, K_c = (0.005 and 0.002 per min) at Δx = 200m and (T_1 = 1.7 min, T_2 = 2.3 min, and T_3 = 6.0min

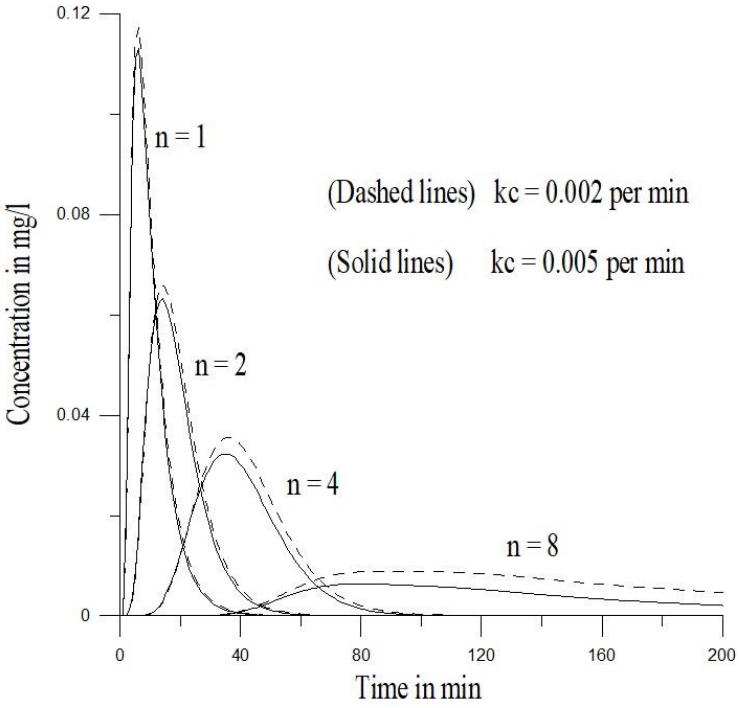

Figure 5.4: Unit impulse responses of the HCIS-NO_3 model for a denitrification rate coefficient, K_c = (0.005 and 0.002 per min), at Δx (= 200m, 400m, 800m, and 1600m) and (T_1 = 1.7 min, T_2 = 2.3 min, and T_3 = 6.0min)

The influence of the nitrification process on the nitrate concentration for the hypothetical data sets is presented in Figure 5.5. The figure illustrates the unit impulse for the nitrification rate (k_b = 0.002 and 0.005 per min) for the 1st, 2nd, 4th and 8th hybrid units using Eq. (5.27). Figure 5.5 describes the variations in nitrate concentration as a function of time when k_b = 0.005 and 0.002 per min and allowing other data to be constant. It was observed from the figure that the higher value of k_b contributes to more quantities of nitrate in the water body when compared with the lower value of k_b. Using the HCIS-NO_3 model, it has been possible to investigate the concentration of nitrate loss and gain by denitrification and nitrification at different locations along the river. The peak concentrations were varied with the hybrid units (n), for various values of k_c= (0.002 and 0.005 per min) which are presented in Figure 5.6. The figure shows that the nitrate concentration decreased along the path of the river as it changed into nitrogen gas due to the denitrification process. Furthermore, increases in phytoplankton in the surface water affects the level of nitrate in the water column.

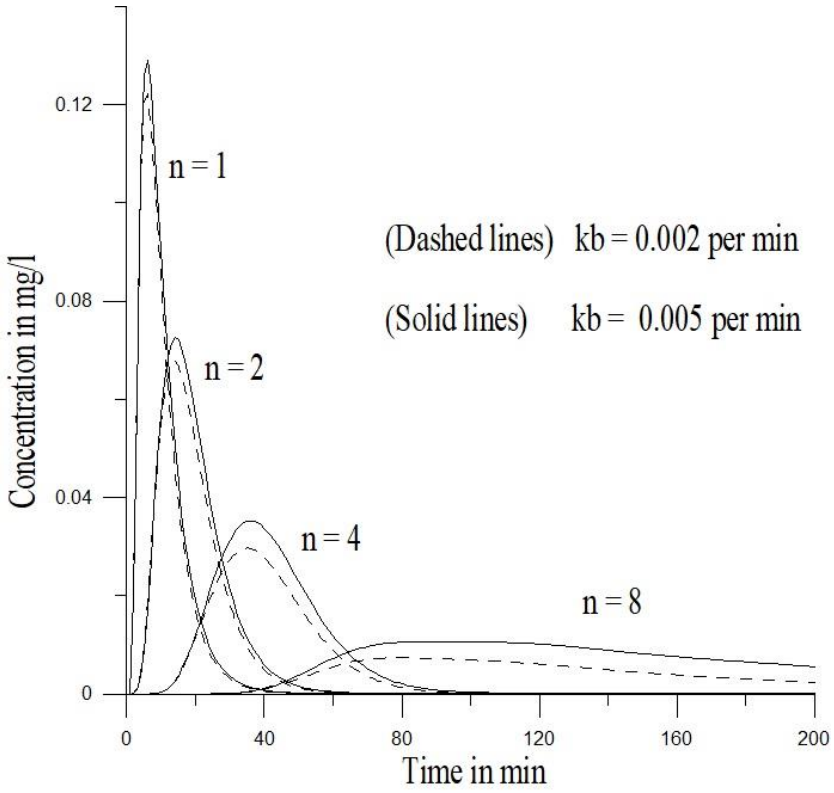

Figure 5.5: Unit impulse responses of the HCIS-NO_3 model for a nitrification rate coefficient, K_b = (0.005 and 0.002 per min), at Δx (= 200m, 400m, 800m, and 1600m) and (T_1 = 1.7 min, T_2 = 2.3 min, and T_3 = 6.0min)

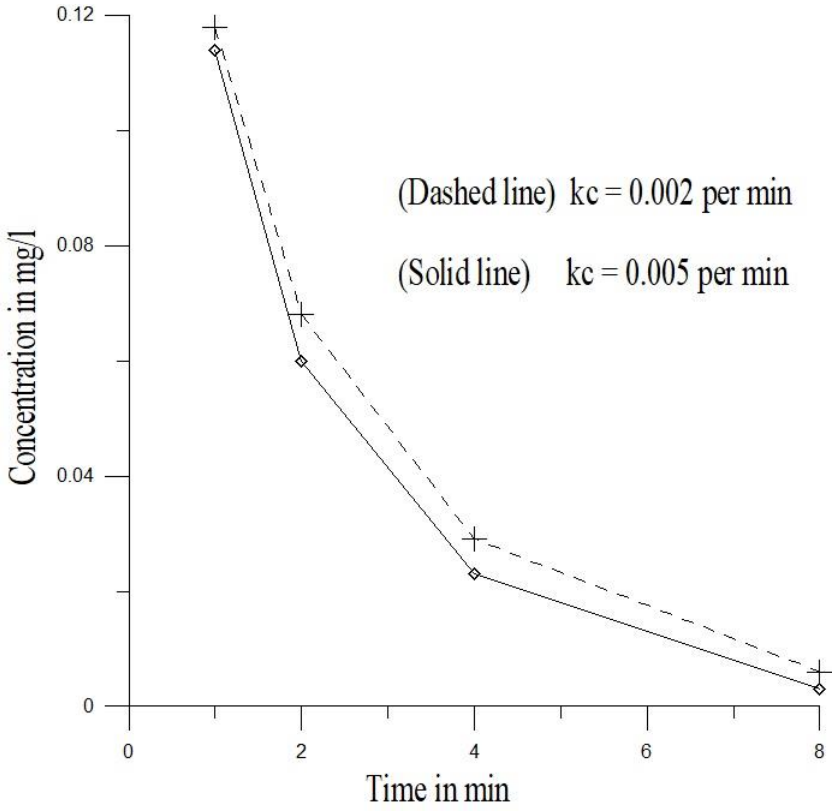

Figure 5.6: Variation of peak concentration at Δx (= 200m, 400m, 800m, and 1600m) for different values of denitrification rate coefficient, k_c = (0.002 and 0.005 per min) and (T_1 = 1.7 min, T_2 = 2.3 min, and T_3 = 6.0min)

Additionally, the solution of the finite difference method was used to verify the HCIS-NO_3 model. The impulse response of the numerical solution was determined numerically by differentiating Eq. (5.23) with respect to the time function. The numerical solutions were solved with the following data set finite difference grid size Δt = 1min, Δx =100m, flow velocity (u) = 20m/min and dispersion coefficient D_L = 1000m^2/min. To simulate the level of nitrate solute in the river downstream at (X =200m, 400m, 800m and 1200m), a numerical convolution was used as presented in Figure 5.7. In addition, the impulse response functions of the ADE-NO_3 model were compared with the responses of the HCIS-NO_3 model obtained in Eq. (5.18). The impulse responses were generated for the first, second, fourth, and sixth hybrid units as indicated in Figure 5.7. The figure shows the relationship between the solution of the HCIS-NO_3 model and the numerical solution of the ADE-NO_3 model when considering more than one hybrid unit. Figure 5.7 demonstrates that the results of both models agreed with each other. The concentration - time profiles agreed with each other and showed similar conditions as the nitrate pollutant moves downstream.

Likewise, both models illustrate typical trends and shapes, also the peak concentration decreases as the number of hybrid units increases. The HCIS response is closely matched with the response of the ADE model, but a marginal difference was observed in the peak concentration of both models. However, the variance is due to space discretization in the hybrid model and the truncation procedure followed in solving the ADE by numerical method.

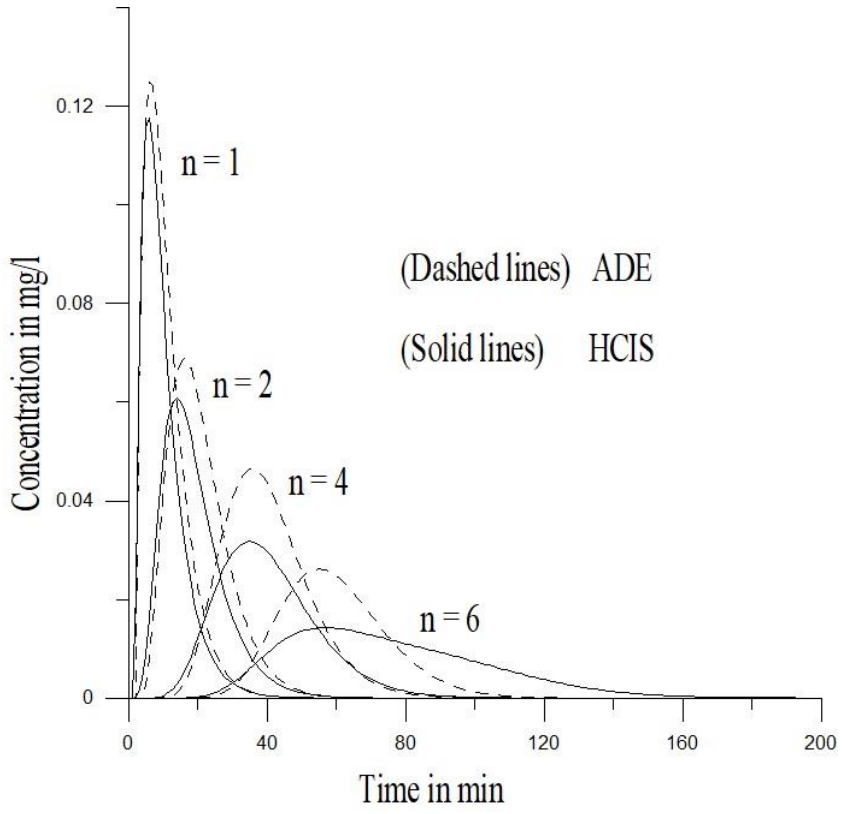

Figure 5.7: Evaluation of unit impulse responses of the HCIS-NO_3 model with the ADE-NO_3 model at X = (200, 400, 800 and 1200m), for denitrification coefficient, k_c = 0.005 per min

Performance of the models were evaluated by incorporating some quantitative measures as presented in Table 5.2. Figure 5.7 was used for the quantitative measures. It was observed that the value for NSE and R^2 were closer to unity. The RMSE and RSR have a very low value. Consequently, the statistical measures show a good agreement between both models. It could be seen that the analytical solution of the HCIS-NO_3 model is reliable and can be applied to simulate pollutant transport in a water body.

Table 5.2: Quantitative measures between the HCIS-NO_3 and ADE-NO_3 models

Unit	R^2	NSE	RMSE	RSR
First	0.988	0.983	0.0025	0.0073
Second	0.964	0.964	0.0029	0.0095
Fourth	0.974	0.932	0.0023	0.0086
Sixth	0.753	0.738	0.0034	0.0243

5.6. Summary

A hybrid model was developed for nitrate transport in rivers and streams by incorporating first-order reaction kinetics of nitrate along with an advection and dispersion process using a mass balance concept. The resulting nitrate transport equation was solved analytically based on the principle of Laplace transform method. A computer programme language presented in C-sharp was used to implement the analytical solution. The analytical solution was used to evaluate the temporal and spatial variation of nitrate concentration in a water body. The study describes the influence of nitrate pollution in surface water, which is attributed to eutrophication of the river system and promotes algae growth. The developed model simulates the transformation of the nitrate nutrients in rivers and streams by considering the effect of nitrification rate, denitrification rate and algae growth rate for its processes. Furthermore, analytical solutions of the HCIS-NO_3 model were compared with numerical solutions of the ADE-NO_3 model and the agreement between them is found to be good. The response obtained by the HCIS-NO_3 model was close to pollutant transport in a natural river. The simplicity of the model to solve ordinary differential equations when linked with partial equations of the ADE model is an advantage to the model. The model is a simple and useful tool for simulating nitrate transport problems in rivers and streams.

CHAPTER 6: APPLICATION OF THE PROPOSED MODEL TO THE UMGENI RIVER

6.1. Overview

In this chapter, the efficiency of the new HCIS model coupled with nutrient kinetics is demonstrated with a practical application involving the simulation of nutrients, i.e., ammonia, nitrite, and, nitrate concentration along the uMgeni River. The developed model was used to predict the nutrients concentration at various locations along the uMgeni River using collected input data for a period from January 2014 to December 2014. Then the simulated results were compared with observed historic data. The model's capability has been analysed with standard error analysis which found the model predicted the nutrient concentrations close to observed data. This chapter also identified model's shortcoming in predicting pollutant concentration during storm event as the current model does not consider non-point source pollution and lateral flows. However, in this chapter, the model was demonstrated to be a promising model for predicting pollutant concentrations along river reaches during non-rainy period.

6.2. Description of Study Area

uMgeni River is an important river situated in KwaZulu-Natal Province of the Republic of South Africa which serves as a source of freshwater for the region. Agunbiade and Moodley (2014) state that the river has a drainage area of 4432km^2 with a length of approximately 232km from the source (Midmar Dam) and exits into the Indian Ocean. Besides, the river takes mean annual precipitation of about 410-1450 mm, and a yearly runoff of 72-680mm. There are four significant dams located along the river which include Midmar, Albert Falls, Nagle, and Inanda as shown in Figure 6.1. The water supply for Pietermaritzburg, Durban, and other local communities comes from these dams. A major tributary to the river is the Msunduzi River which joins the river below Nagle Dam. The Msunduzi River has a catchment area of 875km^2 and a length of approximately 115km and discharges a considerable amount of nutrients into the river.

The uMgeni River plays a significant role in the industrial and urban activities of KwaZulu-Natal Province. However, the river has been characterized by high levels of environmental degradation because of many industries and agricultural operations situated close to the river. Thus, they discharge their waste effluent and agricultural runoff into the water body and increase the pollution level of the river. The water has been one of the most polluted water bodies in South Africa due to excessive nutrient pollution which

is continuously discharged into the river. The high nutrient pollution rate of the stream has caused an adverse effect on the fish life, aquatic biota, human health and the environment. uMgeni Waters Department and the eThekwini Municipality do routine monitoring on the pollution level of the river by carrying out a water quality analysis of the water body. The process is achieved by measuring the nutrient concentration along the water body. It was observed that the river quality around the upper catchment (Midmar Dam) area has reduced because of different anthropogenic activities. Hence, it is significant to assess the nutrient pollutants of the river. Consequently, the model developed in this study was used to evaluate the nutrient concentration of the upper uMgeni River.

6.2.1. Data Sampling Point

Seven sampling locations along the river (Midmar Dam section) were chosen for this research as presented in Figure 6.1. The figure describes the river reach which is approximately 20km in length and stretches between two locations RMG003 (Midmar Dam outflow) and RMG008 (Morton's Drift) having lat-long, 30°12' E – 29°49'S and 30°20'E – 29°43'S respectively. The description of the sampling points is presented in Table 6.1. The distance between the sampling points and the width of the river reach were estimated using a Google Earth map to determine their approximate values. Table 6.2 describes the distance between the river reach and the channel geometries.

Table 6.1: Description of sampling points

Sampling location	**Sampling Site Description**
RMG003	uMngeni Midmar Dam outflow
RMG004	uMngeni Upstream of Midmar WW
RMG005	UMngeni Downstream of Midmar WW
RMG006	uMngeni at Howick
RMG034	uMngeni Upstream Howick WWW outfall
RMG036	uMgeni Downstream Merrivale Stream
RMG008	uMngeni at Morton's Drift

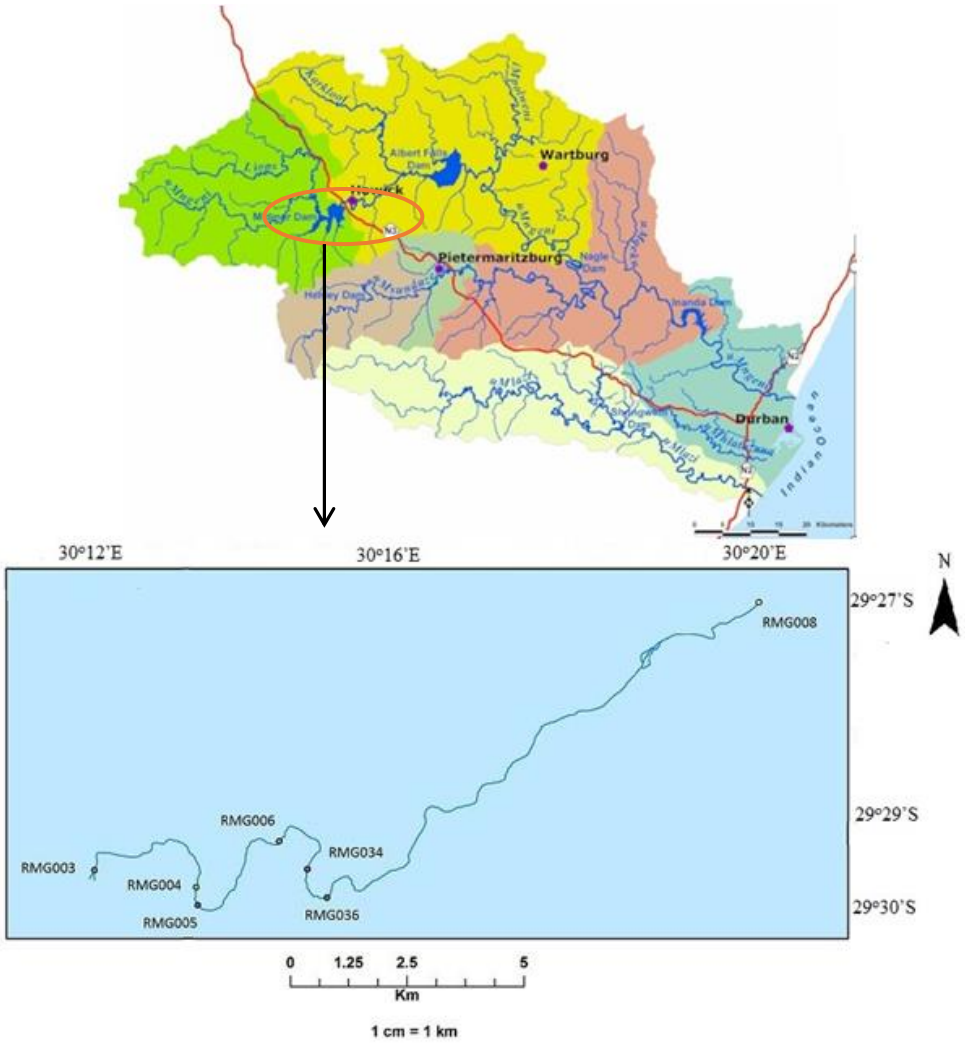

Figure 6. 1: Map of the upper uMgeni River indicating the sampling points

Table 6.2: Estimation of the flow characteristics and channel geometry

Sampling Location	L(m)	W (m)	H (m)	A (m^2)	S
RMG003-RMG004	3200	41.51	0.49	20.34	0.00335
RMG004-RMG005	950	42.81	0.40	17.12	0.0098
RMG005-RMG006	2530	47.29	0.42	19.86	0.0084
RMG006-RMG034	1680	55.40	0.49	27.15	0.0069
RMG034-RMG036	960	34.56	0.34	11.75	0.0037
RMG036-RMG008	11500	33.45	0.30	10.04	0.0017

6.3. Estimation of the Hybrid Model Parameters and Model Setup

The upper uMgeni case study area of 20km was divided into six reaches according to the sampling point presented in Figure 6.1. Each reach was further discretised into several hybrid units having their unit size (Δx) and model parameters as shown in Figure 6.2. To use the hybrid model in assessing the quantity of nutrients in the river, the first step was to estimate the size of each unit (Δx) which depends on the longitudinal dispersion coefficient (D_L), mean flow velocity, and peclet number (P_e). Thus, Δx has been selected in such a way the (Pe =Δx u / D_L) must be equal or greater than 4 (Ghosh *et al.*, 2004; Kumarasamy *et al*., 2011). The total number of hybrid units within a reach as described in Figure 6.2 is calculated by dividing the length of each reach (RL) with respect to the estimated hybrid unit size (Δx) as:

$$n = \frac{RL}{\Delta x} \tag{6.1}$$

The longitudinal dispersion coefficient (D_L) is an essential parameter for analyzing water quality in natural rivers, and different investigators (Seo and Cheong, 1998; Kashefipour and Falconer, 2002; Murphy *et al*., 2007) have presented a range of D_L values. The values were estimated either by experimental, theoretical or empirical equations. Therefore, the process of determining the D_L adopted in this study was the empirical method developed by Etemad-Shahidi and Taghipour (2012) as illustrated in Eqs 6.2-6.3. These equations depend on the fluid properties, channel geometrics and hydraulic characteristics of the reaches. It is a significant parameter in estimating the distribution of solute concentration in a natural waterbody.

If W/ H ≤ 30.6,

$$D_L = 15.49\left(\frac{W}{H}\right)^{0.78}\left(\frac{u}{U_*}\right)^{0.11} * HU_* \tag{6.2}$$

else

$$D_L = 14.12\left(\frac{W}{H}\right)^{0.61}\left(\frac{u}{U_*}\right)^{0.85} * HU_* \tag{6.3}$$

Additionally, the year 2014 flow data were collected from the Department of Water Affairs (DWAF), South Africa for the first sampling point and used for the model calibration. Data on the precipitation conditions were obtained from the South African Weather Services (SAWS). The daily rainfall data for the year were accessible from Cedera station, which is approximately 19.5km from sampling point RMG003.

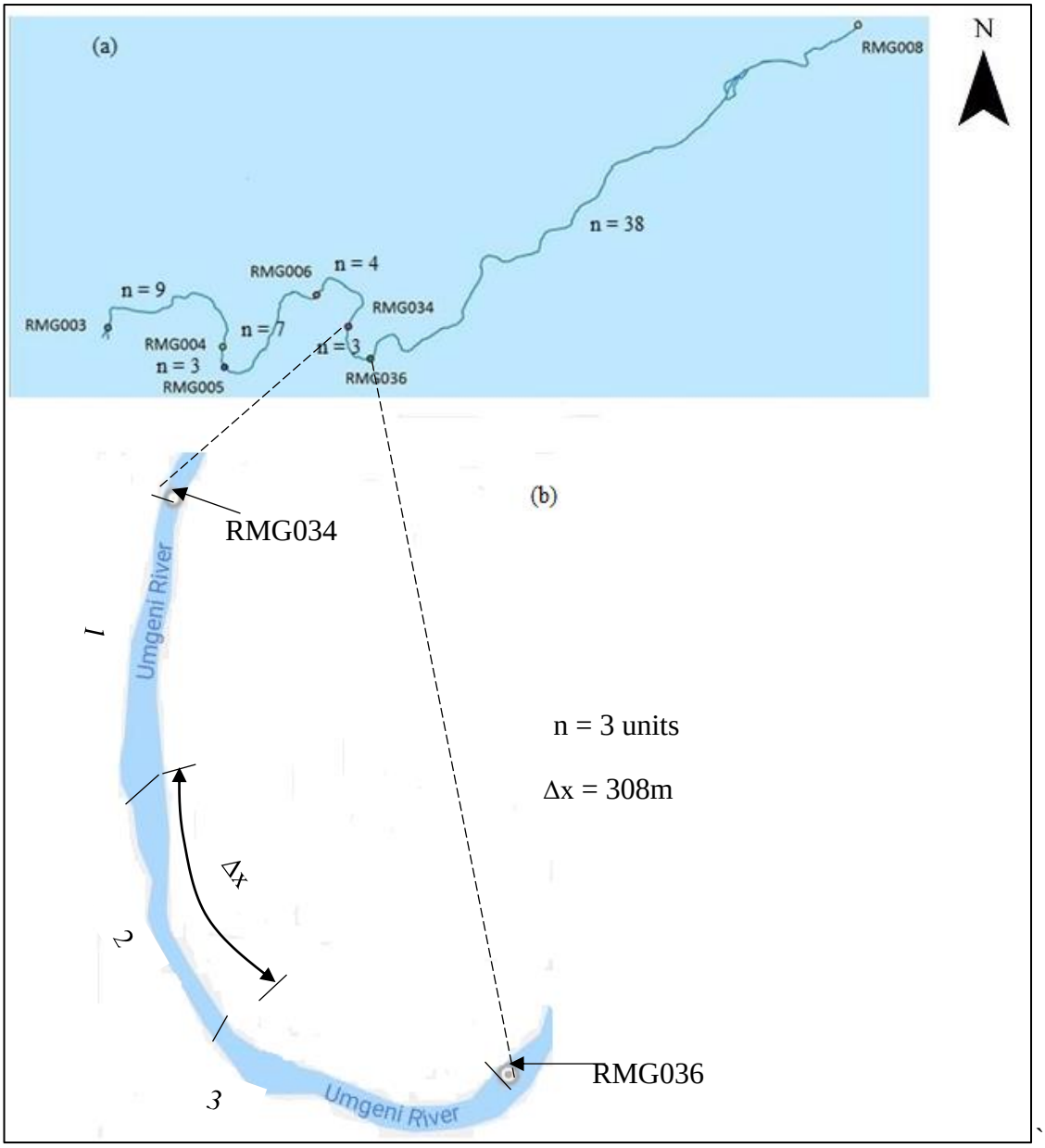

Figure 6. 2: (a) Map showing study reaches of uMgeni River with sampling locations and number of hybrid units in each reach (b) Conceptualized river reach comprising series of hybrid units with a size Δx between sapling point RMG034 and RMG036.

The measured nutrient parameters (ammonia, nitrites, and nitrate) for the year 2014 data were obtained from uMgeni Water. The flow characteristics, average channel geometry, and dispersion coefficient for the first reach were estimated using the first sampling data point.

However, due to non-availability of flow data at other reaches, the observed flow characteristics for the first reach was considered. Consequently, the three-time model parameters (T_1, T_2, and T_3) were estimated using Eq. (3.20) – (3.22) having determined the values of D_L and (Δx). Subsequently, the peclet number (P_e), longitudinal dispersion coefficient (D_L), the hybrid unit size (Δx), the model parameters (T_1, T_2, and T_3), and the total number of hybrid units used for the model simulation are presented in Table 6.3. The developed C-sharp programming code was used to estimate the parameters.

Table 6.3: Estimated model parameters and flow characteristics

	Reaches					
River properties/ HCIS model parameters	RMG003-RMG004	RMG004-RMG005	RMG005-RMG006	RMG006-RMG034	RMG034-RMG036	RMG036-RMG008
L(m)	3200	950	2530	1650	960	11500
Pe	5	5	5	5	5	5
D_L (m^2/s)	25.38	25.86	27.48	30.26	22.69	22.25
Δx (m)	344	351	373	411	308	302
T_1 (s)	187.32	190.96	202.92	223.48	167.58	164.28
T_2 (s)	234.43	238.70	253.65	279.36	209.48	205.35
T_3 (s)	515.11	525.15	558.03	614.59	460.87	451.78
No of hybrid units	9	3	7	4	3	38

6.4. Application of the HCIS-NH_3 Model in Simulating Ammonia Concentration in the River

The ammonia concentration data collected for the year 2014 from uMgeni Water were used for the simulation of the model, and the results were compared with the observed values. The HCIS-NH_3 model was calibrated for the concentration of ammonia under a steady state condition. The calibration was accomplished using the actual flow data for the year 2014 at the sampling location RMG003 as presented in Figure 6.4 and using the upstream values of ammonia concentration as the boundary condition.

Calibration was carried out by a method in which the values of one or two parameters were changed at a time, and other parameters remain constant. A computer run was carried out, and the effects of new parameters values on the simulated results were examined. The calibration was achieved by adjusting model parameter values until acceptable simulation is achieved. Thus, the calibration of the model was intended to modify the kinetics parameters to optimal simulation condition until the predicted values, and measured concentration data agreed.

The calibrated values for the kinetic parameters were 0.005 per sec for ammonia oxidation coefficient, 0.005 per sec for algae growth rate, 0.0002 per sec for algae respiration rate. In addition, the benthic release of ammonia nutrient is 0.00004 mg- N/m2 – sec and the fraction of algal biomass that is nitrogen is 0.004 mg-N/mgA. The ammonia concentration data for sampling point RMG003 for January to December 2014 was used as an input to the hybrid model. Consequently, the ammonia concentration at other sampling points was simulated using successive convolution to determine its concentration at the downstream location for a step input. The data corresponding to other sampling points was then compared with measured values as shown in Figures 6.5 – 6.8.

It can be observed from Figure 6.5 for the period between 11th January 2014 and 13th February 2014 that both the measured and simulated values for ammonia concentration follow the same trend and are very closely matched. The responses presented in Figure 6.5 for the period between January and April indicate that ammonia concentration decreased with an increase in the flow data as shown in Figure 6.4. Therefore, the dilution of ammonia concentration resulted from an increase in the flow condition as the pollutants were transported downstream. The increase in flow condition was due to the increased discharge from Midmar Dam for the same period. The decrease in ammonia concentration within this period was also due to the transformation of ammonia to nitrite as the ammonia pollutant moved downstream. This is true for other sampling points (RMG005, RMG034) as presented in Figures 6.6 and 6.7 for the same period, which were close to the measured data, and the general trends matched between simulated and measured data. From the Figures 6.5–6.7, the simulated and measured ammonia concentration for the period between April and May 2014 were compared. Observation showed an increase in ammonia concentration in April and May, which was due to the high rainfall as seen in Figure 6.3 which resulted in an influx of nutrients from the catchment into the river system. From the Figures 6.5–6.7, it is observed that the measured and simulated ammonia concentrations were very closely matched for the period after August 2014. This was due to the river flow not varying and there being not much rainfall during this period.

Thus, the model parameters remained relatively constant, and there was no influx of nutrients from the catchment. However, there was a significant difference between the simulated and measured data for most of the period at the sampling location RMG008 as shown in Figure 6.8. This was due to the lack of data for the Karkloof River which confluences upstream of the location RMG008. Simulated results did not include the flow and water quality data which resulted in an under predicted profile from the model. However, the general trend was matching between measured and simulated data, like other locations.

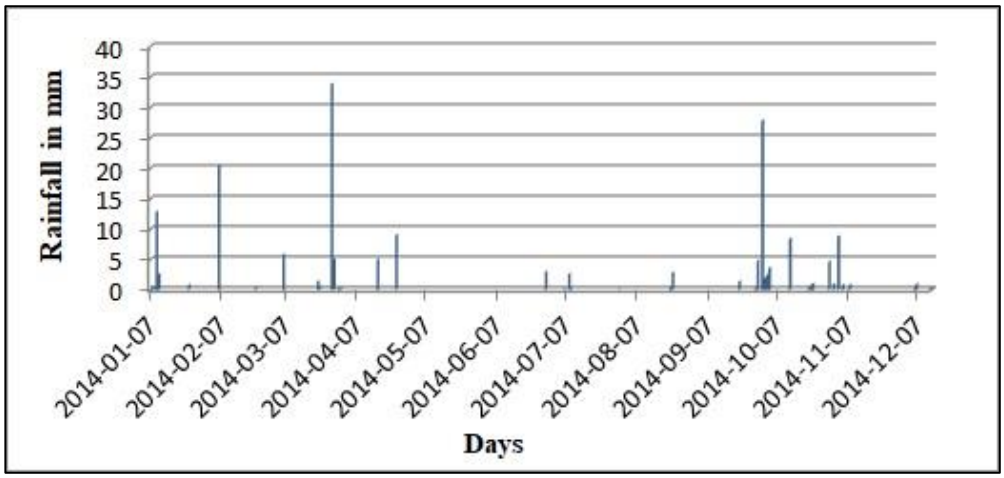

Figure 6. 3: Observed rainfall data for the year 2014 (Source: SAWS)

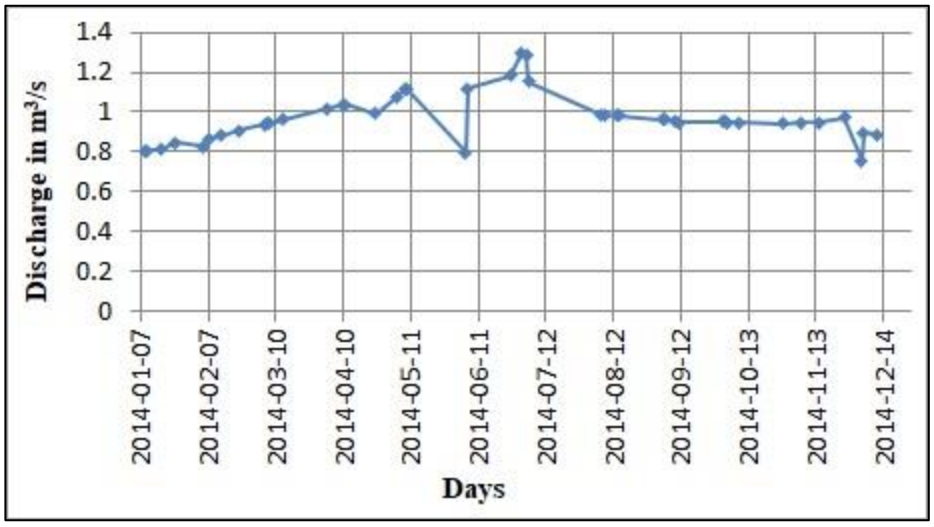

Figure 6. 4: Observed daily discharge data at RMG 003 for the year 2014 (DWAF)

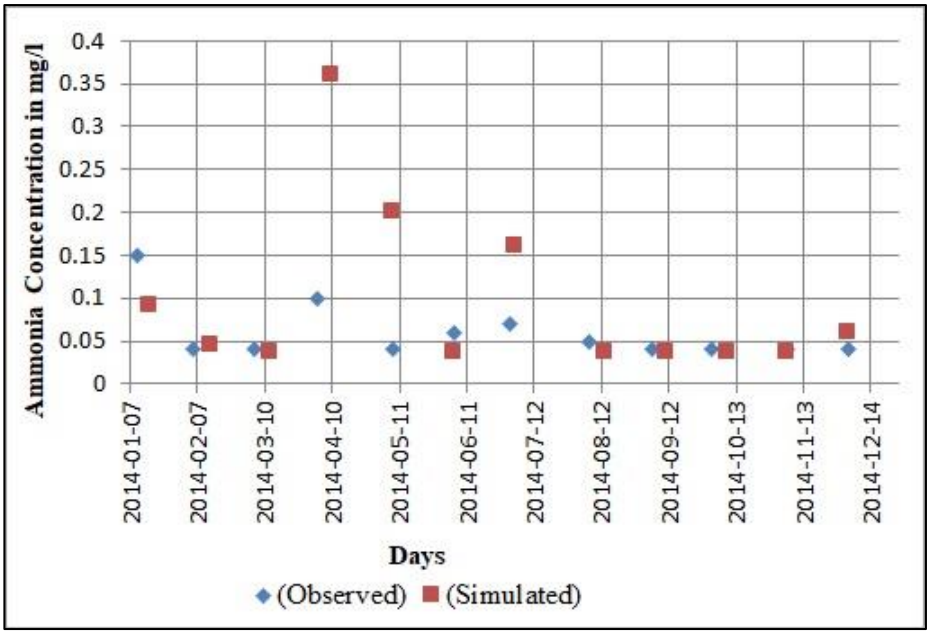

Figure 6. 5: Observed and simulated ammonia concentrations at RMG004

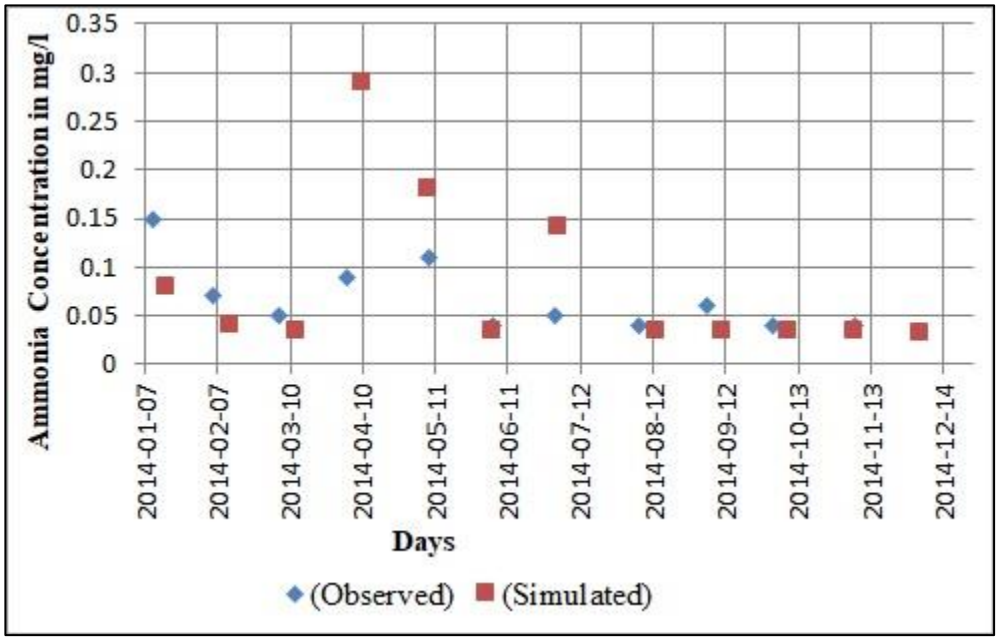

Figure 6. 6: Observed and simulated ammonia concentrations at RMG005

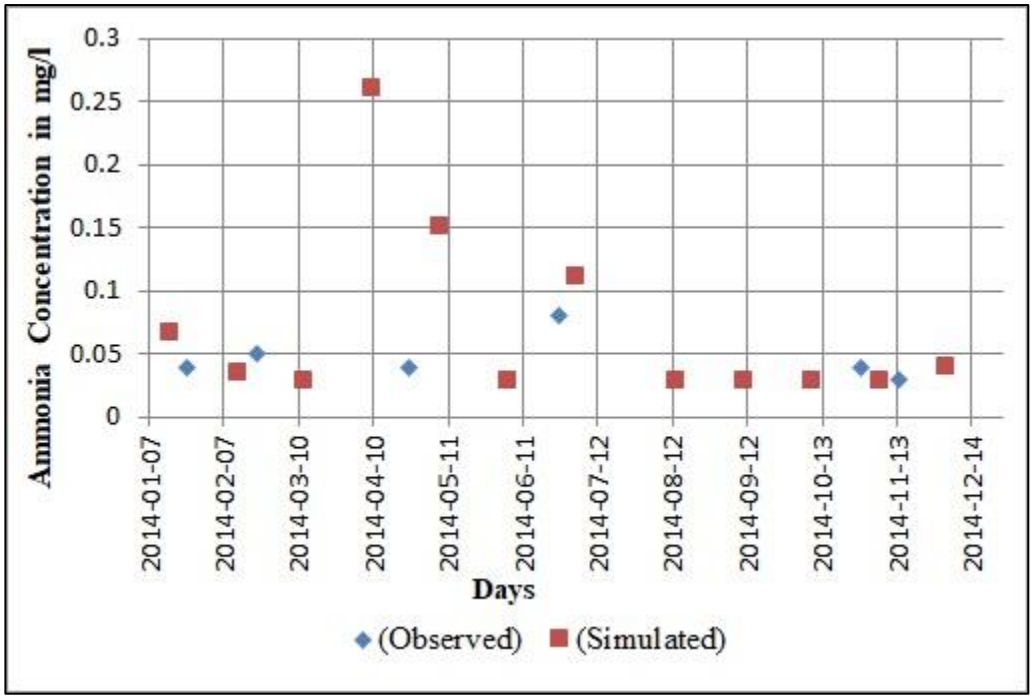

Figure 6. 7: Observed and simulated ammonia concentrations at RMG034

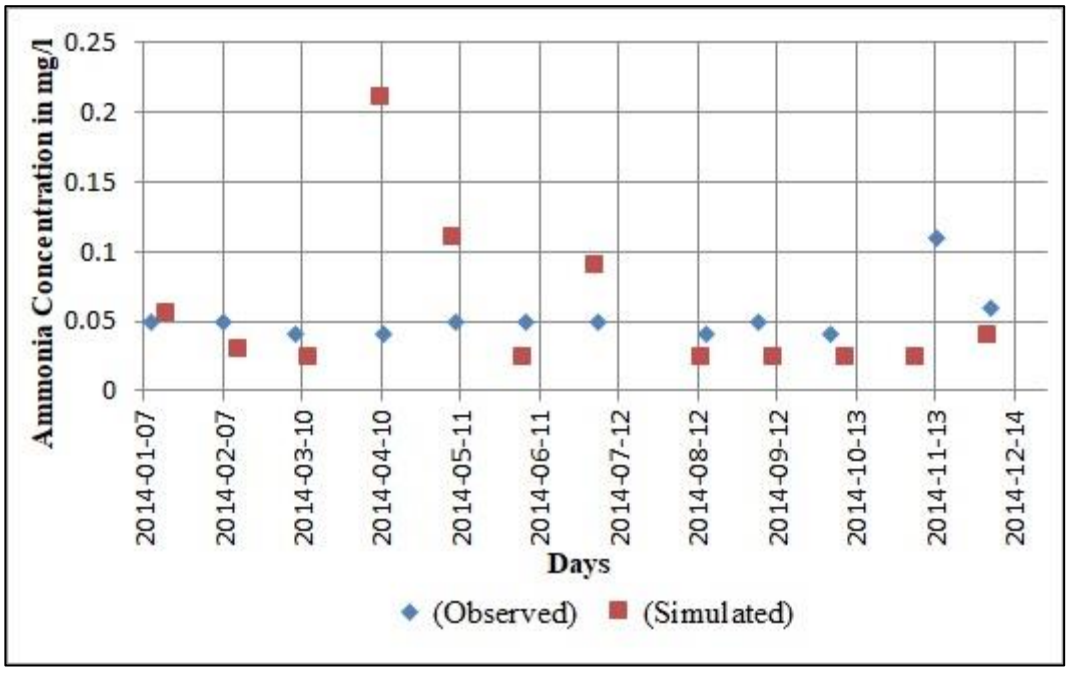

Figure 6. 8: Observed and simulated ammonia concentrations at RMG008

The performance of the model was evaluated using statistical tools based on the coefficient of determination (R^2) which was carried out at a 95 percent level of confidence between the observed and simulated data. Thus, it was observed from the correlation that the observed and simulated values of ammonia concentration in the river demonstrated a high correlation coefficient (R^2) and the standard error (SE) was low as presented in Table 6.4. The result of the statistical analysis shown in the table indicates a strong significance of the model in simulating the concentration of ammonia pollutant in rivers. Hence, the model equation could be used for predicting ammonia concentration in rivers and streams.

$$R^2 = \left[\frac{\sum_{i=1}^{n} \left(O_i - \overline{O}\right)\left(P_i - \overline{P}\right)}{\sqrt{\sum_{i=1}^{n} \left(O_i - \overline{O}\right)^2} \sqrt{\sum_{i=1}^{n} \left(P_i - \overline{P}\right)^2}} \right]^2 \tag{6.4}$$

$$SE = \frac{\delta}{\sqrt{n}} \tag{6.5}$$

Where, P is the predicted values and O is the observed values. δ represents the standard error and n is the number of samples.

Table 6.4: Correlation between observed and simulated values of ammonia concentration

River reach	R^2	F	P value	SE
RMG 004	0.787	36.91	0.00012	0.011
RMG 005	0.748	29.78	0.00027	0.018
RMG 034	0.746	30.38	0.00032	0.012
RMG 008	0.728	26.83	0.00041	0.005

6.5. Application of the HCIS-NO_2 model in Simulating Nitrite Concentration in the River

The year 2014 observed data of nitrite concentration were obtained from uMgeni water. The actual flow data presented in Figure 6.4 for the sampling location RMG003 was applied for the calibration of the HCIS-NO_2 model. Furthermore, the values of nitrite concentration for sampling location RMG003 were taken as the boundary condition for the model. The other parameters such as ammonia and nitrite oxidation rates were taken as 0.002 per sec and 0.005 per sec respectively.

To perform the model simulation, the concentration of nitrite data for the first sample location was applied as a step input into the model. Consequently, the predicted values of nitrite concentration downstream were compared with the measured data collected from uMgeni Water in 2014 as presented in Figures 6.9–6.12. Thus, the figures demonstrate the evaluation of the measured and simulated data of nitrite in the uMgeni River for the period January to December 2014. The results illustrate that the general trends of the predicted data set show a good agreement with the measured values set for the period between January and March 2014. It was observed that the concentration of nitrite decreases merely in both measured and simulated profiles. Moreover, the reduction in nitrite concentration for the period was because of a low flow rate presented in Figure 6.4, and the influence of high temperature which could possibly be associated with the summer season. An increase in river temperature would intensify the activity of nitrifying bacteria resulting in the formation of nitrate concentration in the river through the nitrification process. Hence the agreement between both sets of results could be deemed as satisfactory. The trends of nitrite concentration for the period of April to July were also compared and it was observed that there was an agreement between the measured and observed values. Furthermore, it could be seen from the figures that there was a significant increase in nitrite concentration for this period. However, the increment in nitrite concentration for this period was because of a high rainfall event indicated in Figure 6.3. The high precipitation around this period tends to result in the increase of nutrient loads into the river. Also, the nitrite concentration for the period between August and December were also compared and a reduction in the concentration of nitrite was observed in both profiles. The figures indicate a good agreement between the measured and observed for this period. However, the discrepancy between the measured and simulated profiles for Figure 6.12 was because of a lack of data from the Karkloof River that joins the sampling point RMG008. Consequently, it can be concluded that the general trends of the model prediction agree with the measured data sets as observed from the figures.

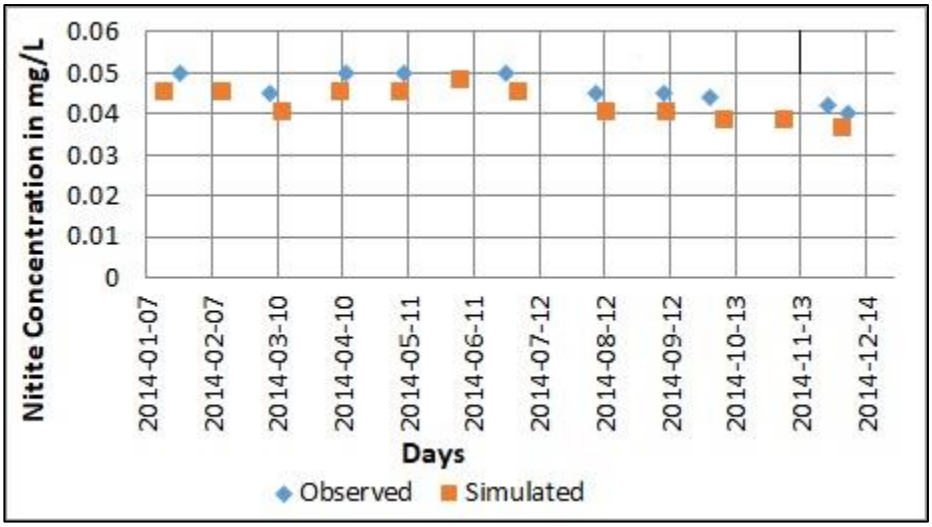

Figure 6. 9: Simulated and observed concentration of nitrite at RMG004

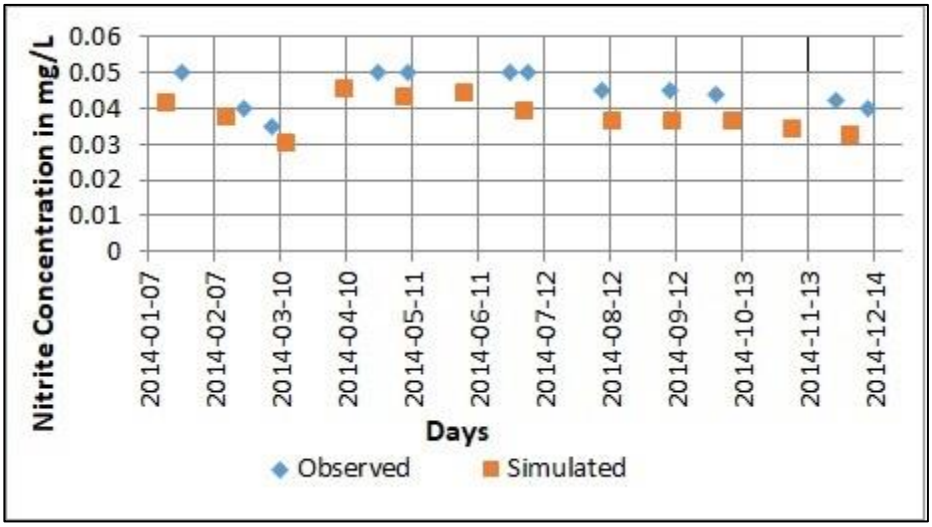

Figure 6. 10: Simulated and observed concentration of nitrite at RMG006

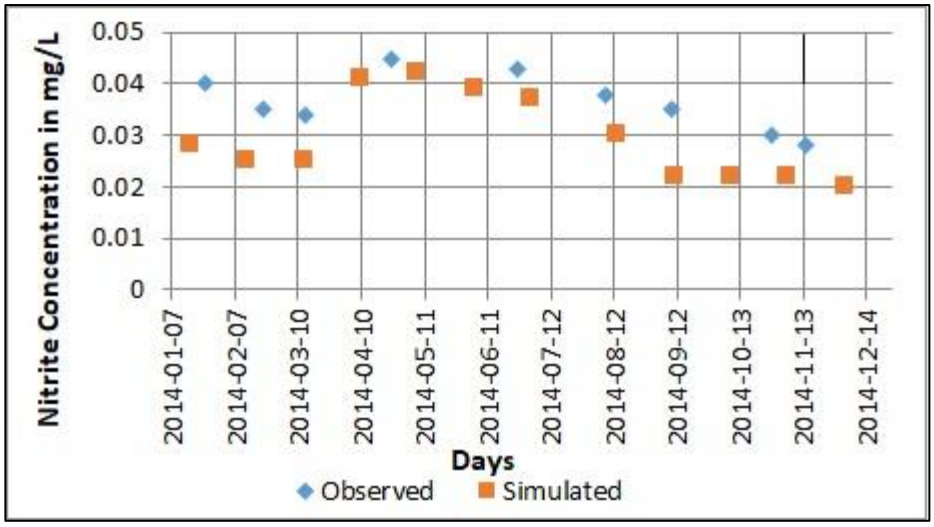

Figure 6. 11: Simulated and observed concentration of nitrite at RMG034

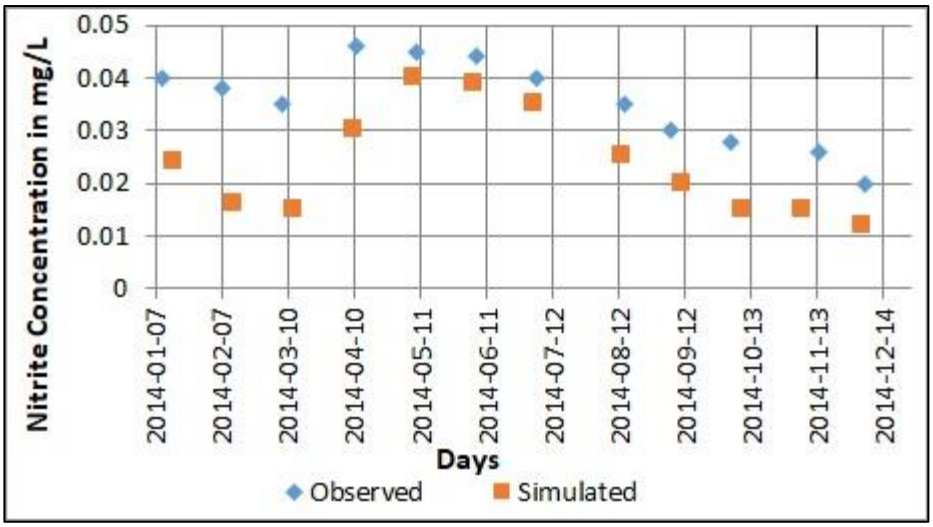

Figure 6. 12: Simulated and observed concentration of nitrite at RMG008

To provide a more quantitative measure of the performance of the HCIS-NO_2 model, the model outputs were compared with the observed values. Statistical analysis in the form of a coefficient of determination (R^2) and standard error (SE) was estimated for all the sampling locations shown in Table 6.5. The results of the statistical measures presented in Table 6.5 indicate high R^2 values and low values of SE which exhibits a high significance of the model to simulate nitrite concentration in the river. The R^2 and SE values, which were closer to unity and zero respectively shows that the HCIS-NO_2 model closely reproduces the measured data in the river.

Table 6.5: Correlation between measured and simulated values of nitrite concentration

Reach(RMG)	R^2	F	P value	SE
004	0.794	38.87	0.00015	0.010
006	0.768	30.62	0.00023	0.013
034	0.754	28.55	0.00037	0.011
008	0.735	26.90	0.00046	0.006

6.6. Application of the HCIS-NO_3 Model in Simulating Nitrate Concentration in the River

The usefulness of the HCIS-NO_3 model was verified with a practical application involving the simulation of nitrate concentration in the uMgeni River. The nitrate enrichment through sewage contamination and fertilizer runoff has increased the pollution level of the river. Increases in pollution and destruction of the catchment areas due to urbanization and agriculture have decreased the quality of the fresh water in the river. The observed nitrate concentration data obtained from uMgeni Water for the year 2014 were used to assess the model. Thus, the observed value for the first sampling point (RMG003) was applied as the boundary condition for the model simulation. The results of the model simulation were compared with the measured data obtained from other sampling points. Table 6.6 described the final calibrated data for other kinetic parameters considered for the model simulation.

Figure 6.13 – 6.16 illustrate the comparisons between the measured and simulated monthly nitrate concentration at different sampling locations. Between January and March 2014, observation shows a decrease in nitrate concentration in both the measured and simulated profiles for this period. The reduction is probably because of the low flow rates experienced during this period as shown in Figure 6.4, which results in a high denitrification process within the river. Also, there were indications of high temperature and light intensity during this period, which have a substantial direct impact on the denitrification process. Thus, a good agreement exists between the simulated and observed values of nitrate concentration for this period. It was seen from Figures 6.13–6.15 for the period between April and December that both observed and measured values of nitrate indicate a similar trend and show a good agreement with each other. There were indications of a significant increase in nitrate concentration in both the measured and simulated data for this phase due to increase in flow rates as presented in Figure 6.4**.** The increase in nitrate concentration for this period was also due to high rainfall which occurred during this period as shown in Figure 6.3. During the high rain for this period, there was an indication of the high influx of nitrate concentration into

the water body from the different watersheds. Besides, low temperatures during this rainy season also reduce the denitrification rate. Therefore, the concentrations of nitrate tend to increase during high intensive precipitation and high flow rate as supported in Hill *et al*. (1999). The response presented in Figure 6.16 for the period between April and December 2014 shows that the simulated profile under-predicted the nitrate concentration for this period. The discrepancy was because of a lack of water quality information and flow data from the Karkloof River which flows into sampling location RMG008. Though, the figure indicates the same trend for both profiles.

Table 6.6: The calibrated parameters applied for the model simulation

Notation	Description	Units	values
K_b	Nitrite oxidation rate	sec-^{1}	0.005
K_c	Denitrification rate at 20°C	sec-^{1}	0.002
μ	Algal growth rate	sec-^{1}	0.002
ρ	Algal respiration rate	sec-^{1}	0.0005
α	Fraction of algal biomass that is Nitrogen	mg-N/mg A	0.0006

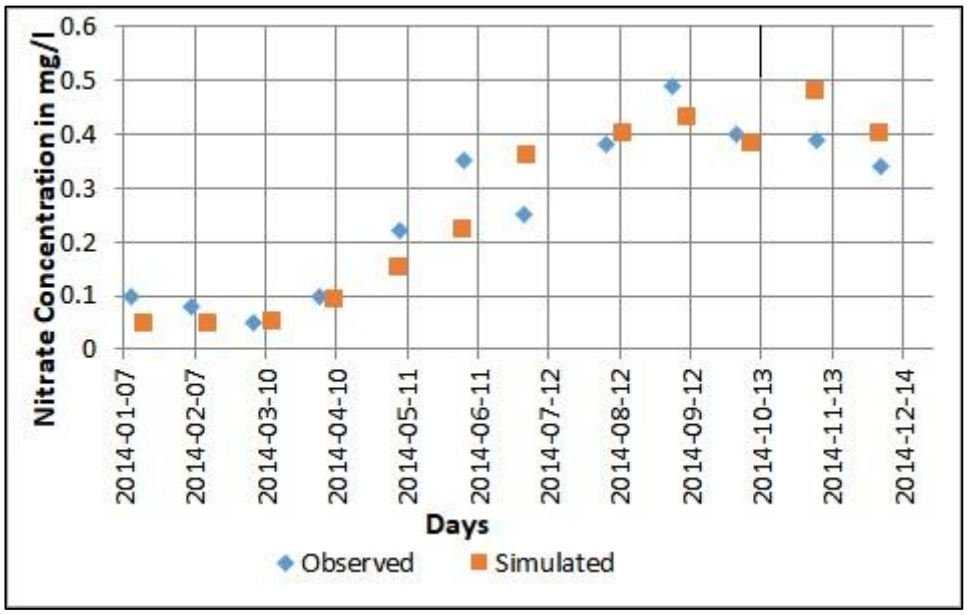

Figure 6. 13: Simulated and observed concentration of nitrate at RMG004

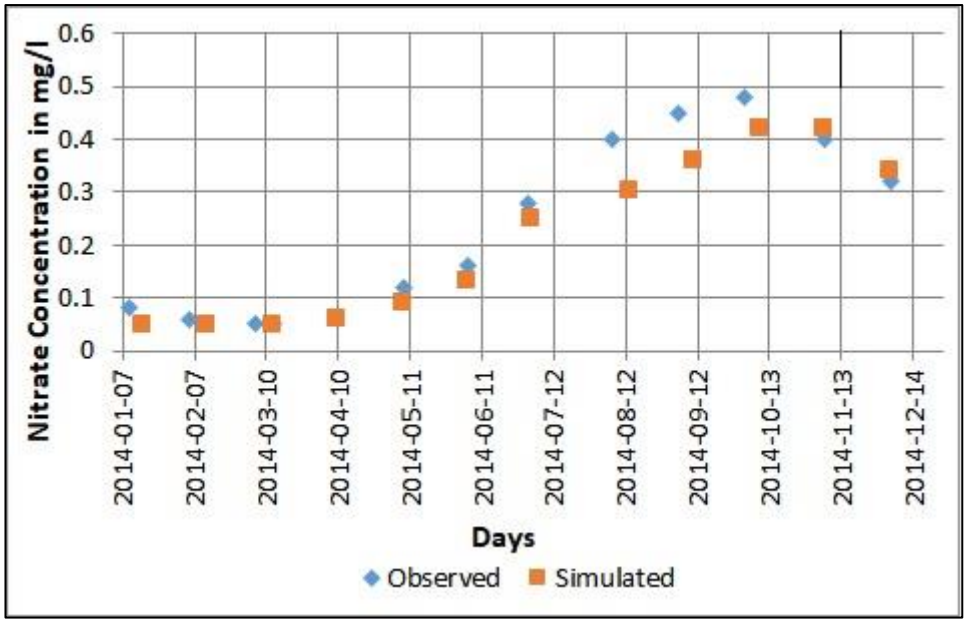

Figure 6. 14: Simulated and observed concentration of nitrate at RMG005

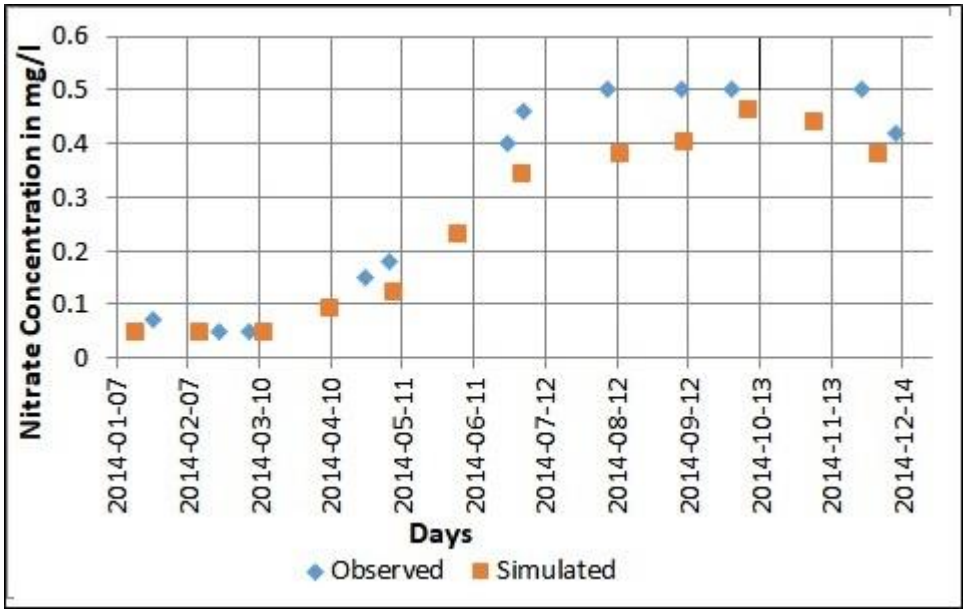

Figure 6. 15: Simulated and observed concentration of nitrate at RMG006

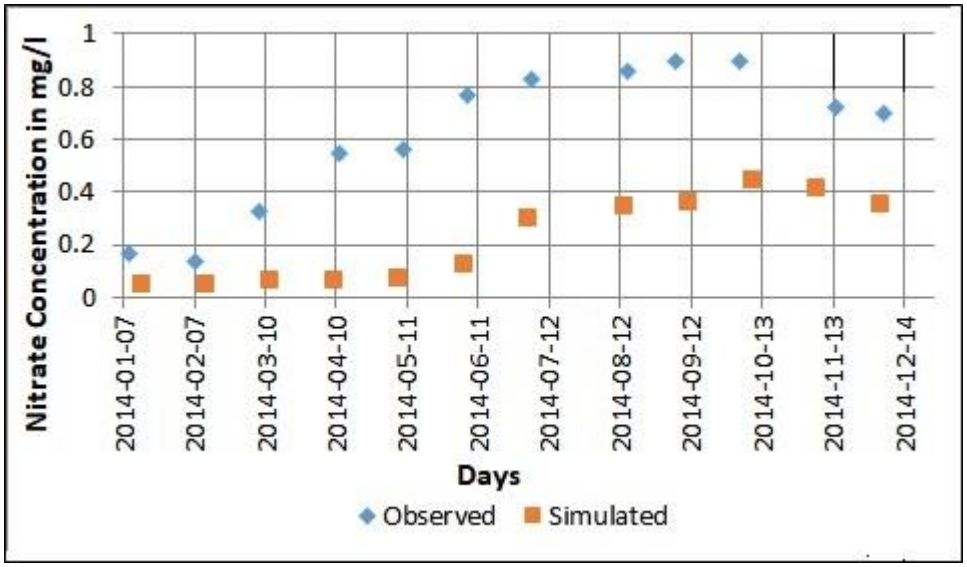

Figure 6. 16: Simulated and observed concentration of nitrate at RMG008

Table 6.7: The quantitative measures between the observed and simulated nitrate concentration

Reach(RMG)	R^2	F	P value	SE
004	0.711	24.54	0.0005	0.014
005	0.742	28.87	0.0003	0.017
006	0.683	21.55	0.0007	0.005
008	0.704	22.64	0.0006	0.004

The use of water quality models is becoming a significance focus in simulating solute transport in a water body. Thus, the need to assess the performance of the developed model is essential for accurate management of water quality. The efficiency of the model was evaluated using quantitative measures to determine the model outputs against the measured values. Statistical analysis described in Table 6.7 indicates that the coefficient of determination (R^2) is more than 0.75 with a low standard error (SE). The results demonstrate an excellent sign of the model in simulating nitrate pollutant in natural rivers and streams.

6.7. Summary

The assessment of water quality parameters in the surface water has been an essential requirement for appropriate management of the water bodies. The adequate supervision of the river would result in effective measures of the nutrient pollution level of the water column and keep solute within acceptable limits. In this chapter, the developed HCIS models were used to evaluate the nutrients, i.e., ammonia, nitrite and, nitrate concentration of the uMgeni River. The twenty kilometres of the upper uMgeni River was divided into six reaches during the model simulation. Each reach was subdivided into a number of hybrid units having different hybrid unit size and model parameters. The model parameters were estimated for a known hybrid unit size, dispersion coefficient, and flow velocity. A Peclet number of five was chosen for the model simulation, and it was observed that the non-dimensional term $((T_1 + T_2 + T_3)\ u)/\ \Delta x)$ is approximately equal to one. The model results were compared with the observed data of nutrient concentration from some selected reach along the uMgeni River. The observed data for nutrient concentration was obtained from uMgeni Water. Also, the details of the data sets which include the channel geometries, flow characteristics and the observed nutrient concentration at different sampling locations was used for the model simulation. The variation in flow velocity from reach to reach was accounted for in the developed model. Statistical analysis of measured and predicted nutrient data was undertaken using R^2 and SE. Thus, it was observed from the model results that the HCIS model simulates the observed nutrient solute transport satisfactorily in the river. In conclusion, analytical solutions can be described as supportive tools for the confirmation of numerical solutions which provide fast and precise results for practical problems. Consequently, using the new model as a tool for simulating nutrients pollutant in water bodies is an excellent option for water quality management.

CHAPTER 7: CONCLUSION AND RECOMMENDATIONS

7.1. Conclusion

A few complex situations concerning the movement of nutrient pollutant in natural water body occur in practical cases for which the nutrient concentration along the river cannot be simulated directly using Fickian based ADE model. The model has a limitation in reproducing the observed behaviour of natural rivers adequately due to constraints in the assumption used for the model derivation and difficulties in its parameter estimations. However, the limitation related to the existing methods have necessitated the development of an alternative solute transport model for rivers and streams. Results from this research described the development of an alternate pollutant transport model that can be used to simulate nutrient concentration along river reaches adequately. This research presents the development and application of a hybrid model for the non–conservative transport of ammonia, nitrite, and nitrate pollutant in a natural river.

The HCIS model, which consists of a plug flow component and two thoroughly mixed cells of distinct sizes, was developed as an alternative method of solving solute transport. The components represented both the advection and dispersion process in a river and were effectively used in simulating pollutants transport in surface water. The plug flow component in the HCIS model predicts the first arrival time of the pollutant at any sampling location which represent the pure advection process of pollutant transport, whereas this arrival time has not been clearly identified by other existing models. The parameters of the hybrid model are the residence times of the plug flow cell and the thoroughly mixed cells (i.e., T_1, T_2, and T_3) which can be determined using the estimated longitudinal dispersion coefficient and the river flow velocity. Nevertheless, the model parameters may also be calculated using the observed concentration graph at any sampling point. Further, the hybrid model also considered variation in flow from one reach to another which affects its parameters.

A conceptual hybrid cell in series model component was developed for a first-order kinetic reaction of ammonia, nitrite, and nitrate along with advection and dispersion processes using mass balance concept. Accordingly, analytical solutions were obtained for the plug flow and two thoroughly mixed cells using Laplace transform method. The results were used to predict the temporal and spatial variation of nutrients, i.e., ammonia, nitrite, and nitrate concentration in a river. An analytical expression for a nutrient concentration of the effluent from the hybrid model has been derived for a step boundary input. Likewise,

the unit impulse responses function was estimated by differentiating the response from the step input to time. Discretising the river into a series of hybrid unit, the nutrient solute concentration for a unit impulse boundary input has been computed along the river using successive convolution technique. The capabilities of the developed models for studying nutrient pollution processes under steady-state flow conditions are demonstrated using hypothetical and field experiment data.

Firstly, the relevance of the HCIS model coupled with nutrient kinetics is tested using hypothetical data, where the unit step and impulse response functions of the hybrid model are described. The effect of nitrification rate, denitrification rate, and algae growth rate were considered during the nutrients simulation processes. For a peclet number greater than 4, the response of the impulse and step response profiles produced by the new model were close to the nutrient transport in a natural stream. The addition of first-order kinetic reaction of nutrients along with the advection-dispersion process decreases the peak concentration and stretches the falling limb of the impulse response profile. Furthermore, the profile of the unit impulse response which described the rising limb, falling limp, time to peak and the peak concentration could be applied to estimate the model parameters. Additionally, a numerical solution of the Fickian based ADE model with kinetics reaction of the nutrients were also computed. Comparison of the responses indicates that the HCIS and ADE models were in good agreement and it provides verification that the solution of the new model is correct. The statistical analysis results show a good correlation between both models. Thus, the HCIS model can be used in predicting pollutant transport in a water body.

The usefulness of the developed models was verified with a practical application involving the simulation of NH_3, NO_2, and NO_3 concentration in the uMgeni River using the data obtained from uMgeni Water, South Africa. The model parameters were estimated by using flow characteristics, average channel geometrics, and dispersion coefficients observed from the river. The model considered the effects of the nitrification rate, the denitrification rate and the algae growth rate during the nutrient simulation. The study shows that increases in nutrient concentration observed in the river were due to precipitation and a high flow rate which has an adverse effect on the river quality. The model was tested during different months of the year with satisfactory results. The simulated results of the model are in good agreement with measured values. Statistical analysis was used to evaluate the developed model by applying some quantitative measures to assess the model outputs against the measured values. The study was conducted based on the coefficient of determination (R^2) and standard error (SE). The results established an excellent

sign of the model in estimating ammonia, nitrite, and nitrate pollutant in natural rivers and streams. Thus, the HCIS model has effectively simulated the nutrient pollutants transport in the river near to the point source as well as far away from the source of the pollutants. The model can be useful in guiding engineering and management decision concerned with the efficient utilization of uMgeni River and the protection of its quality. Therefore, the study has demonstrated that the model can simulate the measured nutrient concentration thoroughly along the selected reaches of the study area, which addresses the aim of this study.

The algorithm has been implemented in a C-sharp programming language to generate the simulated results. A program code in C-sharp has been developed and pre-compiled. A standalone executable file has been created with user notes which helps the users to prepare and capture required input data and generate water quality simulations in MS excel file format. The details are presented in Appendix B that includes C# Programming codes, screenshots of input files, instructions describing data preparation and a generic algorithm for programme developments. Thus, the fourth objective, in this study to develop user friendly pack, has been achieved effectively.

The simplicity of the HCIS model in solving an ordinary first-order differential equation and its flexibility to include additional reaction kinetics has been an advantage to the model. However, it is essential to understand the limitations associated with this new model. The model does not consider the effect of lateral flow due to its restriction to non-rainy period. Also, the model finds the river reach as being prismatic and applies a constant parameter within each reach of the river.

The developed model will be useful for government agencies in charge of river quality monitoring to have a better understanding of the level of nutrient pollution in the river. Model outputs can provide information for decision making and taking active measures against nutrient pollution. Based on the new model's performance in the reproduction of the observed real-time data and the ADE model, it can be concluded that the developed HCIS model coupled with nutrient kinetics is suitable for the simulation of nutrient solute transport in a river. Furthermore, the solution can be used to verify other models that are developed to simulate nutrient pollutants in natural streams. Therefore, the main theoretical contribution of this study is the development of a nutrient solute transport model and solution techniques needed for the evaluation of ammonia, nitrite, and nitrate nutrients in different water bodies.

7.2. Recommendations for Continuation of the Study

The process of water quality modelling has shown to be a very complicated procedure and time-consuming. In this study, a significant effort was made to develop a hybrid cell-in-series model considering nutrient kinetics processes, which can predict some nutrient parameters, i.e., ammonia, nitrite, and nitrate in different water bodies. Based on this study, the following recommendations were made for further research:

(i) The new model does not consider the effect of lateral flow due to its restriction to non-rainy periods. It can be improved in the future to examine the impact of non-point source pollution in its process.

(ii) The model concept can incorporate some other water quality parameters such as phosphorus, heavy metals and sediment transport in its formulation.

(iii) The HCIS model was applied to the uMgeni River. Application of the new model to other South African and overseas water bodies can demonstrate more the capabilities of the model for nutrient simulation.

(iv) The model considers the river reach as being prismatic and applies a constant parameter within each range of the river. It can be enhanced to include channel irregularities in its process.

REFERENCES

Abbaspour, K. C., Faramarzi, M., Ghasemi, S. S. and Yang, H. (2009). Assessing the impact of climate change on water resources in Iran. Water resources research, 45(10).

Agunbiade, F. O. and Moodley, B. (2014) Pharmaceuticals as emerging organic contaminants in uMgeni River water system, KwaZulu-Natal, South Africa. Environmental Monitoring and Assessment. 186: 7273-7291.

Aissa-Grouz, N., Garnier, J., Billen, G., Mercier, B. and Martinez, A. (2015). The response of river nitrification to changes in wastewater treatment (The case of the lower Seine River downstream from Paris). In Annales de Limnologie-International Journal of Limnology (Vol. 51, No. 4, pp. 351-364). EDP Sciences.

Akkoyunlu, A. and Karaaslan, Y. (2015). Assessment of improvement scenario for water quality in Mogan Lake by using the AQUATOX Model. Environmental Science and Pollution Research, 22(18), 14349-14357.

Alam MJ, Islam MR, Muyen Z, Mamun M. and Islam S. (2007) Water quality parameters along rivers. International Journal of Environmental Science & Technology, 4(1): 159-167.

Aliverdi A. and Eslami H. (2014) Modelling of BOD and Ammonia in Karkheh River using WASP6. Bull. Env. Pharmacol. Life Science. 4: 01-09.

Ambrose, R. B., Wool, T. A. and Martin, J. L. (1993). The water quality analysis simulation program,WASP5, Part A: Model documentation. Environmental Research Laboratory, US Environmental Protection Agency, Athens, GA.

Ani EC, Hutchins MG, Kraslawski A. and Agachib P.S. (2010) Assessment of pollutant transport and river water quality using mathematical models. Revue Roumaine de Chimie, 55(4): 285-291.

Anyadike CC, Mbajiorgu, CC. and Ajah GN. (2013). Prediction of the Physico-Chemical Interactions of Vimtim Stream Water Quality using the Aquatox Model. IOSR Journal Engineering. 3: 1-6.

Arnold, J. G., Srinivasan, R., Muttiah, R. S. and Williams, J. R. (1998). Large area hydrologic modeling and assessment part I: model development. JAWRA Journal of the American Water Resources Association, 34(1), 73-89.

Arthington, Á.H., Naiman, R.J., Mcclain, M.E. and Nilsson, C. (2010). Preserving the biodiversity and ecological services of rivers: new challenges and research opportunities. Freshwater Biology, 55(1), pp.1-16.

Atashgahi, S., Aydin, R., Dimitrov, M.R., Sipkema, D., Hamonts, K., Lahti, L., Maphosa, F., Kruse, T., Saccenti, E., Springael, D. and Dejonghe, W. (2015). Impact of a wastewater treatment plant on microbial community composition and function in a hyporheic zone of a eutrophic river. Scientific reports, 5, p.srep17284.

Bailey, R.T. and Ahmadi, M. (2014). Spatial and temporal variability of in-stream water quality parameter influence on dissolved oxygen and nitrate within a regional stream network. Ecological modelling, 277, pp.87-96.

Banks RB. (1974) A Mixing Cell Model for Longitudinal Dispersion in Open Channel. Water Resource Research. 10: 357-358.

Bear J. (1972) Dynamics of fluids in porous media. New York: American Elsevier Publishing Company, Inc. P.764.

Beer, T. and Young, PC. (1983) Longitudinal dispersion in natural streams. Journal of Environmental Engineering. 109: 1049-1067

Benaman, J., Shoemaker, C.A. and Haith, D.A. (2001). Calibration and Validation of the Soil and Water Assessment Tool on the Cannonsville Reservoir Watershed, J. of Hydrologic Engineering, 10(5), pp. 363-374.

Benedini, M. and Tsakiris, G. (2013) Water Quality Modelling for Rivers and Streams, Water Science and Technology Library: 272.

Bingli, L., Huang, S., Min, Q., Tianyun, L. and Zijian, W. (2008). Prediction of the environmental fate and aquatic ecological impact of nitrobenzene in the Songhua River using the modified AQUATOX model. Journal of Environmental Sciences, 20, 769-777.

Birgand, F. (2004). Evaluation of QUAL2E. Agricultural non-point source water quality models: their use and application. Southern Cooperative Series Bulletin, 398, 99-107.

Blancher, E. C. (2010). Modeling nutrients and multiple algal groups using AQUATOX: Watershed management implications for the Braden River Reservoir, Bradenton Florida. Proceedings of the Water Environment Federation, 2010, 6393-6410.

Bouraoui, F. and Grizzetti, B. (2014), Modelling mitigation options to reduce diffuse nitrogen water pollution from agriculture. Science of the Total Environment, 468, 1267-1277.

Boyer, E.W., Alexander, R.B., Parton, W.J., Li, C., Butterbach-Bahl, K., Donner, S.D., Skaggs, R.W. and Grosso, S.J.D. (2006). Modeling denitrification in terrestrial and aquatic ecosystems at regional scales. Ecological Applications, 16(6), pp.2123-2142.

Brown, L. C. and Barnwell, T. O. (1987). The enhanced stream water quality models QUAL2E and QUAL2E-UNCAS: documentation and user manual, US Environmental Protection Agency. Office of Research and Development. Environmental Research Laboratory.

Cameron, D. R. and Klute, A. (1977). "Convective dispersive solute transport with combined equilibrium and kinetic adsorption model." Water Resource. Res., 13(1), 183–188.

Cebron, A. and Garnier, J. (2005). Nitrobacter and Nitrospira genera as representatives of nitrite-oxidizing bacteria: detection, quantification and growth along the lower Seine River (France). Water research, 39(20), pp.4979-4992.

Chapra, S.C. (2008). Surface water-quality modeling. McGraw-Hill, New York.

Chatwin, P.C. (1980) 'Presentation of longitudinal dispersion data', J. Hydraul. Div., ASCE, Vol. 106, No.1, pp.71–83.

Chatwin, P.C. and Allen, C.M. (1985). Mathematical models of dispersion in rivers and estuaries. Annual Review of Fluid Mechanics, 17(1), pp.119-149.

Conley, D. J., Paerl, H. W., Howarth, R. W., Boesch, D. F., Seitzinger, S. P., Havens, K. E., Lancelot,C. and Likens, G. E. (2009). Controlling eutrophication: nitrogen and phosphorus. Science, 323, 1014-1015.

Connolly, J. P. and Winfield, R. P. (1984). A user's guide for WASTOX, a Framework for Modeling the fate of toxic chemicals in aquatic environments. Environmental Research Laboratory,Office of Research and Development, US Environmental Protection Agency.

Corriveau, J., van Bochove, E., Savard, M.M., Cluis, D. and Paradis, D. (2010). Occurrence of high in-stream nitrite levels in a temperate region agricultural watershed. Water, air, and soil pollution,206(1-4), pp.335-347.

Cosgrove, W. and Rijsberman, F. (2000) World Water Vision: Making Water Everybody's Business. World Water Council. Earthscan Publications, London, UK.

Cox, B. (2003). A review of currently available in-stream water-quality models and their applicability for simulating dissolved oxygen in lowland rivers. Science of the Total Environment, 314, 335-377.

Crabtree, R., Squibbs, G., Mitchell, G. and Ellor, B. (2010). A river catchment modelling approach to urban wet weather discharge control strategies for the Water Framework Directive. Proc. 7th Int. Conf. Sustainable Techniques and Strategies in Urban Water Management. NOVATECH7.GRAIE, Lyon, France.

Dodds, W.K. (2006). Eutrophication and trophic state in rivers and streams. Limnology and Oceanography, 51(1part2), pp.671-680.

Dortch, M., Schneider, T., Martin, J., Zimmerman, M. and Griffin, D. M. (1990). CE-QUAL-RIV1: Dynamic, One-Dimensional (Longitudinal) Water Quality Model for Streams. User's Manual (No. WES/IR/E-90-1). Army Engineer Waterways Experiment Station Vicksburg Ms Environmental Lab.

Donner, S.D., Coe, M.T., Lenters, J.D., Twine, T.E. and Foley, J.A. (2002). Modeling the impact of hydrological changes on nitrate transport in the Mississippi River Basin from 1955 to 1994. Global biogeochemical cycles, 16(3).

Elder, J.W. (1959). The dispersion of marked fluid in turbulent shear flow. Journal of fluid mechanics, 5(4), pp.544-560.

Ernst, M. R. and Owens, J. (2009). Development and application of a WASP model on a large Texas reservoir to assess eutrophication control. Lake and Reservoir Management, 25, 136-148.

Etemad-Shahidi, A. and Taghipour, M. (2012). Predicting longitudinal dispersion coefficient in natural streams using M5′ model tree. Journal of hydraulic engineering, 138: 542-554.

Fewtrell, L. (2004). Drinking-water nitrate, methemoglobinemia, and global burden of disease: a discussion. Environmental health perspectives, 112(14), p.1371.

Fischer, H.B. (1966). A note on the one-dimensional dispersion model. WM Keck Laboratory of Hydraulics and Water Resources, California Institute of Technology.

Fisher HB, List EJ, Koh RC, Imberger J. and Brooks, N.H. (1979). Mixing in Inland and Coastal Waters Academic Press. New York :229-242.

Foley, B., Jones, I.D., Maberly, S.C. and Rippey, B. (2012). Long-term changes in oxygen depletion in a small temperate lake: effects of climate change and eutrophication. Freshwater Biology, 57(2), pp.278-289.

Gao, X., LI, G., LI, G. and Zhang, C. (2015). Modeling the effects of point and non-point source pollution on a diversion channel from Yellow River to an artificial lake in China. Water Science and Technology, 71, 1806-1814.

Gassman, P. W., Reyes, M. R., Green, C. H. and Arnold, J. G. (2007). The soil and water assessment tool: historical development, applications, and future research directions. Transactions of the ASABE, 50(4), 1211-1250.

Gavrilescu, M., Demnerová, K., Aamand, J., Agathos, S. and Fava, F. (2015). Emerging pollutants in the environment: present and future challenges in biomonitoring, ecological risks and bioremediation. New biotechnology, 32(1), 147-156.

Genuchten MT, Leij FJ, Skaggs TH, Toride N, Bradford, S.A. and Pontedeiro, E.M. (2013). Exact analytical solutions for contaminant transport in rivers 1. The equilibrium advection-dispersion equation. Journal of Hydrology and Hydromechanics, 61(2): 146-160

Ghosh, N.C. (2001). Study of solute transport in a river. Ph. D thesis, Dept of Civ. Eng., IIT. Roorkee, INDIA.

Ghosh, N.C., Mishra, G.C. and Ojha, C.S. (2004). A hybrid-cells-in-series model for solute transport in a river. Journal of Environmental Engineering Division ASCE. 130: 1198–1209.

Ghosh, N.C., Mishra, G.C. and Kumarasamy, M. (2008). Hybrid-cells-in-series model for solute transport in streams and relation of its parameters with bulk flow characteristics. Journal of Hydraulic Engineering. 134: 497-502.

Gooseff, M.N., Bencala, K.E. and Wondzell, S.M. (2008). Solute transport along stream and river networks. River Confluences, Tributaries and the Fluvial Network, pp.395-418.

Gotovtsev, A. (2010). Modification of the Streeter-Phelps system with the aim to account for the feedback between dissolved oxygen concentration and organic matter oxidation rate. Water Resources. 37: 245-251.

Gotovtsev, A. V. (2014). A new method for estimating BOD and the rate of biochemical oxidation based on modified Streeter-Phelps equations. Water Resources, 41, 330-334.

Gregor, J. and Maršálek, B. (2004). Freshwater phytoplankton quantification by chlorophyll a: a comparative study of in vitro, in vivo and in situ methods. Water Research. 38: 517-522.

Hart, D.R. (1995). Parameter estimation and stochastic interpretation of the transient storage model for solute transport in streams. Water Resources Research, 31(2), pp.323-328.

Hill, A.R., Kemp, W.A., Buttle, J.M. and Goodyear, D. (1999). Nitrogen chemistry of subsurface storm runoff on forested Canadian Shield hillslopes. Water Resources Research, 35(3), pp.811-821.

Holly Jr, F. M., and Preissmann, A. (1977). Accurate calculation of transport in two dimensions. Journal of the Hydraulics division, 103 (ASCE 13336 Proceeding).

Howarth, R.W. (2008). Coastal nitrogen pollution: a review of sources and trends globally and regionally. Harmful Algae, 8(1), pp.14-20.

Jacobs, U. (2007). Appendix 24.5–SIMCAT Modelling Assessment of the Operational Phase of the AWPR affecting the River Dee and its Tributaries.

Jaiswal, D. K., Kumar, A. and Yadav, R. R. (2011). Analytical solution to the one-dimensional advection-diffusion equation with temporally dependent coefficients. Journal of Water Resource and Protection, 3, 76.

Jha M, Gu. R. (2010). Risk analysis of seasonal stream water quality management. Water Science and Technology 62: 2075-2082.

Jirka, G. H. and Weitbrecht, V. (2005). Mixing models for water quality management in rivers: continuous and instantaneous pollutant releases. In Water quality hazards and dispersion of pollutants (pp. 1-34). Springer US.

Kamal, M. M., Malmgren-Hansen, A. and Badruzzaman, A. (1999). Assessment of pollution of the River Buriganga, Bangladesh, using a water quality model. Water science and technology, 40, 129-136.

Kamer K, Fong P, Kennison RL. and Schiff, K. (2004). The relative importance of sediment and water column supplies of nutrients to the growth and tissue nutrient content of the green macroalga Enteromorpha intestinalis along an estuarine resource gradient. Aquatic ecology, 38(1): 45-56.

Kannel, P.R., Lee, S., Lee, Y.S., Kanel, S.R. and Pelletier, G.J. (2007). Application of automated QUAL2Kw for water quality modeling and management in the Bagmati River, Nepal. ecological modelling, 202(3), pp.503-517.

Kannel, P. R., Kanel, S. R., Lee, S., Lee, Y.-S. and Gan, T. Y. (2011). A review of public domain water quality models for simulating dissolved oxygen in rivers and streams. Environmental Modeling & Assessment, 16, 183-204.

Karadžić, V., Subakov-Simić, G., Krizmanić, J. and Natić, D. (2010). Phytoplankton and eutrophication development in the water supply reservoirs Garaši and Bukulja (Serbia). Desalination, 255(1), pp.91-96.

Kiedrzyńska, E., Kiedrzyński, M., Urbaniak, M., Magnuszewski, A., Skłodowski, M., Wyrwicka, A. and Zalewski, M. (2014), Point sources of nutrient pollution in the lowland river catchment in the context of the Baltic Sea eutrophication. Ecological engineering, 70, 337-348.

Kashefipour, S.M. and Falconer, R.A. (2002). Longitudinal dispersion coefficients in natural channels. Water Research, 36(6), pp.1596-1608.

Kaufman, G. B. (2011). Application of the Water Quality Analysis Simulation Program (WASP) to evaluate dissolved nitrogen concentrations in the Altamaha River estuary, Georgia (Doctoral dissertation, uga).

Kazmi, A. A. and Hansen, I. S. (1997). Numerical models in water quality management: a case study for the Yamuna river (India). Water science and technology, 36, 193-200.

Kinnunen, K., Nyholm, B., Niemi, J., Frisk, T., Kylä-Harakka, T. and Kauranne, T. (1982). Water quality modelling of Finnish water bodies. Vesihallitus. National Board of Waters.

Kumar, R.N. (2011). An assessment of seasonal variation and water quality index of Sabarmati River and Kharicut canal at Ahmedabad, Gujarat. Electronic Journal of Environmental, Agricultural and Food Chemistry (EJEAFChe), 10(5), pp.2248-2261.

Kumarasamy, M. (2015). Deoxygenation and Reaeration Coupled hybrid Mixing cells Based Pollutant Transport Model to Assess water Quality Status of a River. International Journal of Environmental Research. 9: 341-350.

Kumarasamy, M, Ghosh NC, Mishra GC. and Kansal ML. (2013). Hybrid model development for the decaying pollutant transport in streams. International Journal of Environment and Waste Management, 12(2): 130-145.

Kumarasamy M, Mishra GC, Ghosh NC. and Kansal ML. (2011). Semianalytical solution for nonequilibrium sorption of pollutant transport in streams. Journal of Environmental Engineering, 137(11): 1066-1074.

Kuo JT, Lung WS, Yang CP, Liu WC, Yang MD. and Tang TS. (2006). Modelling Eutrophication of reservoirs in Taiwan. Environmental Modelling & Software, 21(6): 829-844

Lai, Y., Tu, Y., Yang, C., Surampalli, R. and Kao, C. (2013). Development of a water quality Modeling system for river pollution index and suspended solid loading evaluation. Journal of Hydrology, 478, 89-101.

Lam, Q.D., Schmalz, B. and Fohrer, N. (2010). Modelling point and diffuse source pollution of nitrate in a rural lowland catchment using the SWAT model. Agricultural Water Management, 97(2), pp.317-325.

Lees, M.J., Camacho, L.A. and Chapra, S. (2000). On the relationship of transient storage and aggregated dead zone models of longitudinal solute transport in streams. Water resources research, 36(1), pp.213-224.

Lewis JR, W. M., Wurtsbaugh, W. A. and Paerl, H. W. (2011). Rationale for control of anthropogenic nitrogen and phosphorus to reduce eutrophication of inland waters. Environmental science & technology, 45, 10300-10305.

Liangliang, G. and Daoliang, L.(2015). A review of hydrological/water-quality models. Frontiers of Agricultural Science and Engineering, 1: 267-276.

Lin, L. and Webster, J. (2012). Sensitivity analysis of a pulse nutrient addition technique for estimating nutrient uptake in large streams. Limnology and Oceanography: Methods. 10: 718-727.

Liu, S., Taylor, J. S., Randall, A. and Dietz, J. D. (2005). Nitrification modeling in chloraminated distribution systems. Journal (American Water Works Association), 97, 98-108.

Marchant, H.K., Holtappels, M., Lavik, G., Ahmerkamp, S., Winter, C. and Kuypers, M.M. (2016). Coupled nitrification–denitrification leads to extensive N loss in subtidal permeable sediments. Limnology and Oceanography, 61(3), pp.1033-1048.

María, EPL, Sanchez-Martinez, MG. and Leon, MT. (2013). Eutrophication Levels through San Pedro-Mezquital River Basin. Journal of Environmental Protection, 4(11): 45 - 50.

Martin, J., Wool, T. and Olson, R. (2002). A dynamic one-dimensional model of hydrodynamics and water quality (EPD-RIV1), version 1.0. Model Documentation and User Manual. Atlanta, GA: Georgia Environmental Protection Division.

Mirbagheri, S., Abaspour, M. and Zamani, K. (2009). Mathematical modeling of water quality in river systems. European Water, 31-41.

Murphy, E., Ghisalberti, M. and Nepf, H. (2007). Model and laboratory study of dispersion in flows with submerged vegetation. Water Resources Research, 43(5).

Neitsch, S., Arnold, J., Kiniry, J. E. A., Srinivasan, R. and Williams, J. (2002). Soil and water assessment tool user's manual version 2000. GSWRL report, 202.

Neitsch, S. L., Arnold, J. G., Kiniry, J. R. and Williams, J. R. (2011). Soil and water assessment tool theoretical documentation version 2009. Texas Water Resources Institute.

Neuman, SP. and Tartakovsky, DM. (2009). Perspective on theories of non-Fickian transport in heterogeneous media. Advances in Water Resources, 32: 670-680.

Ning, S.-K., Chang, N.-B., Yang, L., Chen, H.-W. and Hsu, H.-Y. (2001). Assessing pollution prevention program by QUAL2E simulation analysis for the Kao-Ping River Basin, Taiwan. Journal of Environmental Management, 61, 61-76.

Nordin, C.F. and Troutman, B.M. (1980). Longitudinal dispersion in rivers: The persistence of skewness in observed data. Water Resources Research, 16(1), pp.123-128.

Nyenje, P. M., Foppen, J. W., Uhlenbrook, S., Kulabako, R. and Muwanga, A. (2010). Eutrophication and nutrient release in urban areas of sub-Saharan Africa—a review. Science of the Total Environment, 408(3), 447-455.

Oeurng, C., Cochrane, T.A., Arias, M.E., Shrestha, B. and Piman, T. (2016). Assessment of changes in riverine nitrate in the Sesan, Srepok and Sekong tributaries of the Lower Mekong River Basin. Journal of Hydrology: Regional Studies, 8, pp.95-111.

Oliveira, B., Bola, J., Quinteiro, P., Nadais, H. and Arroja, L. (2012), Application of Qual2Kw model as a tool for water quality management: Cértima River as a case study. Environmental monitoring and assessment, 184(10), 6197-6210.

Olowe, K. O. and Kumarasamy, M. (2017). Development of the hybrid cells in series model to simulate ammonia nutrient pollutant transport along the Umgeni River. Environmental Science and Pollution Research, 24(29), 22967-22979.

O'neil, J., Davis, T. W., Burford, M. A. and Gobler, C. (2012), The rise of harmful cyanobacteria blooms: the potential roles of eutrophication and climate change. Harmful Algae, 14, 313-334.

Paerl, H.W. (1997). Coastal eutrophication and harmful algal blooms: Importance of atmospheric deposition and groundwater as "new" nitrogen and other nutrient sources. Limnology and oceanography, 42(5part2), pp.1154-1165.

Paerl, H.W., Hall, N.S. and Calandrino, E.S. (2011). Controlling harmful cyanobacterial blooms in a world experiencing anthropogenic and climatic-induced change. Science of the Total Environment, 409(10), pp.1739-1745.

Park, R. and Clough, J. (2004). AQUATOX (release 2) Modeling Environmental Fate and Ecological Effects in Aquatic Ecosystems. Volume 2: Technical Documentation. EPA-823-R-04-002. US Environmental Protection Agency, Washington, DC.

Park, R. A., Clough, J. S. and Wellman, M. C. (2008). AQUATOX: Modeling environmental fate and ecological effects in aquatic ecosystems. Ecological Modelling, 213, 1-15

Park, S. S. and Lee, Y. S. (2002). A water quality modeling study of the Nakdong River, Korea. Ecological Modelling, 152, 65-75.

Paredes, J., Andreu, J. and Solera, A. (2010). A decision support system for water quality issues in the Manzanares River (Madrid, Spain). Science of the Total Environment, 408(12), 2576-2589.

Parsaie, A. and Haghiabi, A.H. (2015). Computational Modelling of Pollution Transmission in Rivers. Applied Water Science. :1-10.

Pohlert, T., Huisman, J.A., Breuer, L. and Frede, H.G. (2005). Modelling of point and non-point source pollution of nitrate with SWAT in the river Dill, Germany. Advances in Geosciences, 5, pp.7-12.

Pimentel, D., Berger, B., Filiberto, D., Newton, M., Wolfe, B., Karabinakis, E., Clark, S., Poon, E., Abbett, E. and Nandagopal, S. (2004). Water resources: agricultural and environmental issues. BioScience, 54(10), pp.909-918.

Purandara, B., Varadarajan, N., Venkatesh, B. and Choubey, V. (2012). Surface water quality evaluation and modeling of Ghataprabha River, Karnataka, India. Environmental monitoring and assessment, 184, 1371.

Rabalais, NN, Turner, RE, Díaz, RJ. and Justić D. (2009). Global change and eutrophication of coastal waters. ICES Journal of Marine Science: Journal du Conseil, 66: 1528-1537.

Radwan, M., Willems, P., El-Sadek, A. and Berlamont, J. (2003). Modelling of dissolved oxygen and biochemical oxygen demand in river water using a detailed and a simplified model. International Journal of River Basin Management, 1, 97-103.

Rahaman, MM. and Varis, O. (2005). Integrated water resources management: evolution, prospects and future challenges. Sustainability: Science, Practice and Policy. 1: 1-9.

Raimonet, M., Vilmin, L., Flipo, N., Rocher, V. and Laverman, A. M. (2015). Modelling the fate of nitrite in an urbanized river using experimentally obtained nitrifier growth parameters. Water research, 73, 373-387.

Rakib Z, Barber M. and Mahler R. (2015). Modelling flow, nutrient and dissolved oxygen concentrations in the Spokane River under multiple year conditions. WIT Transactions on Ecology and the Environment. 196: 127-138.

Rode M, Klauer B, Petry D, Volk M, Wenk G. and Wagenschein, D. (2008). Integrated nutrient transport modelling with respect to the implementation of the European WFD: The Weiβe Elster Case Study, Germany. Water Sa, 34(4): 490-496.

Runkel, R.L. and Bencala, K.E. (1995). Transport of reacting solutes in rivers and streams. In Environmental hydrology, pp. 137-164. Springer Netherlands.

Runkel, R.L. (1998). One dimensional transport with inflow and storage (OTIS): A solute transport model for streams and rivers. Water Resources Investigation Rep. No 98-4018., USGS, Denver.

Rutherford, J.C. (1994). River mixing. John Wiley & Son Ltd.

Sakalauskienė, G. (2001). Dissolved oxygen balance model for Neris. Nonlinear Analysis: Modelling and Control, 6, 105-131.

Samatya, S., Kabay, N., Yüksel, Ü., Arda, M. and Yüksel, M. (2006). Removal of nitrate from aqueous solution by nitrate selective ion exchange resins. Reactive and Functional Polymers, 66(11), 1206- 1214. Santhi, C., Srinivasan, R., Arnold, J.G. and Williams, J.R. (2006). A modeling approach to evaluate the impacts of water quality management plans implemented in a watershed in Texas. Environmental Modelling & Software, 21(8), pp.1141-1157.

Savci, S. (2012). An agricultural pollutant: chemical fertilizer. International Journal of Environmental Science and Development, 3(1), p.73.

Sayre, W.W. and Chang, F.M. (1968). A laboratory investigation of open-channel dispersion processes for dissolved, suspended, and floating dispersants: US Geol. Survey Prof. Paper.

Schlesinger, W.H., Reckhow, K.H. and Bernhardt, E.S. (2006). Global change: The nitrogen cycle and rivers. Water Resources Research, 42(3).

Schütze M, Reussner F. and Alex, J. (2011). SWQM–a simple river water quality model for assessment of urban wastewater discharges. Proc. 11th International Conference on Urban Drainage (11ICUD): 11-15.

Seibel, B. A. (2011). Critical oxygen levels and metabolic suppression in oceanic oxygen minimum zones. Journal of Experimental Biology, 214, 326-336.

Seo, I.W. and Cheong, T.S. (1998). Predicting longitudinal dispersion coefficient in natural streams. Journal of Hydraulic Engineering, 124(1), pp.25-32.

Shao-Chen S, Zu-Hao Z, Wei-Hua X. and Hao, W. (2014). Impact analysis on water quality of the Second Songhua river based on mathematical model. Journal of Clean Energy Technologies, 2(3): 240-243

Sharma, D. and Kansal, A. (2013). Assessment of river quality models: a review. Reviews in Environmental Science and Bio/Technology, 12, 285-311.

Shoemaker, L., Dai, T., Koenig, J. and Hantush, M. (2005). TMDL model evaluation and research needs, National Risk Management Research Laboratory, US Environmental Protection Agency.

Shu, F. Y., Liu, Y. P., Zhao, Y., Wu, Y. P., and Li, A. H. (2012). Spatio-temporal distribution of TN and TP in water and evaluation of eutrophic state of Lake Nansi. Huan jing ke xue Huanjing kexue, 33(11), 3748-3752.

Silva, M. A. M., Souza, M. F. and Abreu, P. C. (2015). Spatial and temporal variation of dissolved inorganic nutrients, and chlorophyll-α in a tropical estuary in northeastern Brazil: dynamics of nutrient removal. Brazilian Journal of Oceanography, 63(1), 1-15.

Slaughter A.R. (2011). Modelling the relationship between flow and water quality in South African rivers. Doctor of Philosophy, Rhodes University, South Africa.

Smith, V. H. and Schindler, D. W. (2009). Eutrophication science: where do we go from here? Trends in Ecology & Evolution, 24(4), 201-207.

Stefan, H. G. and Demetracopoulos, A. C. (1981). "Cells in series simulation of riverine transport." J. Hydraulic Division, 107(6), 675-697.

Sui, Y. and Frankenberger, J.R. (2008). Nitrate loss from subsurface drains in an agricultural watershed using SWAT2005. Transactions of the ASABE, 51(4), pp.1263-1272.

Szomorová, L. and Halaj, P. (2015). Numerical simulations in the Mala Nitra Stream By 1D Model.Acta Scientiarum Polonorum. Formatio Circumiectus. 14: 185-194.

Thomann, R.V. and Mueller, J.A. (1987). Principles of surface water quality modelling and control. New York: Harper and Row Publishers.

Tisseuil, C., Wade, A.J., Tudesque, L. and Lek, S. (2008). Modeling the stream water nitrate dynamics in a 60,000-km European catchment, the Garonne, southwest France. Journal of environmental quality, 37(6), pp.2155-2169.

Tolson, B. A. and Shoemaker, C. A. (2004). Watershed modeling of the Cannonsville Basin using SWAT2000: Model. Cornell Library Technical Reports and Papers.

Tolson, B. A. and Shoemaker, C. A. (2007). Cannonsville Reservoir Watershed SWAT2000 model development, calibration and validation. Journal of Hydrology, 337, 68-86.

Tsakiris, G. and Alexakis, D. (2012). Water quality models: an overview. European Water, 37, 33-46.

Tufford, D.L. and McKellar, H.N. (1999). Spatial and temporal hydrodynamic and water quality modelling analysis of a large reservoir on the South Carolina (USA) coastal plain. Ecological Modelling. 114: 137-173.

Tyagi, B., Kapoor, R., Sinha, D. and Bhargava, D.S. (2012). Mathematical Modeling and Simulation for Predicting DO Condition in Rivers. International Journal of Environmental Protection, 2(10), pp. 29-34

Valent, P., Howden, N., Szolgay, J. and Komorníková, M. (2011). Analysis of nitrate concentrations using nonlinear time series models. Journal of Hydrology and Hydromechanics, 59(3), 157-170.

Varol, M. and Sen, B. (2012). Assessment of nutrient and heavy metal contamination in surface water and sediments of the upper Tigris River, Turkey. Catena, 92, 1-10.

Vonder Wiesche, M. and Wetzel, A. (1998). Temporal and spatial dynamics of nitrite accumulation in the River Lahn. Water Research, 32(5), pp.1653-1661.

Wadi, A.S., Dimian, M.F. and Ibrahim, F.N. (2014). Analytical solutions for one-dimensional advection–dispersion equation of the pollutant concentration. Journal of Earth System Science. 123: 1317-1324.

Wang, Q., Zhao, X., Yang, M., Zhao, Y., Liu, K. and Ma, Q. (2011). Water quality model establishment for middle and lower reaches of Hanshui River, China. Chinese Geographical Science, 21(6), pp.646-655.

Wang Q, Li S, Jia P, Qi, C. and Ding, F. (2013). A review of surface water quality models. The Scientific World Journal, 2013 :1–7

Wang, G. T. and Chen, S. (1996). A new model describing convective-dispersive phenomena derived by using the mixing-cell concept. Applied mathematical modelling, 20(4), 309-320.

Wang, T., Huang, S., Du, H. and Zhang, G. (2012). Studies on Retrieval of the Initial Values and Diffusion Coefficient of Water Pollutant Advection and Diffusion Process. In Mathematical Methods for Surface and Subsurface Hydrosystems (pp. 174-190).

Warn, A. (1987). SIMCAT-A catchment simulation model for planning investment for river quality. Systems Analysis in Water Quality Management. Pergamon Press New York. 1987. p 211-218.

Warn, T. (2007). SIMCAT 10.1-A guide and reference for users. Environment Agency, 210.

Wool, T.A., Ambrose, R.B., Martin, J.L., Comer, E.A. and Tech, T. (2006). Water quality analysis simulation program (WASP). User's Manual, Version, 6, US Environment protection Agency, Athens, GA.

Yang, C.-P., Kuo, J.-T., Lung, W.-S., Lai, J.-S. and Wu, J.-T. (2007). Water quality and ecosystem modeling of tidal wetlands. Journal of Environmental Engineering, 133, 711-721.

Yang, L., Mei, K., Liu, X., Wu, L., Zhang, M., Xu, J. and Wang, F. (2013). Spatial distribution and source apportionment of water pollution in different administrative zones of Wen-Rui-Tang (WRT) river watershed, China. Environmental Science and Pollution Research, 20, 5341-5352.

Yang, X.-E., Wu, X., Hao, H.-L. and He, Z.-L. (2008). Mechanisms and assessment of water eutrophication. Journal of Zhejiang University Science B, 9, 197-209.

Yin, Y., Jiang, S., Pers, C., Yang, X., Liu, Q., Yuan, J., Yao, M., He, Y., Luo, X. and Zheng, Z. (2016). Assessment of the spatial and temporal variations of water quality for agricultural lands with crop rotation in China by using a HYPE Model. International journal of environmental research and public health, 13(3), p.336.

Yuceer, M. and Coskun, M. A. (2016). Modeling water quality in rivers: a case study of Beylerderesi river in Turkey. Applied Ecology and Environmental Research, 14(1), 383-395.
Zamparas, M. and Zacharias, I., (2014), Restoration of eutrophic freshwater by managing internal nutrient loads. A review. Science of the Total Environment, 496, 551-562.

Zhang, Z., Li, C., Zeng, X.-L. and Zhang, Y. (2006). Application of QUAL2E Model to Chongqing Urban Section of the Yangtze River [J]. Environmental Science & Technology, 1, 200 - 212.

Zheng, X., Fu, C., Xu, X., Yan, X., Huang, Y., Han, S., Hu, F. and Chen, G. (2002). The Asian nitrogen cycle case study. AMBIO: A Journal of the Human Environment, 31(2), pp.79-87.

Zhu Z, Yuan H, Wei Y, Li P, Zhang P. and Xie, D. (2015). Effects of ammonia nitrogen and sediment nutrient on growth of the submerged plant Vallisnerianatans. CLEAN–Soil, Air, Water. 43: 1653-1659.

Ziemińska-Stolarska, A. and Skrzypski, J. (2010). Review of mathematical models of water quality. Copernican Letters, 1, 36-49.

APPENDIX A

A1. List of Publications from this thesis

(1) **Olowe, K.O**. and Kumarasamy, M. (2017). Development of the hybrid cells in series model to simulate ammonia nutrient pollutant transport along the uMgeni River. *Environmental* Science and Pollution Research, 24(29), pp.22967-22979 **(Published).**

(2) **Olowe, K. O**. and Kumarasamy, M. (2017). Assessment of existing water quality models. Nature Environment and Pollution Technology **(Accepted)**

(3) **Olowe, K. O**., and Kumarasamy, M. (2017). Analytical solution of a mathematical model to simulate nitrite pollutant transport along a river. Environmental Modeling & Assessment **(Under review)**

(4) **Olowe, K. O**. and Kumarasamy, M. (2017). A mathematical model development for simulating Nitrate pollutant transport along uMgeni River (**Submitted**)

(5) **Olowe, K. O**., and Kumarasamy, M. (2017). Development of Hybrid-Cell-In -Series Model to Simulate Nitrite Nutrient Pollutant Transport Along A River. International Journal of Arts & Sciences. Prague, Czech Republic, October 31-November 3, 2017. (**Conference Paper**)

APPENDIX B

B1. Program for simulating HCIS - NH_3 model using a C# programming language.

```
using System;
using System. Collections. Generic;
using System.Linq;
using System.Text;
using System.IO;
using Microsoft. Office. Interop. Excel;

namespace HCIS
{
public class Program
{
static void Main (string [] args)
{
        double discrete = 0;
        List<double> sumTotalAtEdge = new List<double> ();
        List<double> sumTotal = new List<double> ();
        int inputtracker = 1;
        double Co = 0;
        double Ka = 0;
        double T1 = 0;
        double T2 = 0;
        double T3 = 0;
        double Ao = 0;
        double A1 = 0;
        double A2 = 0;
        double A3 = 0;
        double A4 = 0;
        double A5 = 0;
        double tv = 0;
        double s = 0;
        double nth = 0;
```

```
double Kb = 0;
int Nr = 0;
string desktopPath = Environment.GetFolderPath(Environment.SpecialFolder. Desktop Directory);
string desktopFolderPath = Path. Combine (desktopPath, "Ammonia. Output Folder");
if (! Directory.Exists(desktopFolderPath))
{
Directory.CreateDirectory(desktopFolderPath);
}
String [] lines;
var list = new System. Collections. Generic. List<string>();
var fileStream = new FileStream(@"input1.txt", FileMode.Open, FileAccess.Read);
using (var streamReader = new Stream Reader(fileStream, Encoding.UTF8))
{
streamReader.ReadLine();
{
list. Add(line);
}
}
string startUPP = System.IO.Directory. GetCurrentDirectory () + "\\input1.txt";
FileStream fss = new FileStream(startUPP, FileMode.Open);
StreamReader srr = new StreamReader(fss);
string tvv = srr.ReadLine();
while (tvv != null)
{
if (inputtracker == 1)
{
string[] c = tvv.Split(' ');
Co = Convert.ToDouble(c[1]);
 }
if (inputtracker == 2)
{
string[] c = tvv.Split(' ');
```

```
Nr = Convert.ToInt32(c[1]);
}
inputtracker = inputtracker + 1;
tvv = srr.ReadLine();
}
int counter = 0;
string startUP = System.IO.Directory. GetCurrentDirectory () + "\\input2.txt";
FileStream fs = new FileStream (startUP, FileMode.Open);
StreamReader sr = new StreamReader(fs);
string tc = sr.ReadLine();
{
if (counter == 0)
{
string[] c = tc.Split(' ');
Ka = Convert.ToDouble(c[1]);
}
if (counter == 1)
{
string[] c = tc.Split(' ');
Ao = Convert.ToDouble(c[1]);
}
if (counter == 2)
{
string[] c = tc.Split(' ');
A1 = Convert.ToDouble(c[1]);
}
if (counter == 3)
{
string[] c = tc.Split(' ');
A2 = Convert.ToDouble(c[1]);
}
if (counter == 4)
{
```

```
string[] c = tc.Split(' ');
A3 = Convert.ToDouble(c[1]);
}
if (counter == 5)
{
string[] c = tc.Split(' ');
A4 = Convert.ToDouble(c[1]);
}
if (counter == 6)
{
string[] c = tc.Split(' ');
A5 = Convert.ToDouble(c[1]);
if (counter == 7)
{
string[] c = tc.Split(' ');
A6 = Convert.ToDouble(c[1]);
}
if (counter == 8)
{
string[] c = tc.Split(' ');
tv = Convert.ToDouble(c[1]);
}
if (counter == 9)
{
string[] c = tc.Split(' ');
s = Convert.ToDouble(c[1]);
}
counter = counter + 1;
tc = sr.ReadLine();
}
Console.WriteLine("Choose output type:");
Console.WriteLine("1: The maximum concentration at the end of the reaches.");
Console.WriteLine("2: The step response at the end of the last reach.");
```

```
Console.Write("Enter your choice: ");
string input = Console.ReadLine();
bool outputMax = input == "1" ? true : false;
FileStream file;
string fileName = "";
if (outputMax)
{
Console.Write("Enter output file name: ");
fileName = Console.ReadLine();
fileName = desktopFolderPath + "/" + fileName + ".txt";
file = new FileStream(fileName, FileMode.Create);
file.Close();
file = new FileStream(fileName, FileMode.Open);
StreamWriter writer = new StreamWriter(file);
writer.WriteLine("Reach Length   Max Concentration");
writer.Close();
file.Close();
}
int ne = Nr;
int counterr = 1;
while (counterr <= ne)
{
double t = 0;
int globalCounter = 0;
int x = Convert.ToInt32(s) - 1;
List<ResultItem> item = new List<ResultItem>();
List<Nitrite> nit = new List<Nitrite>();
List<double> currentration = new List<double>();
List<double> cholder = new List<double>();
List<double> A = new List<double>();
List<double> B = new List<double>();
List<double> D = new List<double>();
List<double> E = new List<double>();
```

```
List<double> F = new List<double>();
List<NthClass> nt = new List<NthClass>();
```

ESTIMATION OF MODEL PARAMETERS

```
cholder.Add(0);
int k = 0;
if (counterr >= 1)
{
lines = list.ToArray();
string i = list[counterr - 1];
string[] mycol = i.Split();
double w = Convert.ToDouble(mycol[0]);
double u = Convert.ToDouble(my col[1]);
double H = Convert.ToDouble(mycol[2]);
double Q = Convert.ToDouble(mycol[3]);
double S = Convert.ToDouble(mycol[4]);
double L = Convert.ToDouble(mycol[5]);
double Qt = Convert.ToDouble(mycol[6]);
double Ct = Convert.ToDouble(mycol[7]);
double pe = 5;
double U = 0.05 * u;
double Dl = (14.12 * (Math.Pow(((w) / H), 0.61)) * (Math.Pow((u / U), 0.85)) * H * U);
{
double delx = ((pe * Dl) / (u));
T1 = (((0.04 * delx * delx) / Dl));
T2 = (((0.05 * delx * delx) / Dl));
T3 = (((delx / u) - ((0.09 * delx * delx) / Dl)));
nth = (Convert.ToInt32(L / delx));
Co = (((Co * Q) + (Ct * Qt)) / (Q + Qt));
}
```

```
for (int ii = 1; ii <= s; ii++)
{
t = ii * tv;
double C3 = 0;
if (t < T1)
{
C3 = 0;
}
else
{
double f = (((1 + (Ka * T3)) / T3) * (T1 - t));
double f9 = (((1 + (Kb * T3)) / T3) * (T1 - t));
double f10 = (((1 + (Kb * T2)) / T2) * (T1 - t));
double a = (1 - (Math.Exp((f))));
double j = Co * ((Math.Exp((-Ka * T1))));
double m = (1 + (Ka * T2)) * (1 + (Ka * T3));
double y1 = (n) * (a);
double b1 = (T1 / T2);
double d1 = (Math.Exp((b1)));
double b4 = ((t / T3) - (t / T2));
double d4 = (Math.Exp((b4)));
double f1 = ((1 + (Ka * T3)) / T3);
double f2 = Co * T2 * ((Math.Exp((-f1 * t))));
double f33 = (1 + (Ka * T2));
double f34 = (T2 - T3);
double f5 = ((1 + (Ka * T2)) * (t - T1));
double f6 = (Math.Exp((-f5)));
double b3 = (T1 / T3);
double d3 = (Math.Exp((b3)));
double d0 = (((d4 * d1) / f33) - d3);
double y2 = ((f2 / f34) * (d0));
```

```
double k0 = (A4 * A2 * Ao * A1);
double k8 = (A3 * Ao * A1);
double k9 = k8 - k0;
double k1 = ((1) + (Ka * T2) + (A2 * T2) - (A3 * T2));
double k6 = Ka == 0.0 ? 0.0 : (k9 / (Ka * k1));
double X1 = ((Math.Exp((-T1 * (Ka + A2 - A3)))));
double X2 = ((Math.Exp((-t * (A3 + A2)))));
double k2 = ((1) + (Ka * T3) + (A2 * T3) - (A3 * T3));
double q1 = ((X1 * X2) / (k2));
double x3 = (Math.Exp((b3)));
double x4 = T2 * x3 * ((Math.Exp((-f1 * t))));
double q2 = ((x4) / (T2 - T3));
double x5 = (Math.Exp((b3))) * ((Math.Exp((-f1 * t))));
double q3 = (x5 / k2);
double x6 = T2 * d1 * d4 * ((Math.Exp((-f1 * t))));
double q4 = ((x6) / (T2 - T3));
double y3 = ((k6) * (q1 - q2 - q3 - q4));
double x7 = (Math.Exp((A3 - A2) * (T1 - t)));
double q5 = Ka == 0.0 ? 0.0 : ((x7) / (k2 * Ka));
double l0 = ((((1 + (Ka * T2)) / T2)) * T1);
double x8 = (Math.Exp((l0))) * T2 * d4 * ((Math.Exp((-f1 * t))));
double q6 = Ka == 0.0 ? 0.0 : ((x8) / ((T2 - T3) * Ka));
double r6 = ((1) + (Ka * T3));
double q7 = (((T2 * ((Math.Exp((-T1 * (A3 - A2)))))) * (h7)) / (r6));
double k7 = ((1) + (Ka * T3) - (A3 * T3) + (A2 * T3));
double q8 = (((T2 * ((Math.Exp((t * (A3 - A2)))))) * (h7)) / (k7));
double x9 = (((Math.Exp((-f1 * t)))) * ((Math.Exp((f1 * T1)))));
double q9 = Ka == 0.0 ? 0.0 : ((x9) / (Ka * k2));
double g1 = Ka == 0.0 ? 0.0 : ((T2 * x9) / (Ka * (T2 - T3)));
double g2 = (((T2 * x9) * ((Math.Exp((-T1 * (A3 - A2)))))) / (1 + (Ka * T3)));
double g3 = (((T2 * x9) * ((Math.Exp((-T1 * (A3 - A2)))))) / (k7));
double g4 = ((k9) / (k1));
double y4 = ((g4) * (q5 - q6 - q7 + q8 - q9 + g1 + g2 - g3));
```

```
double z2 = ((1 / T2) * (t - T1));
double z1 = ((1 / T3) * (t - T1));
double z5 = ((1 / T3) * (T1 - t));
double z6 = ((1 / T2) * (T1 - t));
double z3 = ((1) - ((T2 * (Math.Exp((-z2)))) / (T2 - T3)) - (Math.Exp((-z1))) + ((T2 *
(Math.Exp((-z1)))) / (T2 - T3)));
double z = Ka == 0.0 ? 0.0 : A5 == 0.0 ? 0.0 : (((A5) * ((Math.Exp((-Ka * t))))) / (A6 * Ka));
double y6 = ((z) * (z3));
double c1 = ((1) / (1 + (Ka * T3)));
double c2 = (((Math.Exp((-z2))) * ((Math.Exp((-Ka * (t - T1)))))) / (T2 - T3));
double c3 = (((Math.Exp((-f1 * (t - T1))))) / (1 + (Ka * T3)));
double c4 = (((T2) * ((Math.Exp((-f1 * (t - T1)))))) / (T2 - T3));
double y8 = Ka == 0.0 ? 0.0 : A5 == 0.0 ? 0.0 : ((((A5) * (T2)) / ((A6) * (1 + (Ka * T2))))
double c5 = ((1) - ((Math.Exp((-f1 * (t - T1)))))));
double y9 = Ka == 0.0 ? 0.0 : A5 == 0.0 ? 0.0 : (((((A5) * (T3)) / ((A6) * (1 + (Ka * T3)))))
C3 = ((y1) - (y2) - (y3) + (y4) - (y6) + (y7) + (y8) + (y9));
cholder.Add(C3);
}
{
ResultItem rs = new ResultItem();
rs.C3 = C3;
rs.Co = Co;
rs.t = t;
rs.z = 0;
rs.impulse = (rs.C3 - rs.z) / tv;
rs.discrete = discrete;
item.Add(rs);
}
else
{
k = (cholder.Count() - 2);
ResultItem rs = new ResultItem();
rs.C3 = C3;
```

```
rs.Co = Co;
rs.t = t;
rs.z = cholder.ElementAt(k);
rs.impulse = (rs.C3 - rs.z) / tv;
rs.discrete = discrete;
item.Add(rs);
}
}
}
ResultItem rst = new ResultItem();
rst.Co = 0;
rst.t = 0;
rst.impulse = (rst.C3 - rst.z) / tv;
item.Add(rst);
```

SIMULATION OF NUTRIENTS CONCENTRATION FOR D/S LOCATIONS USING CONVOLUTION TECHNIQUES

```
int counterkb = 0;
for (int i = 1; i <= s; i++)
{
int kb = i;
double Sum = 0;
if (!((kb + 1) > s))
{
for (int d = 1; d <= kb; d++)
{
double L = i - d + 1;
ResultItem result;
if ((result = item.FirstOrDefault(a => a.t == L)) != null)
{
int concentrationOfPol = (d + 1);
ResultItem result2 = item.ElementAt(concentrationOfPol - 1);
```

```
int concentrationOfPolkb = d;
ResultItem resultkb = item.ElementAt(concentrationOfPolkb - 1);
double cc1 = (result2.C3 + resultkb.C3) * 0.5;
Sum = Sum + (cc1 * result.discrete);
}
}
ResultItem rv = item.ElementAt(counterkb);
rv.sum = Sum;
item.RemoveAt(counterkb);
item.Insert(counterkb, rv);
counterkb = counterkb + 1;
}
}
foreach (ResultItem rx in item)
{
nt.Add(new NthClass { nthConc = rx.sum, nthDis = rx.discrete, nthT = rx.t });
}
nt.RemoveAt(x + 1);
int third = 1;
int noRemforNth = Convert.ToInt16(nth) - 2;
int countLong = 0;
int countFromPre = Convert.ToInt16(s);
while (noRemforNth > 0)
{
currentration = new List<double>();
noRemforNth = noRemforNth - 1;
int numberOfValPreDis = item.Count() - 1;
int count = 0;
globalCounter = globalCounter + 1;
List<NthClass> ntcut = new List<NthClass>();
foreach (NthClass c in nt)
{
ntcut.Add(c);
```

```
}
{
int concentrationOfPol = (d);
NthClass result2 = ntcut.ElementAt(concentrationOfPol - 1);
int concentrationOfPolkb = d;
NthClass resultkb = new NthClass();
double cc1 = 0;
if (concentrationOfPolkb == s)
cc1 = (result2.nthConc + 0) * 0.5;
}
{
resultkb = nt.ElementAt(concentrationOfPolkb);
}
Sum = Sum + (cc1 * result.discrete);
}
}
currentration.Add(Sum);
}
{
third = 0;
foreach (ResultItem re in item)
{
if (count == 0 && count <= x)
{
discrete = re.sum / Co;
nt.Add(new NthClass { nthDis = discrete, nthT = count + 1, nthConc =
currentration.ElementAt(count) });
count = count + 1;
countLong = countLong + 1;
}
else if (count != 0 && count <= x)
{
if ((count <= x))
```

```
{
discrete = (re.sum - item.ElementAt(count - 1).sum) / (Co);
nt.Add(new NthClass { nthDis = discrete, nthT = count + 1, nthConc =
currentration.ElementAt(count) });
count = count + 1;
countLong = countLong + 1;
}
}
else
{
foreach (double d in currentration)
{
if (count == 0)
{
discrete = nt.ElementAt(countFromPre).nthConc / Co;
nt.Add(new NthClass { nthDis = discrete, nthT = count + 1, nthConc =
currentration.ElementAt(count) });
countFromPre = countFromPre + 1;
count = count + 1;
countLong = countLong + 1;
}
else if (count != 0)
{
discrete = (nt.ElementAt(countFromPre).nthConc - nt.ElementAt(countFromPre - 1).nthConc)
(Co);
nt.Add(new NthClass { nthDis = discrete, nthT = count + 1, nthConc =
currentration.ElementAt(count) });
count = count + 1;
countFromPre = countFromPre + 1;
countLong = countLong + 1;
}
}
NthClass maxSumItem = nt.First(a => a.nthConc == nt.Max(i => i.nthConc));
```

```
List<NthClass> last200 = new List<NthClass>();
ExportToExcel(item);
public static void appendToFile(string fileName, string data)
{
try
{
FileStream file = new FileStream(fileName, FileMode.Append);
StreamWriter fileWriter = new StreamWriter(file);
fileWriter.WriteLine(data);
fileWriter.Close();
file.Close();
}
catch (Exception ex)
{
Console.WriteLine("Exception while writing to file: " + ex);
}
}
public static void ExportToExcel(List<ResultItem> item)
{
Microsoft.Office.Interop.Excel.Applicationexcel
Microsoft.Office.Interop.Excel.Application();
excel.Workbooks.Add();
Microsoft.Office.Interop.Excel._Worksheet workSheet = excel.ActiveSheet;
try
{
// Creation of header cells
workSheet.Cells[1, "A"] = "Time (t)";
workSheet.Cells[1, "B"] = "Co";
workSheet.Cells[1, "C"] = "Step C";
workSheet.Cells[1, "D"] = "Z";
workSheet.Cells[1, "E"] = "Impulse";
workSheet.Cells[1, "F"] = "Sum";
workSheet.Cells[1, "G"] = "Discrete";
```

```
int row = 2;
foreach (ResultItem r in item)
{
workSheet.Cells[row, "A"] = r.t;
workSheet.Cells[row, "B"] = r.Co;
workSheet.Cells[row, "C"] = r.C3;
workSheet.Cells[row, "D"] = r.z;
workSheet.Cells[row, "E"] = r.impulse;
workSheet.Cells[row, "F"] = r.sum;
workSheet.Cells[row, "G"] = r.discrete;
row++;
}
workSheet.Range["A1"].AutoFormat(Microsoft.Office.Interop.Excel.XlRangeAutoFormat.xlRa
ngeAutoFormatClas
stringfolderPath=
Path.Combine(Environment.GetFolderPath(Environment.SpecialFolder.DesktopDirectory), );
if (!Directory.Exists(folderPath))
{
Directory.CreateDirectory(folderPath);
}
string fileName = string.Format(@"{0}\HCSOutput.xlsx", folderPath);
Console.WriteLine("Enter file name for the second one\n");
string theFile = Console.ReadLine();
fileName = fileName.Replace("HCSOutput", theFile);
workSheet.SaveAs(fileName);
}
catch (Exception)
{
excel.Quit();
if (excel != null)
System.Runtime.InteropServices.Marshal.ReleaseComObject(excel);
if (workSheet != null)
System.Runtime.InteropServices.Marshal.ReleaseComObject(workSheet);
```

```
excel = null;
workSheet = null;
GC.Collect();
}
public static void ExportToExcel2(List<NthClass> item, double tv)
{
List<NthClass> theItem2 = new List<NthClass>();
theItem2 = item;
while (item.Count > 200)
{
theItem2.RemoveAt(0);
}
item = theItem2;
Microsoft.Office.Interop.Excel._Worksheet workSheet = excel.ActiveSheet;
workSheet.Range["A1"].AutoFormat(Microsoft.Office.Interop.Excel.XlRangeAutoFormat.xlRa
neAutoFormatClassic1);
stringfolderPath=
Path.Combine(Environment.GetFolderPath(Environment.SpecialFolder.DesktopDirectory),
if (!Directory.Exists(folderPath))
{
Directory.CreateDirectory(folderPath);
}
string fileName = string.Format(@"{0}\excel.xlsx", folderPath);
Console.WriteLine("Enter the file name\n");
string theFile = Console.ReadLine();
fileName = fileName.Replace("excel", theFile);
workSheet.SaveAs(fileName);
}
catch (Exception)
{
}
finally
{
```

```
excel.Quit();
if (excel != null)
System.Runtime.InteropServices.Marshal.ReleaseComObject(excel);
if (workSheet != null)
System.Runtime.InteropServices.Marshal.ReleaseComObject(workSheet);
excel = null;
workSheet = null;
GC.Collect();
}
}
}
}
```

```
Initial-Concentration-of-Ammonia-pollutants(Co) 0.05
Number-of-River-Reaches------------------------ 6

Details of River profile
Width   Veloc   Depth   Flow    Slope   Length  Qt      Ct
41.51   0.368   0.544   0.947   0.005   3200    0       0
42.81   0.368   0.544   0.947   0.005   950     0       0
47.29   0.368   0.544   0.947   0.005   2530    0       0
55.4    0.368   0.544   0.947   0.005   1650    0       0
34.56   0.368   0.544   0.947   0.005   960     0       0
33.45   0.368   0.544   0.947   0.005   11500   0       0




Column (1) to (6) are the river geometry and hydraulic properties
Each row represent a river reach.User can enter the average values for
the reach
Where Column (7) and (8) are the Tributary flow and concentration
If there is no tributary joining the reach, user should leave it as zero,
Else the numeraical value should be provided
For spacing between columns user should tab button for spacing and should be pressed once.
```

Figure B1. 1: Input file for the River characteristics and Initial concentration of Ammonia

```
Initial-Concentration-of-Ammonia-pollutants(Co) 0.05
Initial-Concentration-of-Nitrite-pollutants(Cb) 0.05
Number-of-River-Reaches------------------------ 6

Details of River profile
Width   Veloc   Depth   Flow    Slope   Length  Qt      Ct
41.51   0.368   0.544   0.947   0.005   3200    0       0
42.81   0.368   0.544   0.947   0.005   950     0       0
47.29   0.368   0.544   0.947   0.005   2530    0       0
55.4    0.368   0.544   0.947   0.005   1650    0       0
34.56   0.368   0.544   0.947   0.005   960     0       0
33.45   0.368   0.544   0.947   0.005   11500   0       0




Column (1) to (6) are the river geometry and hydraulic properties
Each row represent a river reach.User can enter the average values for
the reach
Where Column (7) and (8) are the Tributary flow and concentration
If there is no tributary joining the reach, user should leave it as zero,
Else the numeraical value should be provided
For spacing between columns user should tab button for spacing and should be pressed once.
```

Figure B1. 2: Input file for the River characteristics and Initial concentration of Nitrite

```
Initial-Concentration-of-Ammonia-pollutants(Co) 0.4
Initial-Concentration-of-Nitrite-pollutants(Cb) 0.05
Initial-Concentration-of-Nitrate-pollutants(Cc) 0.05
Number-of-River-Reaches------------------------ 6

Details of River profile
Width   Veloc   Depth   Flow    Slope   Length  Qt      Ct
41.51   0.368   0.544   0.947   0.005   3200    0       0
42.81   0.368   0.544   0.947   0.005   950     0       0
47.29   0.368   0.544   0.947   0.005   2530    0       0
55.4    0.368   0.544   0.947   0.005   1650    0       0
34.56   0.368   0.544   0.947   0.005   960     0       0
33.45   0.368   0.544   0.947   0.005   11500   0       0




Column (1) to (6) are the river geometry and hydraulic properties
Each row represent a river reach.User can enter the average values for
the reach
Where Column (7) and (8) are the Tributary flow and concentration
If there is no tributary joining the reach, user should leave it as zero,
Else the numeraical value should be provided
For spacing between columns user should tab button for spacing and should be pressed once.
```

Figure B1. 3: Input file for the River characteristics and Initial concentration of Nitrate

```
Rate-Constant-for#Ammonia-Oxidation----------------------------------------------------ka 0.001
Algal-biomass-concentration------------------------------------------------------------Ao 0.005
Fraction-of-Algal-biomass-that-is-Nitrogen---------------------------------------------A1 0.0004
Algal-Growth-rate----------------------------------------------------------------------A2 0.002
Algal-Respiration-rate-----------------------------------------------------------------A3 0.0005
Algal-Preference-factor-for-Ammonia----------------------------------------------------A4 0.8
Benthos-source-rate-of-Ammonia-nitrogen------------------------------------------------A5 0.000004
Mean-depth-of-bottom-sediment(Benthos)-------------------------------------------------A6 0.5
Time-Increment-------------------------------------------------------------------------tv 2
Total-number-of-Observation------------------------------------------------------------s 200
Rate-Constant-for#Nitrite-Oxidation----------------------------------------------------kb 0.009
Rate-Constant-for#Nitrate-Oxidation----------------------------------------------------kc 0.01



For spacing between the notations and numerical values user should use the space button for spacing and should
be pressed once.
```

Figure B1. 4: Input file for the kinetics parameters

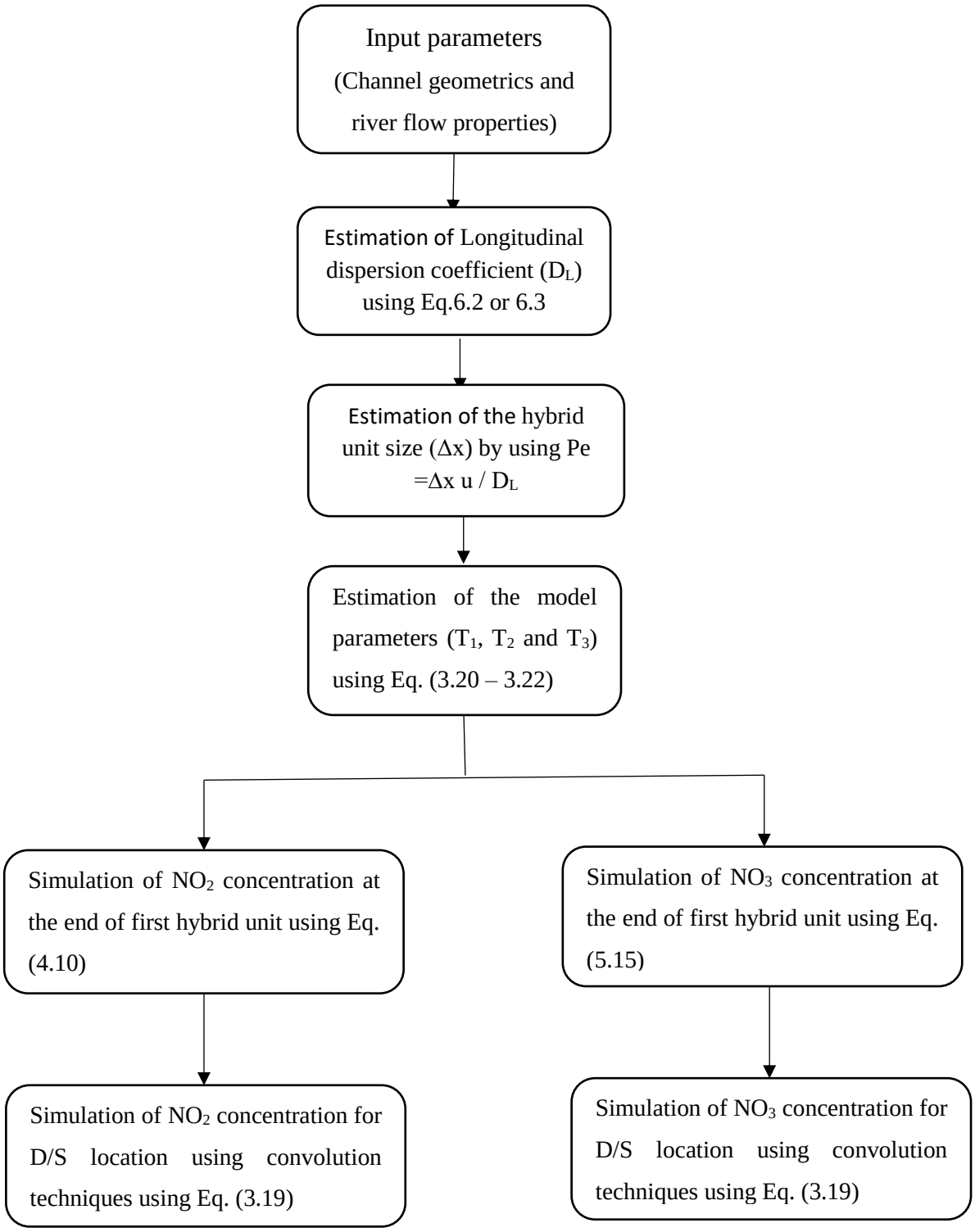

Figure B1. 5: Flow chart representing the general process of simulating the concentration of nitrite and nitrate pollutants using C-sharp programming language similar to Appendix B1.